PB82-220179

REPORT NO.
UCB/EERC-81/20
DECEMBER 1981

EARTHQUAKE ENGINEERING RESEARCH CENTER

OPTIMAL DESIGN OF SEISMIC-RESISTANT PLANAR STEEL FRAMES

by

R. J. BALLING
V. CIAMPI
K. S. PISTER
E. POLAK

Report to the National Science Foundation

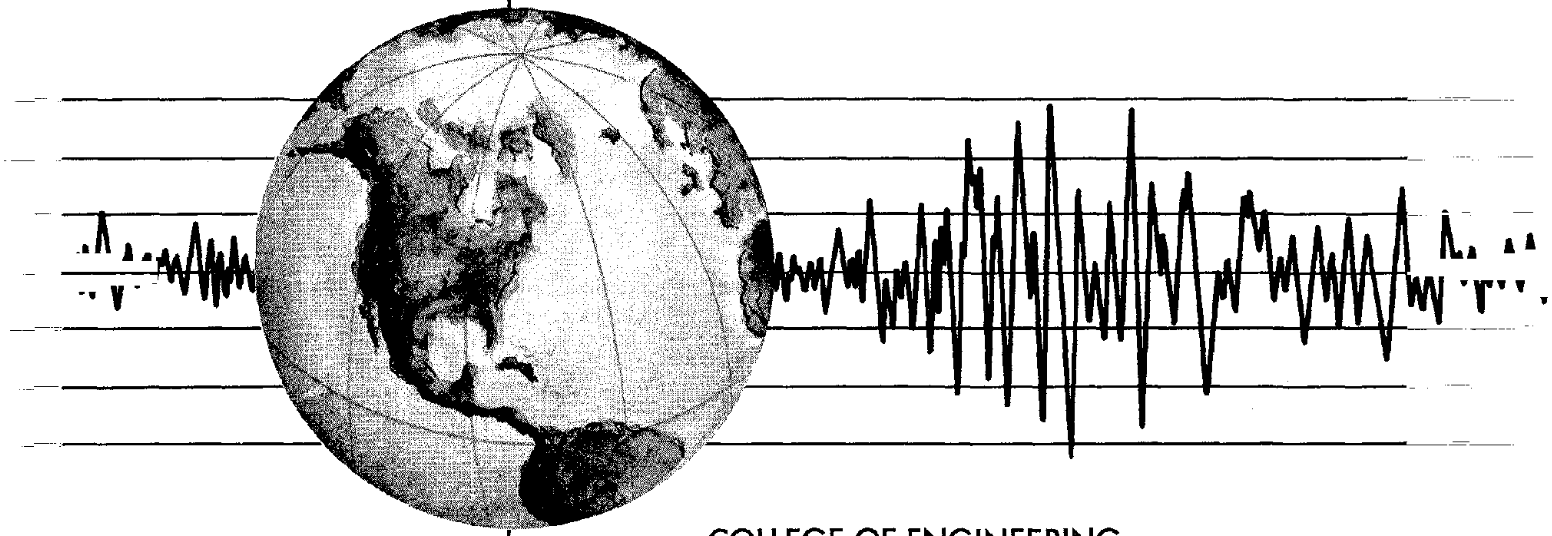

COLLEGE OF ENGINEERING

UNIVERSITY OF CALIFORNIA · Berkeley, California

For sale by the National Technical Information Service, U.S. Department of Commerce, Springfield, Virginia 22161.

See back of report for up to date listing of EERC reports.

Optimal Design of Seismic-Resistant Planar Steel Frames

by

R. J. Balling

V. Ciampi

K. S. Pister

and

E. Polak

Prepared under the sponsorship of
the National Science Foundation
Grant PFR-7908261

Report No. UCB/EERC-81/20
Earthquake Engineering Research Center
College of Engineering
University of California
Berkeley, California

December 1981

ABSTRACT

This report presents a method for the seismic-resistant design of planar rectangular braced or unbraced steel frames. An important feature of the method is that nonlinear step-by-step integration is used as the analysis technique within the design process itself.

The method directly quantifies the accepted seismic-resistant design philosophy that a structure: (1) resists moderate ground motion without structural damage, and (2) resists severe ground motion without collapse. Actual ground motion accelerograms are selected and scaled to levels representing moderate and severe ground motions. Constraints quantifying structural damage and limited non-structural damage are constructed for the case of moderate ground motion. Constraints quantifying collapse and limited structural damage are constructed for the case of severe ground motion. In addition there are serviceability constraints on structural behavior under gravity loads only. Possible objective functions range from the minimization of structural volume to the minimization of response quantities such as story drifts or inelastically dissipated energy. Sophisticated optimization algorithms are utilized to solve the resulting mathematical programming problem.

The frame design method is illustrated by application to a non-trivial example 4-story 3-bay moment-resisting steel frame. The practicality and reliability of the method for this example problem are assessed.

ACKNOWLEDGEMENTS

This research was supported by the National Science Foundation under Grant PFR-7908261 with the University of California, Berkeley. Computing facilities were provided in part by equipment Grant ENG-7810442 from the National Science Foundation.

The support of Professor Ciampi by the Italian National Research Council during the course of the research is gratefully acknowledged.

TABLE OF CONTENTS

1. INTRODUCTION

The design of structures to resist earthquake loading presents one of the most challenging problems facing structural engineers. The major components of this design problem are treated in [1]. Two principal aspects differentiate seismic-resistant design from other branches of engineering [2]: First, there is enormous uncertainty in the prediction of future disturbances; Second, the response of structures to such complicated disturbances is not well understood. Uncertainties arise not only with regard to the number and magnitudes of future earthquakes affecting a structure, but also with regard to the characteristics of the motions themselves. At best, earthquake ground motion can be broadly described as a nonstationary random process. Sources of difficulty related to the second aspect of seismic-resistant design stem from the inability to model properly the nonlinear, dynamic, cyclic behavior of material, which will occur when the structure is subjected to strong ground motion.

Notwithstanding the many obstacles involved, progress has been made in the state of analysis of the response of given structures to prescribed deterministic seismic excitation. At present, it is generally agreed that the analysis of linear elastic structures is most efficiently performed by a mode-superposition procedure, while analysis of inelastic structures require use of step-by-step integration techniques [3].

There is also general consensus in the profession of structural engineering that a proposed structural design should meet the following criteria [4]:

(1) The structure should resist minor earthquakes without damage.

(2) The structure should resist moderate earthquakes without structural damage, but possibly with limited non-structural damage.

(3) The structure should resist the most severe earthquakes without collapse, but possibly with limited structural damage.

These criteria will be referred to as the "accepted design philosophy". It is evident that the process of design should involve at least a two-tier approach to account for the different criteria regarding moderate and severe earthquakes.

Consider now the state of design as prescribed by the Uniform Building Code [5]. The methodology suggested therein may be summarized as follows:

(1) Compute "equivalent static seismic forces" from formulae such as $V = ZIKCSW$ where V = base shear, W = weight of the structure, C = coefficient related to the fundamental period of the structure, and Z,I,K,S are empirical coefficients which account for seismicity, importance of the structure, ductility of the structure, and effect of local soil conditions, respectively.

(2) Place the static seismic forces on a linear-elastic model of the structure.

(3) Design the structure such that the resulting stresses and displacements do not exceed allowable values.

An obvious criticism of this design method is the fact that its relationship to the accepted design philosophy is tenuous. This method makes no distinction between moderate and severe ground motion. Futhermore there is no attempt to quantify structural or non-structural damage, and it is difficult to relate the exceedance of allowable stresses to collapse. Another flaw in the method is its incompatibility with the state of analysis of seismically-excited structures. The linear static method of analysis prescribed by this design scheme is extremely primitive. The capability for performing more sophisticated and more reliable analyses is available; however it is not required by the proposed code design method.

Structural engineers, recognizing the drawbacks to the code method of design, have proposed alternative design methods. Probably the most prominent among these is the method proposed by the Applied Technology Council [6]. In the area of seismic-resistant design of steel framed structures, several methods have emerged from research done in the academic environment [7-9]. In all of these methods the accepted design philosophy is approached more directly, and more sophisticated methods of analysis are employed than are used in the code method. However, all of these methods avoid the use of step-by-step integration analysis within the design process itself. Severe earthquake excitation is certain to cause significant inelastic deformation in structures. The resulting nonlinear response demands the use of a nonlinear analysis technique such as step-by-step integration; however, this alternative is usually dismissed as too costly.

It is the author's opinion that advances in current computational technology make the use of more sophisticated analysis techniques within a design methodology a viable alternative. Specific reasons for this opinion include:

(1) The computational speed and storage capabilities of new computers is increasing rapidly.

(2) Affordable yet powerful mini-computers are becoming available for use by consulting engineering firms.

(3) Computing costs are small in comparison to the cost of construction, or to the cost of insurance, or even to other engineering costs.

In this report, a method is proposed and illustrated by a non-trivial example for the seismic-resistant design of planar, rectangular braced or unbraced steel frames. The accepted design philosophy is approached directly. Moderate and severe earthquake ground motions are selected. Structural damage, non-structural damage, and collapse are quantified directly in terms of mathematical constraint functions, and the problem is cast into a nonlinear programming setting. Flexibility with regard to the objective function is allowed, and some interesting possibilities are explored. Most important, step-by-step integration is used as the analysis technique within the design process itself. Therefore, the approach may be viewed as an attempt to propose a design method compatible with the current state of analysis.

The proposed design method makes use of an interactive, optimization-based structural design software system known as DELIGHT.STRUCT, which is described in a companion report [10]. The system contains a library of software wherein the proposed frame design method is programmed. The software library will be referred to as the "frame software". The design of an example 4-story 3-bay frame using the proposed method will form the central focus of the report. This frame, referred to as the "example frame", is shown in Figure 1 and is typical of frames found in low-rise apartment buildings. The example frame will be designed as a independent planar frame in this report, but in practice its design would have to reflect the complete three-dimensional frame behavior of the building. The example frame is taken from a report by Pique and Roesset [11] where the frame was designed according to the Uniform Building Code to resist gravity, earthquake, and wind loadings.

Section 2 of the report will treat the quantification of design criteria. Here the proposed method will be presented and assumptions made in its formulation will be enumerated. Section 3 will present the computational results obtained by applying the proposed method to the example frame. Section 4 draws some brief conclusions from the results.

2. QUANTIFICATION OF DESIGN CRITERIA

Before the designer can enter the computation part of the design process, the answers to important questions such as the following must be quantified:

(1) What are the loads for which the structure is to be designed?

(2) What is a reasonable mathematical model that can be used for analysis of the structural response?

(3) What structural characteristics should be chosen as design variables?

(4) What is the objective to be used in deciding among competing designs?

(5) What constraints on performance of the structure should be imposed?

The answers to these five questions for both the frame software and the example frame will be treated in Subsections 2.1, 2.2, 2.3, 2.4, and 2.5, respectively.

2.1. LOADING

It is assumed that the frames to be designed will be subjected to gravity loading, moderate earthquake loading, and severe earthquake loading. Wind and other loading conditions are omitted for simplicity; however, more comprehensive loading combinations could be added to the method without significant change. The assumed gravity loads will be described first. A discussion of modelling earthquake loading, followed by an explanation of the earthquake loading model adopted for the example frame, completes the subsection.

2.1.1. Gravity Loads

The frame software allows the user to specify downward gravity loads on nodes of the frame as well as downward uniform gravity loads on girders of the frame. Furthermore, the percentage of uniform load to be designated as live load may be specified by the user. Load factors are not used; thus, one should try to specify the "worst" possible gravity loads and incorporate safety factors in the constraints on response.

For the example four-story, three-bay frame nodal gravity loads are not specified. The specified dead load is 80 psf, and the specified live load is 40 psf for the floors and 20 psf for the roof. These frames are assumed to be spaced 20 feet apart. Thus, the downward gravity uniform loads are 0.2000 kips/in for the floors and 0.1667 kips/in for the roof. Live load is given as one-third of the total uniform load.

2.1.2. Earthquake Loading

One of the most difficult tasks facing the structural engineer is that of specification of an earthquake loading. Many complex geological and geotechnical factors which currently cannot be reasonably modelled affect the nature of ground motion at a given site. The absence of data from actual strong motion earthquakes in the vicinity of a site makes it difficult to statistically quantify future ground motion.

A common approach taken by structural engineers is to use "smoothed design response spectra". This approach assumes that possible future ground motions will have response spectra which are bounded by a smoothed envelope spectrum derived from the spectra of past motions. The drawback to this method is that the notion of a response spectrum is based on the linear elastic properties of structures. Although the design envelope spectrum may contain the most severe frequency content for linear elastic structures, other classes of ground motion may exhibit characteristics which cause more severe response in yielding structures. For example, the long acceleration pulse experienced near the fault during the 1971 San Fernando earthquake is recognized to have been a major cause of the damage potential of that earthquake. Information regarding acceleration pulse size is not available from response spectra. To account for the inelastic properties of structures, "inelastic design response spectra" have been derived from elastic design spectra by various methods. Some of these methods make the crude assumption that for a given ground motion elastic and yielding SDOF systems with the same stiffness will have roughly the same peak displacements; thus, the design forces may be obtained by dividing the design forces on the equivalent elastic structure by the design ductility factor.

Step-by-step integration is used as the analysis technique in the frame software. This requires that the user supply a time history for a design earthquake together with values for peak accelerations of "severe" and "moderate" ground motions. It is assumed that the time history so given is for ground acceleration in the horizontal direction in the plane of the frame, and vertical ground acceleration is neglected for simplicity. Selecting an appropriate design time history for a site poses difficult problems. First, one must construct the time histories of possible motions for a site. This can only be done through statistical procedures which operate on actual past time histories at the site or at similar sites. Recent work in this regard using autoregressive, moving-average (ARMA) models captures the non-stationary nature of earthquake ground motions [12]. Second, one must select from the possible time histories a design history. Normally the design history should be that ground motion which drives the structure to its maximum response. The problem is that this "worst" motion is a function of the structure itself, which has not yet been designed. Thus, any approach to obtain a design time history will have to involve a considerable amount of judgement and assumption.

2.1.3. Adopted Earthquake Loading Model

Since several strong motion records are available for area surrounding El Centro, California, let us assume that the example frame will be constructed at that site. Six actual ground motion histories digitized at time intervals of 0.02 seconds were selected for this site and will be designated as E1, E2, E3, E4, E5, and E6 throughout the remainder of this report. Histories E1 and E2 represent the S00E and S90W components, respectively, of the earthquake which occurred on May 18, 1940 as measured at the El Centro Site Imperial Valley Irrigation District. Histories E3 and E4 represent the S00W and S90W components, respectively, of the earthquake which occured on December 30, 1934 as measured at the El Centro Site Imperial Valley Irrigation District. Histories E5 and E6 represent the N50E and N40W components, respectively, of the earthquake which occurred on October 15, 1979 as measured at the El Centro Community Hospital on Keystone Road. Histories E1 through E4 were obtained from the California

Institute of Technology [13]. Histories E5 and E6 were obtained from the United States Geological Survey [14]. The most severe ten seconds from each history were selected by inspection. The actual histories together with the respective ten-second intervals are shown in Figure 2. After selecting the ten second intervals, each record was translated along the acceleration axis by a small amount so that the residual ground velocity obtained by integrating the record by the trapezoidal rule is zero. The largest ratio of this acceleration translation to the peak acceleration over all the records was 0.0150.

The next step was to scale these records so that they each represent roughly the same damage potential. Initially each record was scaled so as to have the same peak acceleration. However, the example frame was expected to exhibit a strong variance in behavior when analyzed under the motions scaled in this way. It was decided that a more rational approach would be to scale according to the spectral intensity which is a measure of ground motion intensity for linear-elastic structures. The program SPECTR [15] was used for evaluating digitized response spectra at an assumed damping ratio of 2% for each of the records. It was then assumed that the significant vibrational modes of the four-story frame will have periods between 0.1 s and 1.0 s. The spectral intensities for each of the records were obtained by integrating the response spectra between these limits using the trapezoidal rule. Since El Centro, California is a highly seismic region it was decided that the "severe" earthquake should have a peak acceleration of 0.5g and the "moderate" earthquake should have a peak acceleration of 0.15g. Thus, all of the records were normalized so as to have the same spectral intensity. The set of records was then scaled for the severe earthquake so that the maximum peak acceleration over all the records was 0.5g, and scaled for the moderate earthquake so that the maximum peak acceleration over all the records was 0.15g. The resulting spectral intensities, peak accelerations, and scale factors for each record are listed in Figure 3. The response spectra at 2% damping for the records before and after normalization and scaling for the severe earthquake are shown in Figure 4. The ten-second interval time histories for the normalized records scaled for the severe earthquake are shown in Figure 5.

After selecting, normalizing, and scaling the set of records, the final step is to select a design earthquake from the set in a rational manner. An effort was made to obtain a good initial design for the example frame. This initial design was then analyzed under all six motions and the design constraints were evaluated. The destructive potentials of the motions for this design were ranked using the following criteria:

(1) Energy input from the severe earthquake to the structure

(2) Sum of squares of story drifts caused by the moderate earthquake

(3) Energy dissipated inelastically by the entire frame during the severe earthquake

(4) Energy dissipated inelastically by the columns during the severe earthquake

(5) Maximum constraint function violation

These criteria were weighted as depicted by the decision table in Figure 6. It became clear that records E2 and E6 were the most damaging for this frame. By a purely judgemental decision it was decided to use record E6 as the design record. It is assumed that the final design will not differ substantially from this preliminary design; thus, record E6 may be the most damaging motion for the final design as well. Of course, once a final design is obtained, it will be checked by analyses using the other records.

2.2. MODEL OF THE STRUCTURE

The mathematical model used in the frame software to simulate the response of a specified frame under the assumed loads will now be described. This involves a description of the frame geometries allowed in the frame software as well as an explanation of the solution strategies and element models used for simulation.

2.2.1. Geometry Of The Model

The frame configurations which can be treated with the frame software include planar, rectangular braced or unbraced frames. Specifically the desired frame configuration must be derivable from the following three-step process:

(1) A rectangular grid is constructed according to a specified number of stories, number of bays, story heights, and bay widths.

(2) Cross-bracing may be placed in specified panels.

(3) Specified elements and nodes in the resulting grid may be erased.

After the configuration is thus specified, the element types for the model are given. The frame software assumes horizontal elements are modelled as girders, vertical elements are modelled as columns, and diagonal elements are modelled as braces. In addition the user may specify some girders as "shear link" elements, other girders as "dissipator" elements, and some columns as "rubber bearing" elements (see Figure 7).

The boundary condition assumed by the frame software is that the base nodes are fixed against translation and rotation. The user may include additional boundary conditions at specified nodes.

A result of the freedom allowed in specification of configuration, element type, and boundary conditions is that a wide range of frame geometries may be treated. The example frame is but one of many possible geometries. Other examples are shown in Figure 7, which include moment-resistant frame geometries, reduced-degree-of-freedom frame geometries, concentric and eccentric braced frame geometries, and vibration-isolated frame geometries.

2.2.2. Simulation Procedure

The following simulation procedure is adopted in the frame software:

(1) A static nonlinear analysis is made under gravity loads only.

(2) A static linear analysis under gravity loads followed by a dynamic linear analysis under the moderate earthquake loading is made.

(3) A static nonlinear analysis under gravity loads followed by a dynamic nonlinear analysis under severe earthquake loading is made.

The general-purpose structural analysis program, ANSR, is used to compute simulation structural response [16]. Parameters used in the ANSR simulation program are set in the frame software to achieve the desired solution strategies for the several analyses. For all analyses:

(1) Path dependent state determination is used.

(2) The maximum allowable nodal displacement is unlimited.

(3) Convergence tolerances on unbalanced force vector norms are set to 0.01.

(4) The next load or time step is applied regardless of convergence in the previous step.

For all dynamic analyses:

(1) Nodal translational masses are computed by dividing the nodal forces due to gravity dead loads by the acceleration of gravity, and nodal rotational masses are neglected.

(2) Step-by-step integration is made using Newmark's method where parameters are set to yield constant "average" acceleration with no numerical damping (trapezoidal rule).

(3) The time step length is 0.01 seconds, and the number of time steps is chosen so that analysis is carried out one second beyond the end of the earthquake ground acceleration record. Thus, for the example frame 1100 time steps were used in dynamic analysis.

(4) The damping matrix is taken as a linear combination of the mass matrix and the initial stiffness matrix as:

$$\mathbf{C} = \frac{4\xi\pi f s}{n\,(s-1)}\mathbf{M} + \frac{\xi n}{\pi f\,(s-1)}\mathbf{K}$$

where

C = damping matrix

M = mass matrix

K = initial stiffness matrix

ξ = damping ratio

n = number of stories

f = ratio of number of stories to the fundamental period

s = ratio of the fundamental to the second period

The damping ratio, the ratio of the number of stories to the fundamental period, and the ratio of the fundamental period to the second period are specified by the user. For the example frame a damping ratio of 2% was selected and the period ratios were estimated by solving the eigenproblem for the initial design. The damping coefficients given by the above formulae yield the specified damping ratio in the first two modes.

In order to achieve a nonlinear static analysis under gravity loads only, a Newton-Raphson iteration scheme is employed. The loads are applied in a series of five load steps. The maximum number of iterations permitted in any load step is 20, and the stiffness matrix is reformed at each iteration. Axial deformation of columns and girders is considered so that there are 48 degrees of freedom in the example frame.

For the combined gravity and moderate earthquake loads analyses are simplified by neglecting axial deformation in the girders and columns and assuming linear elastic response. The example frame has but 20 degrees of freedom after neglecting axial deformation. Linear analyses are achieved by increasing yield moments and forces in the model by 1000 times, and by allowing only one iteration per load or time step. Only one static load step is needed to represent gravity loads before the moderate earthquake dynamic loads are applied.

For the combined gravity and severe earthquake loads, nonlinear static and dynamic analyses are made employing a Newton-Raphson iteration scheme. Axial deformations are neglected. Five static load steps are applied, representing the gravity loads followed by application of the severe earthquake dynamic loads. The stiffness matrix is reformed at each iteration in each load or time step and the maximum number of iterations within any step is 20.

2.2.3. Element Models

For all elements the frame software requires that the user supply values for the yield stress, the strain hardening ratio, and the initial modulus of elasticity. The values chosen for the example frame are yield stress = 36.0 ksi, strain hardening ratio = 0.05 , and modulus of elasticity = 29000. ksi. Furthermore, shearing deformations, out-of-plane deformations, and end eccentricities are not considered in any of the element models to simplify the analysis.

Columns are modelled by a two-dimensional lumped-plasticity parallel-component beam-column element as depicted in Figure 8 and descibed in reference [17]. The geometric stiffness of columns is considered. A yield interaction diagram is used as shown in Figure 9, where the parameters ym and yp are specified by the user. For the example frame these factors were chosen as $ym = 1.0$ and $yp = 0.15$. Initial axial forces are included on the columns to influence the onset of yielding and the impact of geometric stiffness. These initial axial forces are computed from the gravity loads by approximating the girders as simply supported.

Girders are also modelled by the same beam-column element, however, the geometric stiffness and yield surface interaction are neglected. Initial fixed-end moments for girders with uniform gravity loads are employed to influence the onset of yielding.

Braces can be modelled by a three-dimensional elasto-plastic parallel-component truss element as depicted in Figure 8. Geometric nonlinearity is neglected. The braces yield elasto-plastically in tension and buckle elastically in compression at their Euler load.

For eccentrically braced frames (see Figure 7), the shear links can be modelled by the beam-column element used for columns and girders. Appropriate input parameters can be derived assuming the shear link elements are constrained to deform in pure shear. It is assumed that wide flange sections are used for the shear links and that the web behaves as an elastic perfectly-plastic shear block and the flanges behave elastically in flexure. Thus, in the parallel-component model, the lumped-plasticity component can model the web and the strain-hardening component can model the flanges. A value for Poisson's ratio must be specified by the user. With these assumptions one is able to derive the following expressions for the equivalent model section properties from the actual element dimensions:

$$I_m = \frac{L^2}{4\,(1+\nu)}\left[\frac{A}{4} - \frac{I}{D^2}\right] + \frac{3\,I}{2} - \frac{A\,D^2}{8}$$

$$S_m = \frac{\left[\frac{3\,I}{2} - \frac{A\,D^2}{8}\right]}{I_m}$$

$$M_m = \frac{6\,\sigma_y\,I_m\,(1+\nu)}{L}$$

where

I_m = model moment of inertia

S_m = model strain hardening ratio

M_m = model yield moment

A = actual cross-sectional area

I = actual moment of inertia

D = actual section depth

L = element length

σ_y = yield stress of steel

ν = Poisson's ratio for steel

As with girders, geometric stiffness and yield interaction are ignored while initial end moments due to uniform gravity loads are included.

For frames which involve vibration isolation (see Figure 7), rubber bearing elements can also be modelled by the beam-column element used for the columns and girders. These rubber bearing elements are constrained to deform in pure shear. They are assumed to have a square cross-section and infinite yield stress. The user must supply values for the shear modulus of rubber and the height of the bearings. From these assumptions the following expression can be derived to compute the equivalent model moment of inertia from the actual element dimensions:

$$I_m = \frac{A\,L^3\,G_r}{12\,E\,H}$$

where

I_m = model moment of inertia

A = actual cross-sectional area

L = length of bearing

G_r = shear modulus of elasticity for rubber

E = steel modulus of elasticity

H = height of bearings

Note that the specified length of the bearing is arbitrary. As with the columns, geometric stiffness is considered and initial axial forces due to gravity loads are included.

For frames which involve vibration isolation, triangular dissipator elements (of the type shown in Figure 7) connected by a rigid link to the frame may be modelled by the same truss element used for braces with the exception that the element yields rather than buckles elastically in compression. The user must specify the dissipator height and base width. From these quantities the following expressions can be derived to compute the equivalent model section properties from the actual element dimensions:

$$A_m = \frac{W\,L\,T^3}{6\,H^3}$$

$$\sigma_{ym} = \frac{3\,\sigma_y\,H^2}{2\,L\,T}$$

where

A_m = model cross-sectional area

σ_{ym} = model yield stress

T = actual dissipator thickness

W = actual dissipator base thickness

H = actual dissipator height

L = rigid link length

σ_y = yield stress of steel

Note that the specified length of the rigid link is arbitrary. The dissipator is assumed to yield at the same stress in both tension and compression, and geometric nonlinearity is included.

2.3. DESIGN VARIABLES

To simplify the design problem the frame software assumes that there is only one design variable per element. The design variables considered for the various elements are explained in this subsection. Other section properties needed for analysis for each element are computed by appropriate approximate functional relationships also described.

2.3.1. Element Design Variables

The section moment of inertia is used as the element design variable for columns, girders, and shear elements. For braces the element design variable is the cross-sectional area. The thickness of the dissipator is the design variable for dissipator elements. Cross-section edge length is the design variable for rubber bearing elements. The minimum and maximum values acceptable for each design variable are specified by the user. It is possible to specify some elements as "not subject to design", meaning that their section properties are pre-set and remain constant throughout the design process. It is also possible to designate groups of elements as "equal during design", meaning that the section properties of elements in the group remain equal as they change throughout the design process.

The design variables for the example frame are numbered as follows:

(1) Moment of inertia for the exterior columns of the bottom two stories

(2) Moment of inertia for the interior columns of the bottom two stories

(3) Moment of inertia for the exterior columns of the top two stories

(4) Moment of inertia for the interior columns of the top two stories

(5) Moment of inertia for first story girders

(6) Moment of inertia for second story girders

(7) Moment of inertia for third story girders

(8) Moment of inertia for fourth story girders

It is assumed that column moments of inertia lie in the interval $[50\, in^4, 1500\, in^4]$, and that girder moments of inertia lie in the interval $[125\, in^4, 2500\, in^4]$.

2.3.2. Section Relationships

The frame software assumes that the section depth for columns and girders can be approximated by an expression which is proportional to the moment of inertia raised to a rational power specified in the input. Further, the radius of gyration for columns and girders is taken to be proportional to the section depth raised to a rational power specified in the input. For wide flange sections the cross-sectional area and plastic yield moment can then be computed from the following formulae:

$$A = \frac{I}{R^2}$$

$$M_p = \sigma_y \left(\frac{A\,D}{8} + \frac{3\,I}{2\,D} \right)$$

where

A = cross-sectional area

M_p = plastic yield moment

I = moment of inertia

R = radius of gyration

σ_y = yield stress

D = section depth

It is necessary to compute the moment of inertia for braces in order to derive their critical buckling stress. It is assumed that for braces the moment of inertia can be approximated by an expression which is proportional to the cross-sectional area raised to a rational power specified in the input.

For the example frame many of the functional relationships proposed by Walker [18] are used for the column and girder properties. These relationships were derived from least-square curve fits among "economy" wide flange sections most likely to be used for columns and girders. The relationships thus derived are as follows:

for columns with $I \leqslant 429\, in^4$

$$D = 1.47\, I^{0.368}$$

$$R = 0.39\, D^{1.04}$$

for columns with $I > 429\, in^4$

$$D = 10.5\, I^{0.0436}$$

$$R = 0.39\, D^{1.04}$$

for girders

$$D = 2.66\, I^{0.287}$$

$$R = 0.52\, D^{0.92}$$

where

D = section depth in inches

I = moment of inertia in inches^4

R = radius of gyration in inches

2.4. COST FUNCTION

One must have a specific cost or merit function for the design process in order to choose among the set of designs satisfying the constraints. The cost function must in some way put a scalar "pricetag" on each design. Although a number of cost functions may be used, in seismic-resistant design it may be desirable to formulate cost in terms of energy. This is for the following reasons:

(1) Energy dissipation is an indicator of the amount of inelastic deformation (damage) throughout the structure.

(2) Energy is the mapping of complex mechanical information varying over space and time into a time dependent mathematical scalar.

(3) One has an intuitive feel for what energy represents, since it is used in many aspects of science.

In this subsection the way in which an existing finite-element program was modified to compute terms in the energy balance equation is described. Then, the possible cost functions allowed by the frame software are explained.

2.4.1. Energy Balance

The computation of terms in the energy balance equation adopted herein follows the work of Berg and Thomaides in spirit [19]. In the ANSR simulation program, the following force balance equation is satisfied at each load or time step:

$$F_u = F_l - F_i - F_{dm} - F_e$$

where

F_u = unbalanced nodal force vector

F_l = vector of applied nodal loads

F_i = nodal inertia force vector

F_{dm} = nodal mass proportional damping force vector

F_e = nodal element resistance force vector

The nodal element resistance force vector is evaluated by accumulating the contributions from each element to the proper global degrees of freedom. These contributions from each element consist of three parts:

$$F_e = F_{ee} + F_{ge} - F_{de}$$

where

F_{ee} = nodal forces due to element deformation

F_{ge} = nodal forces due to P-delta effect

F_{de} = nodal forces due to stiffness proportional damping

By rearranging the terms in the force balance equation and multiplying through by the differential nodal displacements one obtains the following differential energy balance equation:

$$dE_q + dE_l = dE_k + dE_d + dE_e + dE_u$$

where

$dE_q = - < F_{ee} , R\ dv_g >$

= earthquake input energy differential

$dE_l = < (F_l + F_{ge}) , (dv_r + R\ dv_g) >$

= differential of work done by applied loads

$dE_k = < F_i , (dv_r + R\ dv_g) >$

= kinetic energy differential

$dE_d = < (F_{dm} - F_{de}) , (dv_r + R\ dv_g) >$

= damped energy differential

$dE_e = < F_{ee} , dv_r >$

= element deformation energy differential

$dE_u = < F_u , (dv_r + R\ dv_g) >$

= error energy differential

dv_r = relative nodal differential displacement vector

dv_g = differential ground displacement

R = boolean ground displacement distribution vector

At each load or time step the ANSR simulation program calls the subroutine energy after the norm of the unbalanced forces has satisfied the convergence tolerance criterion. This subroutine integrates the differential energy balance equation with respect to nodal displacements in order to compute the values of terms in the energy balance equation at each step. The numerical integration must be carried out in a manner consistent with the scheme used by the ANSR simulation to solve the differential equation of motion. Thus, if the Newmark average acceleration scheme is used by the ANSR simulation program, the trapezoidal rule must be used to evaluate the energy integrals. Furthermore, the trapezoidal rule must also be used to evaluate ground velocities from ground accelerations and ground displacements from ground velocities. At each time step the subroutine energy updates the earthquake input energy, kinetic energy, damped energy, and energy error. The element deformation energy is separated into the element elastic and element inelastic energy, which are computed at the element level and accumulated in the subroutine energy. For some elements in ANSR, initial element forces may be applied in order to influence the onset of yielding. Such initial forces represent the effects of distributed element gravity loads which are absent when modelled by equivalent nodal loads. These initial element forces will cause the sum of the element elastic and inelastic energy to be out of balance with the work done by the nodal element resistance forces. The energy difference may be attributed to work done by distributed element gravity loads. Therefore, the subroutine energy evaluates the work done by the applied loads as the opposite of the sum of the other terms in the energy balance equation.

The earthquake input energy so evaluated represents the work done by the base shear force on the frame as it moves through the ground displacement. One would expect this energy to be generally increasing in time, although not monotonically, and to remain constant after the ground motion ceases. The kinetic energy represents the work done by inertial forces. One would expect this energy to be oscillatory and positive, and to be decreasing in amplitude after the ground motion ceases. The damped energy represents work done by the nodal damping forces. The dissipative nature of damping would cause one to expect this energy to be monotonically increasing in time, however the stiffness proportional damping model used permits the possibility of decreasing damping energy to occur. The elastic energy represents the elastic strain energy stored in the elements due to element displacements. This energy is positive and oscillatory in time, and is almost 180 degrees out of phase with the kinetic energy. The elastic energy is initially non-zero at time zero due to strain under gravity loads. Furthermore, if yielding occurs during the earthquake, the axis about which the elastic energy oscillates may shift upward due to the build-up of prestrain in the elements. The inelastic energy represents the energy dissipated by inelastic deformation of the elements. It is expected to be a monotonically increasing in time and may be non-zero under gravity loads only. The work done by the applied loads represents work done by applied nodal loads, work done by axial loads on the columns due to the P-delta effect, and work done by the aforementioned initial element forces. At time zero one would expect this work to be equal to the sum of the elastic and inelastic energy at time zero, but thereafter this work may be increasing or decreasing, and positive or negative. The error energy represents the work done by the unbalanced nodal forces, and is expected to be relatively small.

2.4.2. Possible Cost Functions

The cost function allowed by the frame software is a linear combination of the following six terms:

(1) Volume of design elements;

(2) Sum of squares of maximum story drifts during the moderate earthquake;

(3) Severe earthquake input energy;

(4) Severe earthquake inelastically dissipated energy;

(5) Severe earthquake energy dissipated inelastically by shear link and dissipator elements;

(6) Severe earthquake energy dissipated inelastically by the columns.

The coefficients for each of these terms are set interactively by the user. Terms specified with positive coefficients are minimized, terms specified with negative coefficients are maximized, and terms specified with zero coefficients are ignored.

If one chooses not to minimize volume, then it is wise to have a constraint on volume to keep the problem well posed. The frame software formulates such a constraint according to an interactively supplied value for the maximum volume. The minimization of something other than volume may be viewed as trying to utilize a given amount of material in some optimal way.

Mathematical problems arise when trying to minimize the sum of the squares of the maxima over time of the story drifts by conventional optimization algorithms. These problems stem from the fact that most algorithms require the computation of the gradient of the cost function with respect to the design variables, and the max function is nondifferentiable. To overcome this problem, dummy design variables and constraints are created to shift the nondifferentiable max function from the cost function to constraint functions. This is done because algorithms are available for handling functional max constraints over time. The new formulation is as follows:

minimize

$$\sum_{i=1}^{i=n} X_i$$

subject to

$$\max_{time} D_i^2 < X_i \quad i=1,n$$

where

D_i = story drift for story i

X_i = dummy drift design variable for story i

The choice of cost function is a very complex decision. One might wish to minimize initial construction cost. This may be quantified as the minimization of volume if it is assumed that material and labor costs are roughly proportional to the volume. The minimization of volume or weight is the cost function chosen most often in the literature on optimum structural design. However in real-world situations, the savings of a modest amount of material is not usually an important objective. An structural engineer might wish to design a structure with a given amount of material so as to minimize seismic damage. Non-structural damage during a moderate earthquake may be quantified in terms of the sum of the maxima of the moderate earthquake story drifts since breakage of glass and cracking of walls are roughly functions of the story drift. Likewise, structural damage during a severe earthquake may be quantified in terms of the severe earthquake inelastic energy dissipation. Failure of columns in a severe earthquake usually produces more devastating effects than failure of girders. Thus, an engineer may wish to minimize the energy dissipated inelastically in the columns during a severe earthquake. One may view the role of a structure during an earthquake as dissipating in an acceptable manner the energy imparted to it from ground motion. An optimal way of dissipating this energy may be to maximize the proportion of this energy which is dissipated in "fuses". Such fuses are elements which can locally dissipate large amounts of energy without causing significant damage to the global structure. In the frame software, shear link elements and dissipator elements are classified as fuses. It should be recognized that the amount of energy input from the ground to the structure is a function of the characteristics of both the ground motion and the structure. One may therefore wish to design the structure so as to minimize the input energy during a severe earthquake. Base-isolated structures tend to minimize the amount of input energy imparted to the structure from the ground motion.

2.5. CONSTRAINTS

The frame software defines various constraints on the response of a specified frame under gravity loads only, under combined gravity and moderate earthquake loads, and under combined gravity and severe earthquake loads. There are constraints on both nodal and element quantities. There are both "conventional" and "functional" constraints. Conventional constraints may be represented mathematically as an inequality on a scalar-valued function of the design variables. Functional constraints are represented by an inequality on the maximum of a scalar-valued function over all the time steps. The user may specify certain elements as "no constraint elements" meaning constraints are not formulated for those elements. This may be useful for frames and loadings possessing enough symmetry that constraints on some elements are duplicates of constraints on other elements. Each constraint as formulated by the frame software contains a parameter which may be set interactively to increase or decrease the restriction imposed by the constraint. For the example frame the number of conventional constraints totalled 141 and the number of functional constraints totalled 69.

2.5.1. Constraints Under Gravity Loads Only

Under gravity loads only, the following conventional constraints are placed on the columns, girders, and braces:

$|\text{column axial force}| < \text{Colax} * \text{column axial yield or buckling force}$

$|\text{column end moments}| < \text{Colgra} * \text{column yield moments}$

$|\text{girder end moments}| < \text{Girgra} * \text{girder yield moments}$

$|\text{girder midspan deflection under live load}| < \text{Girdef} * \text{girder span}$

$|\text{brace force}| < \text{Bragra} * \text{brace yield or buckling force}$

For the example frame the values selected for the interactive constants were Colax = 0.5 , Colgra = 0.6 , Girgra = 0.6, and Girdef = 1/240, which are consistent with current design practices.

2.5.2. Constraints Under Combined Gravity And Moderate Earthquake Loads

Under combined gravity and moderate earthquake loads the accepted design philosophy directs that structural damage be resisted. Structural damage is defined in the frame software as element yielding. Thus, the following functional constraints are placed on the element response:

max over time |column end moments| < Colyld * column yield moments

max over time |girder end moments| < Giryld * girder yield moments

max over time |shear element force| < Shryld * shear yield force

max over time |dissipator force| < Disyld * dissipator yield force

max over time |brace force| < Brayld * brace yield or buckling force

For the example frame, the values of the interactive constants Colyld and Giryld were set to unity.

Although non-structural damage is allowed under combined gravity and moderate earthquake loads, it should be limited. One form of non-structural damage is the cracking of glass and any walls, which is strongly related to the amount of interstory drift. Another form of non-structural damage is the falling and tipping over of equipment, which is strongly related to the amount of floor acceleration. Thus, the following functional constraints are placed on nodal response:

max over time |story drift| < Drift

max over time |absolute floor acceleration| < Accel * acceleration of gravity

For the example frame, the interactive drift parameter, Drift, was set to 1/200. The interactive acceleration parameter, Accel, was set to 1/2 which corresponds to the uniform floor acceleration required to initiate the tipping of an unsecured bookshelf twice as tall as it is wide.

2.5.3. Constraints Under Combined Gravity And Severe Earthquake Loads

Under combined gravity and severe earthquake loads the structure should resist collapse. Any collapse of the frame may be detected by large displacements at the top of the frame. The following functional constraint is therefore placed on the frame sway which is the relative horizontal displacement at the top of the frame divided by the total frame height:

$\text{max over time } |\text{structure sway}| < \text{Sway}$

For the example frame, the interactive sway parameter, Sway, was set to 1/100.

Under combined gravity and severe earthquake loads structural damage is allowable, but it should be limited. This may be interpreted as placing a limit on the amount of yielding. Traditionally the limit on element yielding has been defined in terms of the "ductility factor" or the ratio of maximum displacement to yield displacement. This scheme, however, neglects the fact that many cycles at lower ductilities can be just as critical as a single large excursion into the higher ductility range. In order to account for "low-cycle fatigue" failures, the frame software puts a constraint on the inelastic energy dissipation rather than on the ductility allowed in an element. For a given allowable ductility under monotonic loading on an elasto-plastic element, the corresponding constraint on its inelastic energy dissipation is:

$$E_d < E_y\,(mu-1)\,(1-S)\,(2+S\,(mu-1))$$

where

E_d = inelastic energy dissipation

E_y = elastic strain energy at yield

μ = allowable ductility for monotonic loading

S = strain hardening ratio

The equivalent number of cycles at a given ductility for uneven cyclic deformation may be defined in terms of energy as indicated in Figure 10. The energy constraint curve on a plot of equivalent cycles vs. ductility (as shown in Figure 10) reveals that the allowable number of cycles is inversely proportional to the allowable ductility. Experimental results show that cyclic failure criteria have similar form [20].

The frame software places the following conventional constraints on the element inelastic energy dissipation:

column end inelastic energy dissipation < f(Colduc) * yield strain energy

girder end inelastic energy dissipation < f(Girduc) * yield strain energy

shear element inelastic energy dissipation < f(Shrduc) * yield strain energy

dissipator inelastic energy dissipation < f(Disduc) * yield strain energy

brace inelastic energy dissipation < f(Braduc) * yield strain energy

The yield strain energy of each end for the columns and girders was taken to be half the element yield strain energy when loaded in pure shear (ML/6EI). Multiplying the yield strain energy by the function f as in the above inequalities gives the energy dissipated under monotonic loading up to the allowable ductility. For the example frame the values of the interactive allowable monotonic ductility factors Colduc and Girduc were set to 3 and 6, respectively.

For the rubber bearing elements, excessive damage was defined to occur if a tensile bearing stress occurred at any point on the bottom cross-section of the element. This condition can be expressed as a functional constraint on the end moment as follows:

max over time |bearing end moment|

< Berten * edge length * axial force / 6

Here the factor Berten is an interactive factor.

3. COMPUTATION OF A DESIGN FOR THE EXAMPLE FRAME

The computation of a design for the example frame was done in two parts. First, a rational preliminary design was generated. The ground motion to be used in the final design process was chosen as the most destructive motion for the preliminary design. Second, final designs were obtained from the preliminary design by formal optimization procedures. One should try to obtain a preliminary design which will be as close as possible to the final design or else the possibility of another ground motion becoming the critical motion increases. It is also important to obtain a good preliminary design because final design iterations are costly. A feasible directions algorithm [21] was used for final design optimization. This algorithm has the desirable property that once a design satisfying all constraints is produced, successive iterations generate designs which also satisfy all constraints and which have monotonically decreasing costs. Thus, every iteration is guaranteed to generate a superior design. The computational expense limited the number of final design iterations that were performed. The resulting designs should be viewed as "improved" designs rather than "optimal" designs. The results from the preliminary design are presented in Subsection 3.1, and the results from final design are presented in Subsection 3.2.

3.1. PRELIMINARY DESIGN

A preliminary design for the example frame was generated from an iterative procedure which closely follows the design procedure suggested by Bertero and Kamil [22]. The method employs equivalent static seismic forces for the severe earthquake which are derived from "inelastic design spectra" constructed in a manner similar to that suggested by Newmark and Hall [23]. The girders are then designed so as to prevent formation of a collapse mechanism at each story under the design loads, and the columns are designed by using a strong-column weak-girder philosophy. The advantage of using a collapse mechanism based design philosophy for the design of the girders is that plastic design is governed by the equations of equilibrium, which are linear. The resulting linear programming problem can be solved in a finite number of iterations. An iterative scheme was used for preliminary design of the example frame. More detail on the derivation of the inelastic design spectra, the girder and column design, the iterative scheme, and the results of the preliminary design will be presented in this subsection.

3.1.1. Inelastic Design Spectra

As mentioned in Subsection 2.1 of this report, response spectra were obtained for six ground acceleration records at the assumed damping ratio of 2%. These spectra are depicted in Figure 4. From these spectra the maximum envelope spectrum was constructed and then idealized by straight lines on a tripartite plot. The result is a design spectrum for linear elastic structures with 2% damping. The maximum envelope spectrum and the elastic design spectrum are shown in Figure 11.

In order to transform the elastic design spectrum to inelastic design spectra a value for the story ductility is needed. As shown in Figure 12 if one allows no ductility in the columns and assumes a ductility capacity for girder end rotation, the story ductility can be computed to be the following:

$$\mu_s = 1 + \frac{\mu_g - 1}{1 + \frac{R_i}{R_l}}$$

where

μ_s = story ductility

μ_g = assumed girder end rotation ductility

R_i = ratio of girder to column moment of inertia

R_l = ratio of girder to column length

For the example frame, the girder end ductility was taken as 6, the ratio of girder moment of inertia to column moment of inertia was taken as 1, and the ratio of girder length to column length was taken as 2. Thus, the approximate story ductility was computed to be 4.33.

For an elasto-perfectly plastic system the design spectrum for displacement and the design spectrum for force in a ductile structure should differ by a ratio equal to the story ductility. For flexible structures the inelastic design spectrum for displacement would be roughly equal to the elastic design spectrum; and for rigid structures the inelastic design spectrum for force would be equal to the elastic design spectrum. From these assumptions inelastic design spectra for force and displacement at a story ductility of 4.33 are constructed from the elastic design spectrum and depicted in Figure 11.

3.1.2. Girder And Column Design

The required girder plastic moment capacities for each story were computed by a linear programming scheme. For each story there are two design variables which are the plastic moment capacities for the girders on top and the girders on bottom. It was assumed that half the plastic moment capacity and half the gravity uniform load for each girder applied to the story under consideration while the other half applied to the adjacent story. In the case of the top story, all rather than half, of the plastic moment capacity and gravity uniform load was used for the top girders. In the case of the bottom story the uniform load for the bottom girders was taken as zero. Under the equivalent static seismic story shear force and the gravity uniform loads, eighteen non-redundant collapse mechanisms are possible for each story, as shown in Figure 13. Thus, eighteen linear constraints are placed on the two design variables together with the linear constraint that the plastic moment capacity for the girders on the bottom of the story must be greater than the plastic moment capacities for the girders on the top of the story. The cost function used was to minimize weight. If it is assumed that an increase in cross-sectional area of an element yields an increase in its plastic moment capacity and vice-versa, then the weight of an element could be minimized by minimizing the product of its length and its plastic moment capacity. With the linear cost and constraint functions available, the linear program is solved for each story for the plastic moment capacities of the girders.

The plastic moment capacities for the columns were selected by requiring that the sum of the actual plastic moment capacities of the columns was greater than 1.2 times the sum of the girder plastic moment capacities at each joint. This restriction is made to insure a strong-column weak-girder design. The "actual" plastic moment capacities for the columns include reductions due to the interaction of gravity axial forces according to the interaction diagram shown in Figure 9. There is also a constraint that the moment capacity of any column must be greater than the moment capacity of the column above it. The minimum plastic moment capacities were then chosen to satisfy all these constraints.

3.1.3. Iterative Preliminary Design Program

An iterative design program was written for the preliminary design of the example frame. This program applies only to the example frame. It is written in the Rattle language of the DELIGHT.STRUCT package [10], and is listed in Appendix 1. First a subprogram is called, which computes the mass at each of the four stories, the factored uniform loads at each story, and the axial forces due to factored gravity loads in each column. Next, initial values of the moments of inertia for the eight design variables in the example frame are specified by the user. Then the main iteration loop is begun generating new values for the eight moments of inertia until the maximum change in any moment of inertia is less than 1 in^4.

For each iteration in the main loop seven subprograms are called for carrying out the following tasks:

(1) The 20 by 20 stiffness matrix for the frame is assembled from the 4 by 4 element stiffness matrices of the 16 columns and the 12 girders.

(2) Since the mass matrix is only a 4 by 4 diagonal matrix, a condensation is performed on the general eigenproblem equations. Then, the general eigenproblem is transformed to the standard eigenproblem by pre- and post-multiplying the resulting 4 by 4 stiffness matrix by the squareroot matrix of the inverse of the mass matrix. The standard eigenproblem is then solved and the four natural periods and mode shapes of the frame are computed.

(3) The pseudo-accelerations for the four periods are computed from the inelastic force design spectrum, and the pseudo-displacements for the four periods are computed from the inelastic displacement design spectrum.

(4) The maximum shears and drifts at each story for each mode are computed from the pseudo-accelerations and pseudo-displacements respectively. The maximum shears and drifts are then computed from the modal maxima by the squareroot of the sum of the squares (SRSS) method. Finally, the equivalent static story shears are computed by adding to the maximum shears the P-Delta effect due to the maximum drifts.

(5) With the equivalent static seismic story shears and gravity uniform loads available, the linear program is solved for each story to yield the required plastic moment capacities of the girders.

(6) The plastic moment capacities for the columns are computed from the plastic moment capacities of the girders by applying the strong-column weak-girder philosophy as described previously.

(7) The new moments of inertia for the 8 design variables are derived from their respective plastic moment capacities by solving the nonlinear section property relationships given in Subsection 2.3 by a Newton-Raphson scheme.

3.1.4. Results Of The Preliminary Design

The design given by Pique and Roesset [11] was taken as the starting design for the iterative preliminary design program. After 8 iterations an improved preliminary design was reached. The moments of inertia, natural periods, pseudo-accelerations, equivalent static seismic story shears, and plastic moment capacities for the starting and preliminary design are tabulated in Figure 14. The collapse mechanisms for the starting and preliminary designs are shown in Figure 15.

Note that the preliminary design is quite different from the starting design which was made according to the Uniform Building Code. The moments of inertia for the interior columns were approximately doubled during the preliminary design process while the moments of inertia for the exterior columns did not change dramatically. The moments of inertia for the lower girders were increased while the moments of inertia for the upper girders were decreased. Reasons for the dramatic change between the "code" design and the preliminary design may be attributed to the fact that the design earthquake forces used in the preliminary design are higher than those prescribed by the code. Furthermore, the simplifying approximations used in the code design are sure to be a major factor in the difference.

3.2. FINAL DESIGNS

After a satisfactory preliminary design was obtained for the example frame, it was used as the starting design for a formal optimization procedure based on the criteria described in Section 2. The first task was to obtain a "feasible" design or a design which satisfied all the constraints. Minimum volume was chosen as the cost function during the process of obtaining a feasible design in order to keep the problem well-posed. From the feasible design, effort was made to decrease severe earthquake structural damage by minimizing the inelastic energy dissipation during the severe earthquake. Five iterations were carried out with this cost function. It was then decided to diminish moderate earthquake non-structural damage by minimizing the sum of the maxima of the moderate earthquake story drifts. Six further iterations were made with this cost function. Finally these three final designs, i.e. the feasible design, the minimum dissipated energy design, and the minimum story drift design, were analyzed under all six ground motion records. The three final designs are depicted and compared in Figure 16.

3.2.1. Feasible Design

The preliminary design was analyzed under the six ground motions described in Subsection 2.1. From these analyses constraints were evaluated and the percentages of the allowables for all the constraints under each motion are tabulated in Appendix 2. Based on this evaluation the motion E6 was considered to be the most destructive to the preliminary design and was thus chosen as the design ground motion, as previously mentioned. Note that under severe earthquake motions, the ends of nearly all the girders and the bases of the bottom story columns undergo yielding. This is a desirable mechanism since the burden of energy dissipation is shared among many locations in the structure. The constraints which exhibited the worst violations were constraints on severe earthquake energy dissipation at the bottom nodes of the bottom columns. The end moments of the top girders under gravity and moderate earthquake loading, the third story drift under moderate earthquake loading, and the structure sway under severe earthquake loading were also in violation.

Intervention of the designer led to increasing the sizes of the bottom columns and the top girders before formal optimization began. After six iterations of formal optimization a feasible design satisfying all 141 conventional constraints and all 69 functional constraints was found. The iteration histories of the maximum value over all the constraint functions, the structural volume, and the values of the design variables are plotted in Figure 17. Note the large decrease in constraint violation in the first iteration, and the slow decrease in later iterations. This is typical of the performance of many optimization algorithms. Note also that the volume of the structure remained nearly constant for all iterations. Thus the feasible design was not contructed by simply increasing the strengths of all the members, but rather by re-distributing the strength of the structure among the members.

The constraints which are greater than 90% of allowable for the feasible design include the following:

First story girder end moments under gravity loads only (96%).

Second story girder end moments under gravity loads only (99%).

Third story girder end moments under gravity loads only (94%).

Fourth story girder end moments under gravity loads only (95%).

First story girder end moments under moderate earthquake loads (95%).

Second story girder end moments under moderate earthquake loads (100%).

Third story drift under moderate earthquake loads (93%).

First story interior column energy dissipation under severe earthquake loads (96%).

Second story girder energy dissipation under severe earthquake loads (97%).

Structure sway under severe earthquake loads (99%).

The fact that there is a number of these "active" constraints suggests that this feasible design is probably a good design if one subscribes to the notion that an optimal design is a "fully stressed" design.

The process of obtaining a feasible design appears to have modified the preliminary design in two main areas. First, the columns were increased in size, especially the lower interior columns and the upper exterior columns. An increase in the sizes of the lower columns was expected because the ductilities in these columns for the preliminary design were unacceptably high. Increasing the sizes of the upper columns would tend to lessen the third story drift under moderate earthquake loading and the structure sway under severe earthquake loading. The second area of modification occurred in the sizes of the girders. In the preliminary design the sizes of the girders decreased from the bottom story to the top. In the feasible design the girder sizes for the bottom three stories are roughly the same and the girder size for the top girder is slightly less. Thus, the lower girders were decreased in size while the upper girders were increased in size during the feasible design process. This is rational because the constraints under gravity loads only are the controlling constraints for the girders in the feasible design, and the girders on the bottom three stories support the same amount of gravity load, while the top girders support slightly less gravity load.

The feasible design was analyzed under all six ground motion records and the values of the constraint functions were computed. The percentages of allowables for all the constraint functions under each ground motion record are tabulated in Appendix 3. Note that the feasible design is acceptable under ground motions E3 and E5 in addition to the design ground motion E6. Under motion E4 the severe earthquake energy dissipation constraint in a bottom interior column was violated by 3%, and under the motion E1 the moderate earthquake end moment constraints for second story girders were violated by 3%. The motion E2 seems to be the most severe for the feasible design. Under this motion, moderate earthquake end moment constraints for girders in the first two stories were violated by a maximum of 11%. Moderate earthquake story drift constraints in the second and third stories were violated by a maximum of 14%. Severe earthquake energy dissipation constraints in the third story columns were violated by 8%. The worst violation was 32%, which occurred in the constraints on severe earthquake energy dissipation in the second story girders. Under monotonic loading a violation of this much would give a girder rotation ductility of 7.4 rather than the allowable of 6. This is still probably acceptable if attention is placed on detailing. Thus, it appears that the feasible design is an acceptable design for all the ground motions.

3.2.2. Minimum Dissipated Energy Design

The minimization of severe earthquake inelastically dissipated energy was used as the cost function for five iterations starting from the feasible design. The histories of the cost function, cumulative cpu-time, and values for the design variables vs. the five iterations are plotted in Figure 18. Note that the reduction from the feasible design in inelastic energy dissipation was about 14%. There was also a drop of 15% in sum of maxima of moderate earthquake story drifts, and a small drop of 0.1% in volume. Each iteration of the optimization process required about 28 analyses. There was an average of about 700 time steps per analysis meaning there were many dynamic analyses for the full time period which requires 1101 time steps. Furthermore there was an average of about 0.91 reformulations of the stiffness matrix per time step meaning many of the analyses were nonlinear. The fact that many nonlinear dynamic analyses were required is plausible since these analyses were needed to evaluate of the cost function.

Fewer constraints were active for the minimum dissipated energy design than for the feasible design. In particular none of the constraints on severe earthquake dissipated energy were active ---- a reasonable result since this quantity was minimized. Active constraints included the following:

First story girder end moments under gravity loads only (99%).

Second story girder end moments under gravity loads only (99%).

Third story girder end moments under gravity loads only (94%).

First story girder end moments under moderate earthquake loads (94%).

Second story girder end moments under moderate earthquake loads (94%).

Structure sway under severe earthquake loads (100%).

When the severe earthquake inelastic energy dissipation was minimized, the first unanticipated result was the slight decrease in the volume of the structure. Originally it was expected that decreasing the dissipated energy in a yielding structure would require increasing the sizes of the elements to make them stronger and thus yield less. However, a larger element may have a lower amplitude of yield deformation, but it also has more material with which to dissipate energy. Therefore, the slight decrease in volume is plausible. Perhaps a cost function which minimized the dissipated energy divided by the volume of the structure would have quantified severe earthquake damage in a better way.

A second interesting result is depicted in Figure 19 which shows the time histories of energy dissipation in various parts of the structure for the feasible and the minimum dissipated energy designs. In both designs approximately 85% of the dissipated energy was dissipated in the girders. Note, however, that in the minimum dissipated energy design the upper stories dissipated about 16% of the dissipated energy while in the feasible design the upper stories dissipated only 8%. Thus, in this case minimizing the dissipated energy tended to balance the dissipated energy distribution in the structure.

A third interesting result concerns the fifth iteration. In this iteration there was a substantial reduction in energy dissipation, and correspondingly there was an unexpected drop in the size of the upper interior columns and an increase in the size of the top story girders. Upon checking the values of the gradients of the cost and active constraint functions for the fifth iteration, it was discovered that the decrease in the size of the upper interior columns causes a decrease in the dissipated energy, and the increase in the size of the top story girders causes a decrease in the severe earthquake structure sway constraint. These are examples of how the results of a complex constrained optimization problem involving constraints on nonlinear dynamic response are difficult to anticipate before computation.

The minimum dissipated energy design was then analyzed under all six available ground motion records and the percentages of the allowables for the contraints under each record are tabulated in Appendix 4. The design was acceptable for records E3 and E4 in addition to the design record E6. Under record E5 all constraints are satisfied except the structure sway constraint, which was violated by only 5%. Records E1 and E2 appear to produce the greatest response in this design. Although the constraints on moderate earthquake girder end moments were violated by less than 10%, and the constraint on moderate earthquake third story drift was violated by 15%, the energy dissipated by the third story interior columns under severe earthquake loading violates the contraint by up to 139%. A violation by this much under monotonic loading would give a rotation ductility of 5.3 in these columns rather than the allowable of 3. This is probably unacceptable, and the sizes of the upper story interior columns should be increased.

3.2.3. Minimum Drift Design

Since the minimum dissipated energy design had a lower sum of maxima of moderate earthquake story drifts than the feasible design, it was used as the starting design for the minimization of story drift. Six iterations were carried out and the corresponding iteration histories are plotted in Figure 20. The first thing to note is that there was not much change in the cost nor in the design variables. The sum of the maxima of the moderate earthquake story drifts was decreased by a mere 3%. There was also a drop of 2% in severe earthquake dissipated energy and a small drop of 0.3% in volume. An average of 24 analyses was needed per iteration. Each analysis required an average of 414 time steps, which is significantly lower than for the minimum dissipated energy design. Furthermore, there was an average of only 0.54 reformulations of the stiffness matrix per time step, which is about half the number required by the minimum dissipated energy design. Since computation of the cost function does not require full nonlinear dynamic analysis, one would expect less computational effort per iteration. However, although the computational effort per iteration is low for this choice of cost function, the change per iteration in the cost and in the design is also low.

The main change in the minimum drift design from the minimum dissipated energy design is that the third story girder was decreased in size. The girders of the minimum story drift design have nearly the same size. This is a result of the gravity load end moment constraints, which are active in the minimum story drift design. Other active constraints include moderate earthquake end moment constraints on first and second story girders and the constraint on severe earthquake structure sway. Thus the same constraints are active for the minimum story drifts and minimum dissipated energy designs.

Again, one would have expected that a minimization of story drift would have given an increase in volume rather than the decrease that was realized. The reason for the decrease in volume may be explained from the plots of story drift for the minimum story drift and feasible designs as shown in Figure 21. Note that in each story the minimum story drift design exhibits slightly less drift. Note also that the period of the minimum story drifts design is slightly longer than the period of the feasible design. One must therefore conclude that frequency content of the particular design ground motion E6 tends to drive the stiffer feasible design to greater response. This conclusion can be made since the structural response to the moderate earthquake is in the linear elastic range.

The minimum story drift design was analyzed under all six ground motions and the percentages of the allowables for all constraints under each motion are tabulated in Appendix 5. This design was acceptable for motions E3 and E4 in addition to the design motion E6. The only constraint not satisfied under motion E5 was the severe earthquake structure sway constraint, which was violated by only 5%. Under motions El and E2 moderate earthquake end moment constraints were violated in the girders by less than 10%, and the moderate earthquake third story drift constraint was violated by 18%. These results are similar to those for the minimum dissipated energy design. However, the constraint on severe earthquake energy dissipation in the third story interior columns under motions El and E2 was violated by a maximum of 104%, which is less than the 139% violation exhibited by the minimum dissipated energy design. If the loading were monotonic, this 104% violation in energy dissipation constraint would correspond to a column rotation ductility of 4.9 rather than the allowable of 3. This may be unacceptable. Thus, the minimum story drift design appears to be a little less sensitive to change in ground motion than the minimum dissipated energy design; however, it is more sensitive than the feasible design.

4. CONCLUSIONS

Conclusions are now stated in three areas. The practicality of the proposed design method is examined in Subsection 4.1. The reliability of the method is assessed in Subsection 4.2. Finally some generalizations regarding low-rise steel frames, such as the example frame, are drawn in Subsection 4.3.

4.1. PRACTICALITY OF THE PROPOSED DESIGN METHOD

A major consideration of the optimization method developed and used in this study is the amount of computational effort that has been involved. Computation was done on a VAX 11/780 mini-computer. For the minimum dissipated energy design an average of 4.3 hours of cpu-time was required per iteration, for the minimum story drift design 2.1 hours of cpu-time were required per iteration, and for the feasible design the figure was somewhere in between. For an engineering firm that owned an equivalent mini-computer, the cost for computing is minimal. The amount of time it takes for computation becomes a critical factor because it affects the scheduling of the design project itself.

The final design process should be viewed as a refinement process on the preliminary design. One should not expect to carry out a final design to some surprisingly different optimal design. The importance of obtaining a reasonably good preliminary design cannot be overemphasized, since they minimize the number of final design iterations needed. In the case of the example frame, a good preliminary design was obtained by solving a simplier optimization problem. Consequently, a very practical design was produced after only one iteration of final design. The first iteration design was very close to the final feasible design which performed quite well under the different ground motions. However, in general more iterations of final design would be required.

The computation process used a more or less "brute force" method. Many inefficiencies are involved and are described in the companion report [10] in more detail. The computational effort could be reduced by more than an order of magnitude if the more efficient schemes suggested in that report were utilized. These schemes must be incorporated before the method can be applied to the design of frames which are significantly larger than the example frame.

Obviously the proposed method involves more computation than conventional design methods. However, this does not necessarily imply an increase in the amount of real time invested in the design process. The computations in the proposed method are performed by the computer 24 hours a day, while many of the computations required by conventional methods are performed slowly and expensively by hand during "prime" time.

4.2. RELIABILITY OF THE PROPOSED DESIGN METHOD

The proposed method is one of the first seismic-resistant design methods which actually uses nonlinear dynamic analysis in the design process itself, rather than just using such an analysis to check the final design. This method should have greater reliability over state-of-the-art design methods because the cyclic, dynamic, nonlinear behavior exhibited by seismically-excited frames is accounted for in an improved fashion. However, it should be recognized that further improvement could be made in the modelling of the nonlinear behavior of beams and columns. The frame software modelled beams and columns with single lumped-plasticity beam-column elements as available in the ANSR simulation package. Such models are computationally inexpensive and therefore, popular. However, significant errors may be introduced by the approximations involved.

The method should also possess greater reliability because it quantifies accepted design philosophy more directly. Descriptions of moderate and severe ground motion were derived from accelerograms corresponding to actual earthquakes. Constraint functions were constructed to reflect structural damage and excessive non-structural damage in the case of moderate ground motion, and collapse and excessive structural damage in the case of severe ground motion.

A complex mathematical programming problem is generated by the proposed method. In the case of the example frame the problem involved over 200 constraints, most of which were extremely complicated functions of the design variables. This complexity was the reason that a sophisticated optimization algorithm was employed to manage the final design process. Note that a feasible design for the example frame was produced without a noticable increase in the volume of material. An engineer faced with an infeasible design would be tempted to resolve the problem by simply increasing the sizes of relevant members. Thus, the way in which information about a design is generated and utilized in the proposed method definitely contributes to its reliability.

An area which needs improvement in the proposed method is the way in which seismic ground motion is incorporated. Indeed, all deterministic design methods could be improved in this area. The record E6 was chosen as the design record for the example frame because it seemed to be the most destructive to the preliminary design. However, as the final designs moved further away from the preliminary design, it became apparent that records E1 and E2 caused more critical responses. Since the final design process incorporated information about the design record E6 only, the designs became more sensitive to different records as final design iterations were carried out. The optimization process seems to seek out some optimal "corner" in design space, and such corners are dependent on the characteristics of the design record. This problem of sensitivity to different ground motions can only be resolved properly if the design method is modified to utilize information about different possible ground motions.

4.3. LOW-RISE STEEL FRAMES

The following generalizations are proposed on the basis of the results obtained for the example frame:

(1) Girder design seems to be controlled by the constraints on their end moments under gravity loads only. An exception is the design of the top story girder, which may be controlled partially by the severe earthquake sway constraint.

(2) Column design seems to be controlled by moderate earthquake story drift constraints, the severe earthquake sway constraint, and severe earthquake energy dissipation constraints in the columns and girders.

(3) Designs produced by the minimization of severe earthquake inelastically dissipated energy seem to distribute the energy dissipation more evenly among the different stories than conventional designs.

(4) The minimization of moderate earthquake story drift is strongly linked to the frequency content of the design ground motion.

From these generalizations it may be possible to propose "simplified" design methods for the design of low-rise steel frames. One such method would advocate that girder design be made on the basis of constraints under gravity loads only with the use of an empirical dynamic amplification factor for sizing the girders in the top stories. Column design seems to be controlled by constraints under dynamic loading, and little simplification in the final design process is recommended. Nevertheless, the simplifying assumption on girder design would have cut the number of design variables, and thus the computational effort, in half for the example frame.

REFERENCES

1. K.S.Pister, "Optimum Design of Structures under Dynamic Loading", Optimization of Distributed Parameter Structures, (Ed. E.J.Haug and J.Cea), Sijthoff and Noordhoff, Alphen aan den Rihn, Netherlands, 1980, pp. 569-585
2. N.M.Newmark and E.Rosenblueth, Fundamentals of Earthquake Engineering, Prentice-Hall, Englewood Cliffs, N.J., 1971
3. R.W.Clough and J.Penzien, Dynamics of Structures, McGraw-Hill, New York, N.Y., 1975
4. R.V.Whitman and C.A.Cornell, "Design", in Seismic Risk and Engineering Decisions, Editted by C.Lomnitz and E.Rosenblueth, page 339, Elsevier, New York, N.Y., 1976
5. Uniform Building Code, International Conference of Building Officials, Whittier, Ca., 1979 Edition
6. ATC-2 Evaluation of a Response Spectrum Approach to Seismic Design, Applied Technology Council, San Francisco, Ca., Sept., 1974
7. J.H.Robinson and J.M.Biggs, "Inelastic Dynamic Design of Steel Frames to Resist Seismic Loads", Report No. R77-23, Dept. of Civil Engineering, MIT, Cambridge, Mass., July, 1977
8. C.J.Montgomery and W.J.Hall, "Studies on the Seismic Design of Low-Rise Steel Buildings", Report No. 442, Dept. of Civil Engineering, Univ. of Ill., Urbana, Ill., July, 1977
9. F.Y.Cheng, D.Srifuengfung, and L.H.Sheng, "ODSEWS-2D Optimum Design of Static, Earthquake, and Wind Steel Structures", Report No. 81-10, Dept. of Civil Engineering, Univ. of Mo., Rolla, Mo., Jan., 1981
10. R.J.Balling, K.S.Pister, and E.Polak, "DELIGHT.STRUCT: A Computer-Aided Design Environment for Structural Engineering", Report No. EERC 81-19, Earthquake Engineering Research Center, Univ. of Cal., Berkeley, Ca., December, 1981

11. J.R.Pique and J.M.Roesset, "On the Use of Simple Models in Nonlinear Dynamic Analysis", Report No. R76-43, Dept. of Civil Engineering, MIT, Cambridge, Mass., Sept., 1976

12. R.F.Nau, R.M.Oliver, and K.S.Pister, "Simulating and Analyzing Artificial Non-Stationary Earthquake Ground Motions", Report No. ORC 80-16, Operations Research Center, Univ. of Ca., Berkeley, Ca., June, 1980

13. "Strong Motion Earthquake Accelerograms, Index Volume", Report No. EERL 76-02, Earthquake Engineering Research Laboratory, Ca. Inst. of Tech., Pasadena, Ca., August, 1976

14. A.G.Brady, V.Perez, and P.N.Mork, "The Imperial Valley Earthquake, October 15, 1979", Open File Report No. 80-703, USGS, Menlo Park, Ca., April, 1980

15. "SPECTR - Spectra Response Analysis Code", National Information Service for Earthquake Engineering, Univ. of Ca., Berkeley, Ca., 1972

16. D.P.Mondkar and G.H.Powell, "ANSR-I General Purpose Program for Analysis of Nonlinear Structural Response", Report No. EERC 75-37, Earthquake Engineering Research Center, Univ. of Ca., Berkeley, Ca., December, 1975

17. A.Riahi, D.G.Row, and G.H.Powell, "Three Dimensional Inelastic Frame Elements for the ANSR-I Program", Report No. EERC 78-06, Earthquake Engineering Research Center, Univ. of Ca., Berkeley, Ca., August, 1978

18. N.D.Walker, "Automated Design of Earthquake Resistant Multistory Steel Building Frames", Report No. EERC 77-12, Earthquake Engineering Research Center, Univ. of Ca., Berkeley, Ca., May, 1977

19. G.V.Berg and S.S.Thomaides, "Energy Consumption by Structures in Strong-Motion Earthquakes", Proceedings of the 2nd World Conference on Earthquake Engineering, vol II, page 681, July, 1960

20. E.P.Popov and V.V.Bertero, "Cyclic Loading of Steel Beams and Connections", ASCE Jour. of the Structural Division, vol 99, no. 6, June,1973

21. G.Gonzaga, E.Polak, and R.Trahan, "An Improved Algorithm for Optimization Problems with Funtional Inequality Constraints", Mem. No. UCB/ERL/A78/56, Electronics Research Laboratory, Univ. of Ca., Berkeley, Ca., Sept., 1977

22. V.V.Bertero and H.Kamil, "Nonlinear Seismic Design of Multistory Frames", Canadian Journal of Civil Engineering, vol 2, no. 4, page 494, 1975

23. N.M.Newmark and W.J.Hall, "Procedures and Criteria for Earthquake-Resistant Design", Building Practice for Disaster Mitigation, Building Science Series 46, National Bureau of Standards, February, 1973

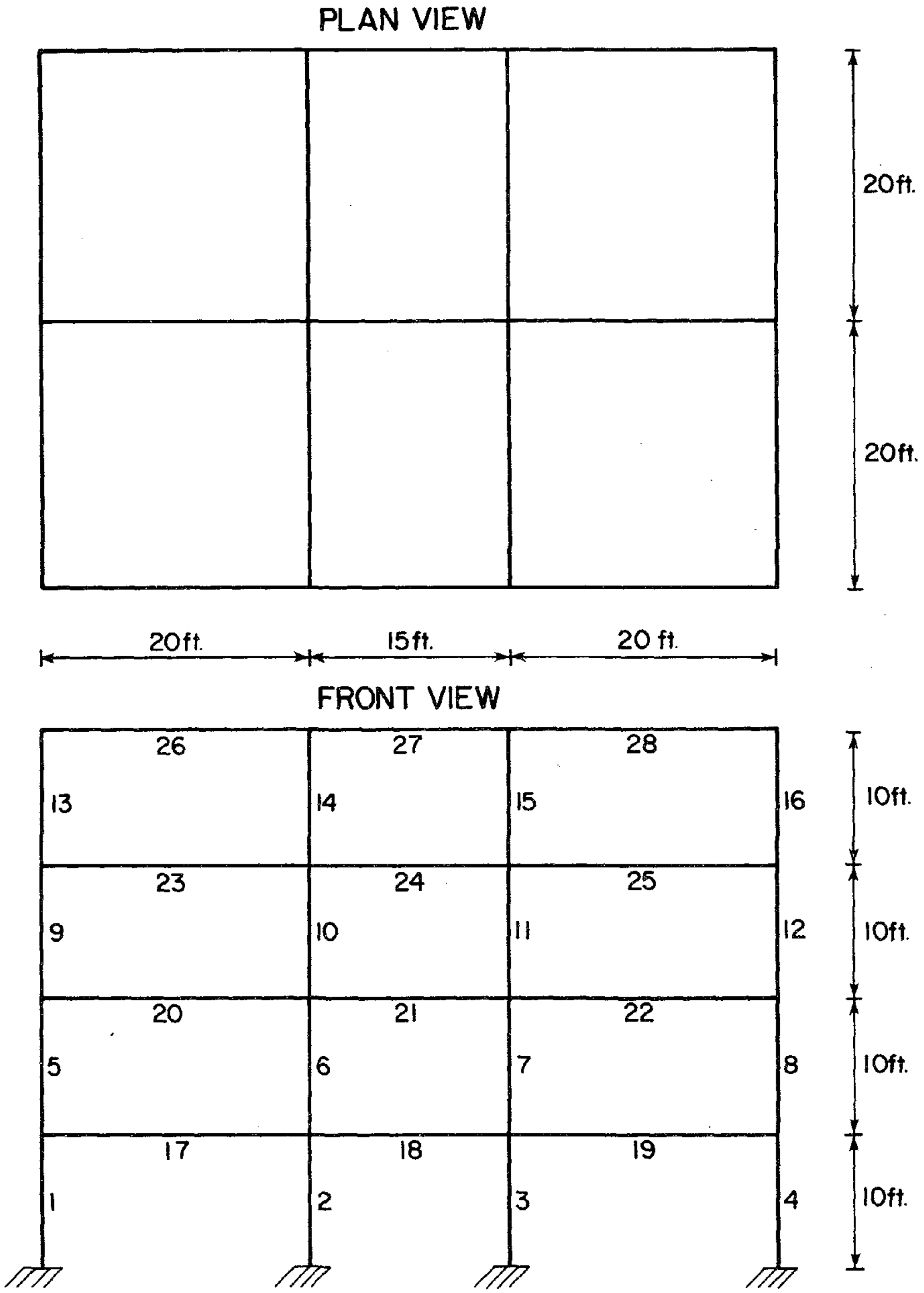

FIGURE 1 : EXAMPLE FRAME DIMENSIONS

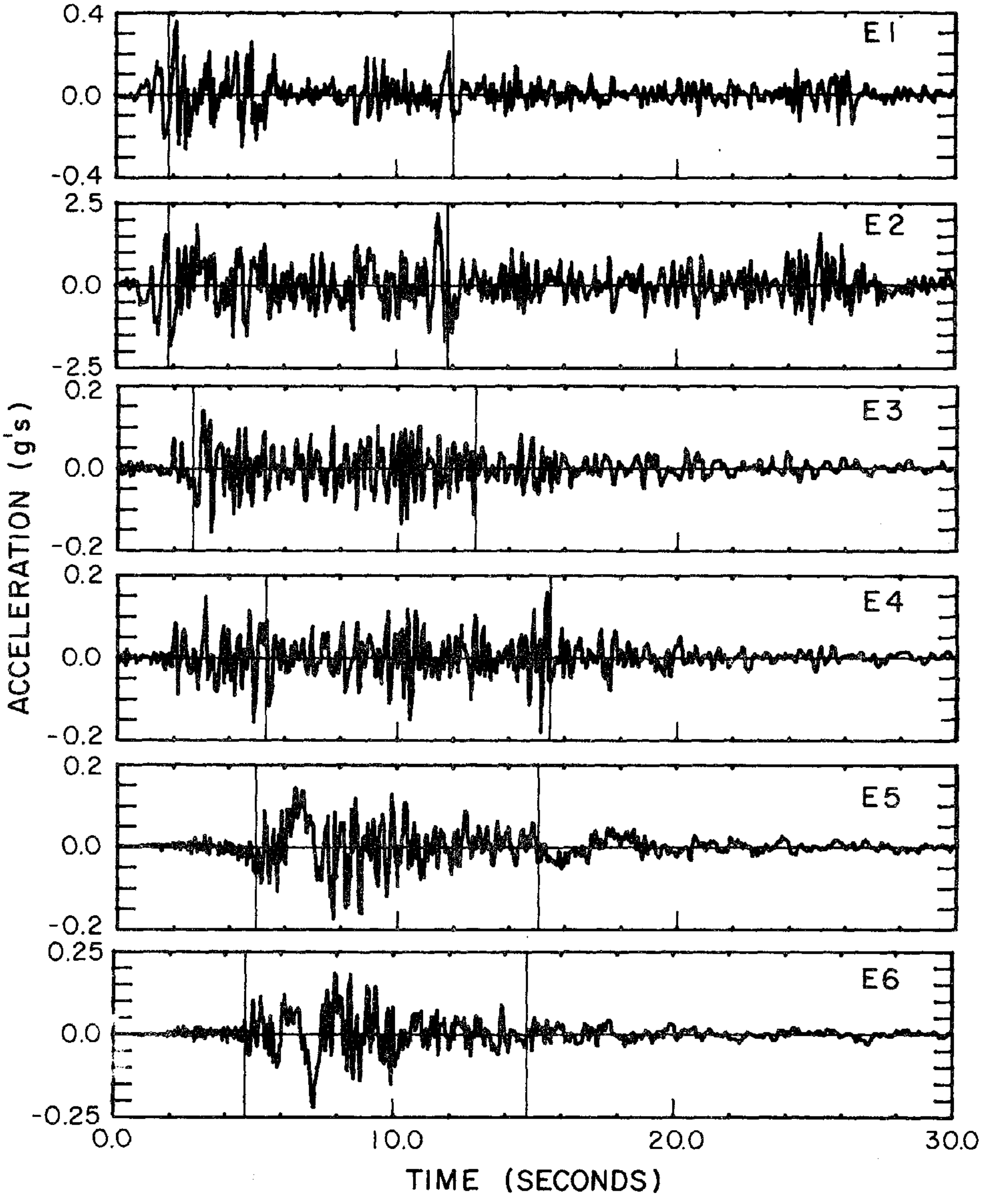

FIGURE 2 : ORIGINAL GROUND MOTION RECORDS
(critical 10-sec. intervals are shown)

RECORD year comp.	PEAK ACCEL (g's)	SPEC INT .1<T<1. (in.)	SCALE FACTOR sev/mod	PK ACCEL (g's) sev/mod	SPEC INT (in.) sev/mod
E1 1940 S00W	0.3463	23.52	1.040 0.3120	0.360 0.108	24.5 7.34
E2 1940 S90W	0.2110	13.85	1.767 0.5301	0.373 0.112	24.5 7.34
E3 1934 S00W	0.1608	10.80	2.266 0.6798	0.364 0.109	24.5 7.34
E4 1934 S90W	0.1821	8.91	2.746 0.8238	0.500 0.150	24.5 7.34
E5 1979 N50E	0.1741	11.30	2.166 0.6498	0.377 0.113	24.5 7.34
E6 1979 N40W	0.2249	12.59	1.944 0.5832	0.437 0.131	24.5 7.34

BEFORE SCALING

AFTER SCALING

FIGURE 3 : GROUND MOTION PROPERTIES

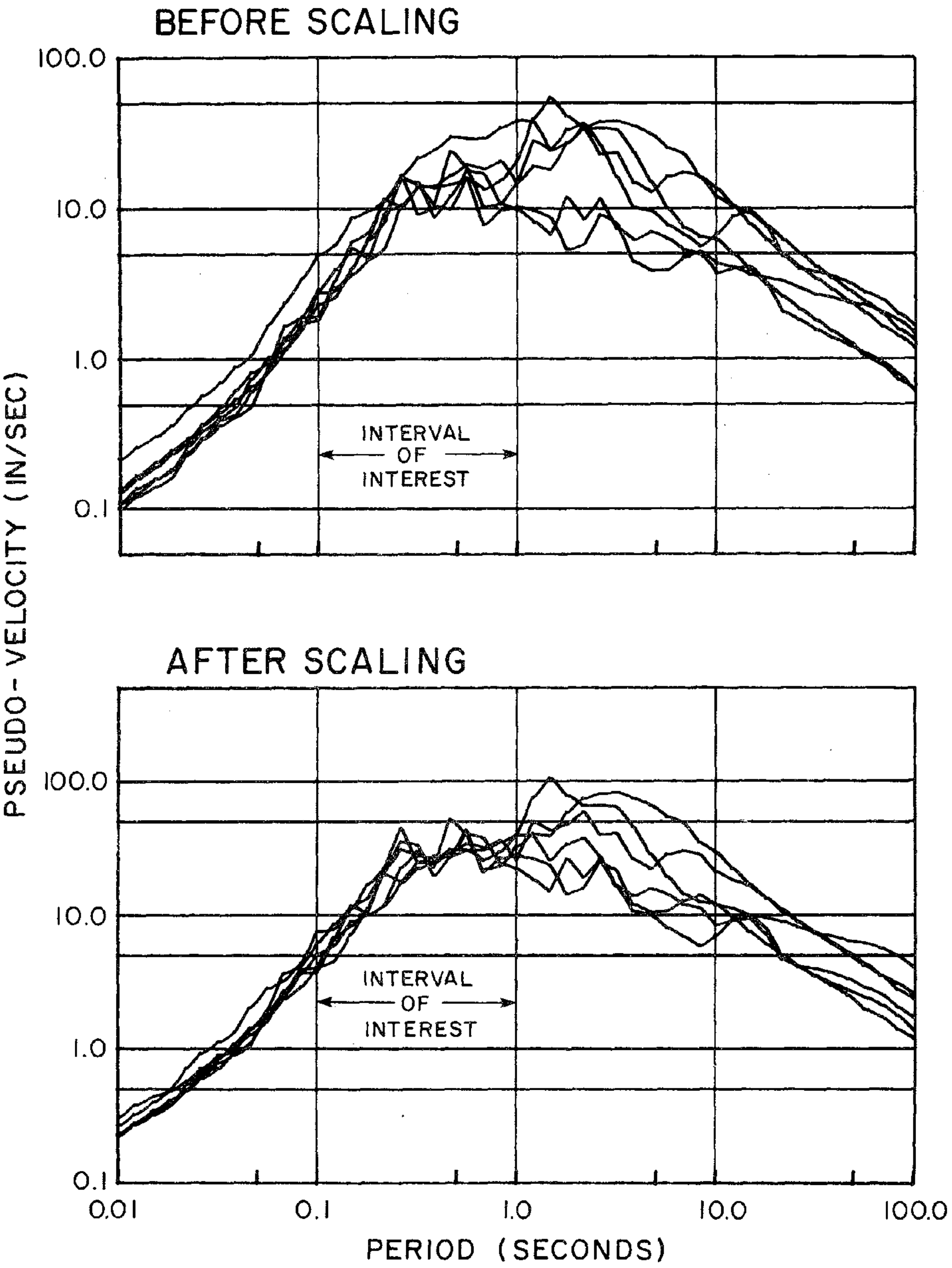

FIGURE 4 : RESPONSE SPECTRA FOR RECORDS

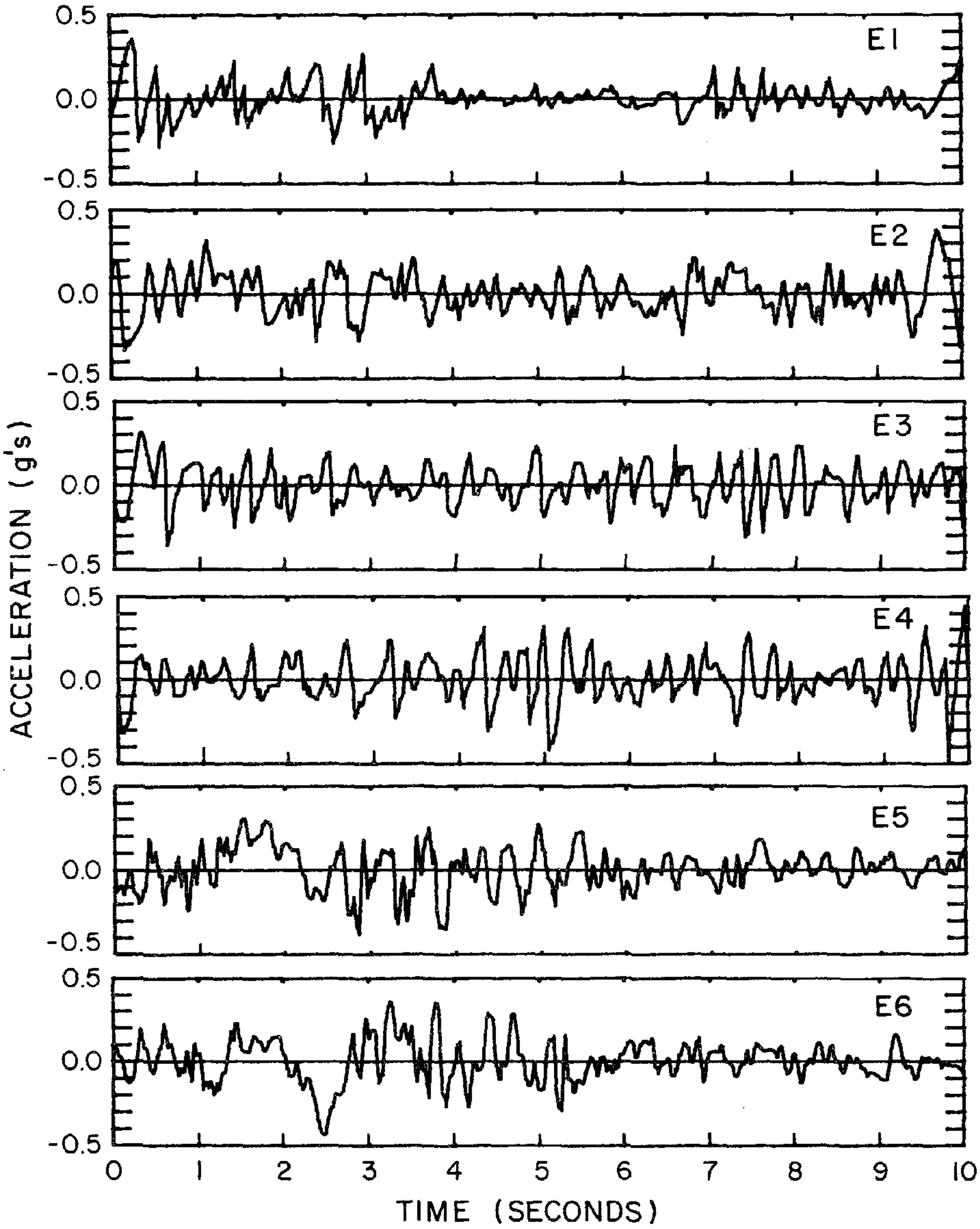

FIGURE 5 : SCALED GROUND MOTION RECORDS

REC NUM	MAX CONST VALUE	pts x 3	COLUMN INELAST ENERGY	pts x 2	QUAKE INPUT ENERGY	pts x 1	TOTAL INELAST ENERGY	pts x 1	SUM OF STORY DRIFTS	pts x 1	TOT PTS
E1	280% allow	12	136.8 kip-in	8	679.4 kip-in	4	450.9 kip-in	4	7.737 x10**-5	5	33
E2	343% allow	15	177.5 kip-in	10	1006. kip-in	6	578.5 kip-in	6	8.554 x10**-5	6	43
E3	190% allow	4.5	13.8 kip-in	2	335.9 kip-in	1	190.1 kip-in	1	6.433 x10**-5	2	10.5
E4	205% allow	9	81.0 kip-in	6	602.7 kip-in	3	293.2 kip-in	3	6.544 x10**-5	3	24
E5	190% allow	4.5	37.1 kip-in	4	406.1 kip-in	2	198.6 kip-in	2	5.759 x10**-5	1	13.5
E6	377% allow	18	179.6 kip-in	12	854.8 kip-in	5	470.4 kip-in	5	7.390 x10**-5	4	44

FIGURE 6 : DESIGN RECORD SELECTION CRITERIA

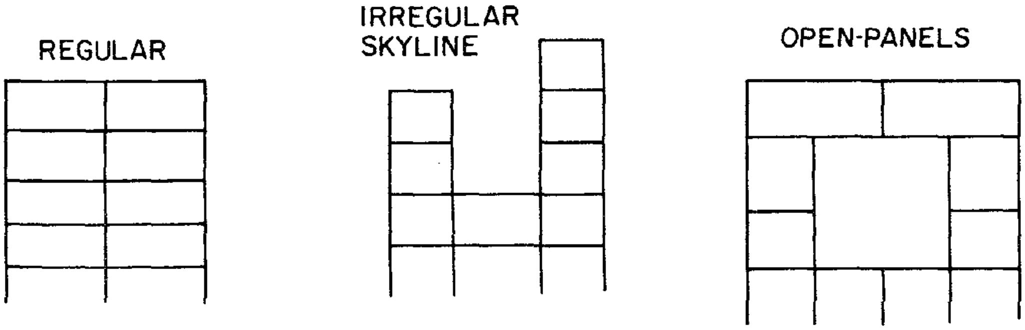

MOMENT-RESISTING FRAMES

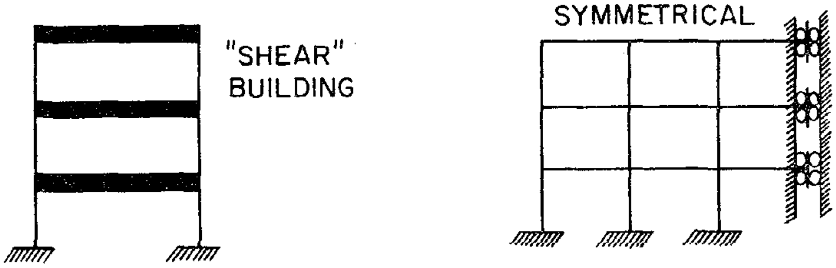

REDUCED-DOF FRAMES

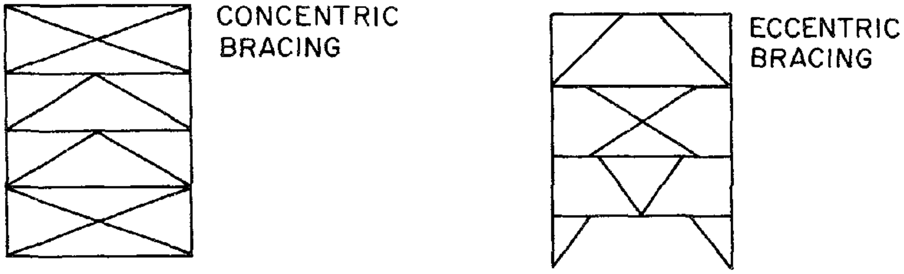

BRACED FRAMES

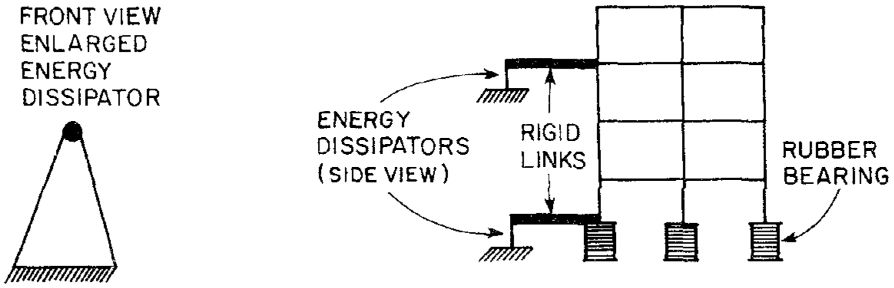

VIBRATION ISOLATED FRAMES

FIGURE 7 : POSSIBLE FRAME GEOMETRIES

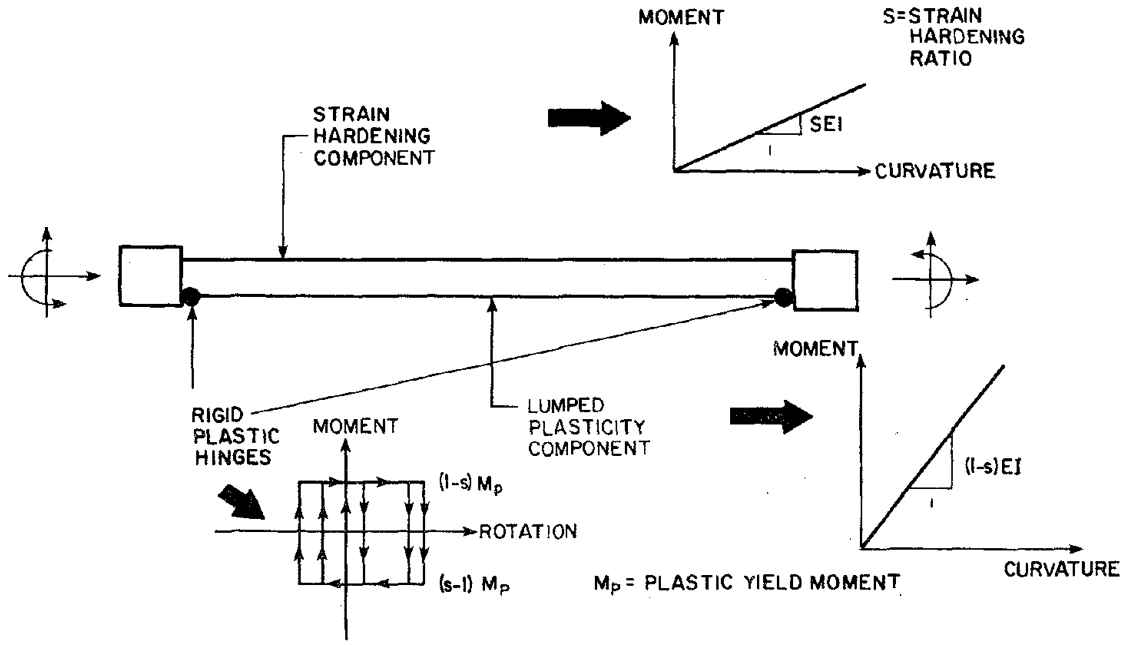

BEAM-COLUMN ELEMENT

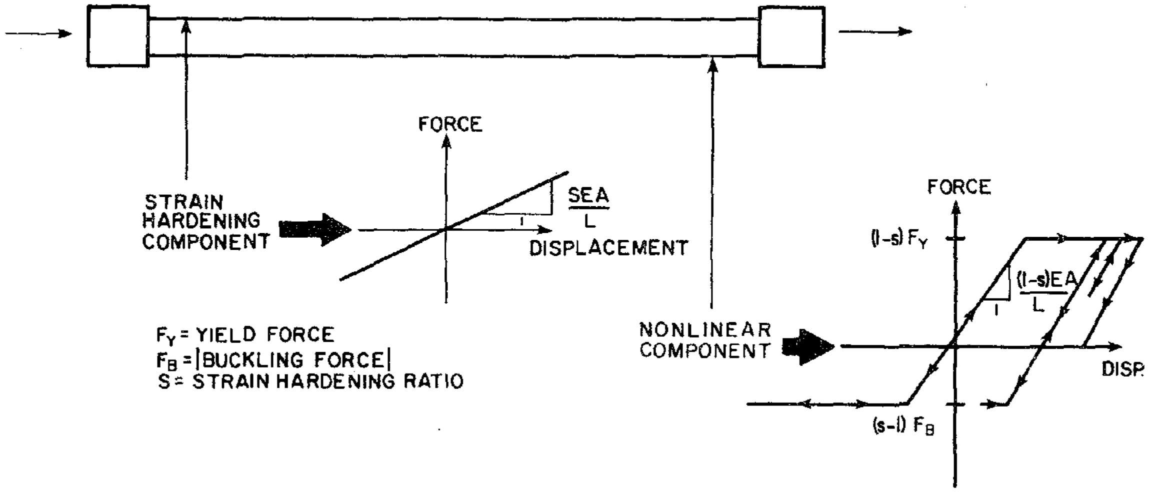

TRUSS ELEMENT

FIGURE 8 : ELEMENT MODELS

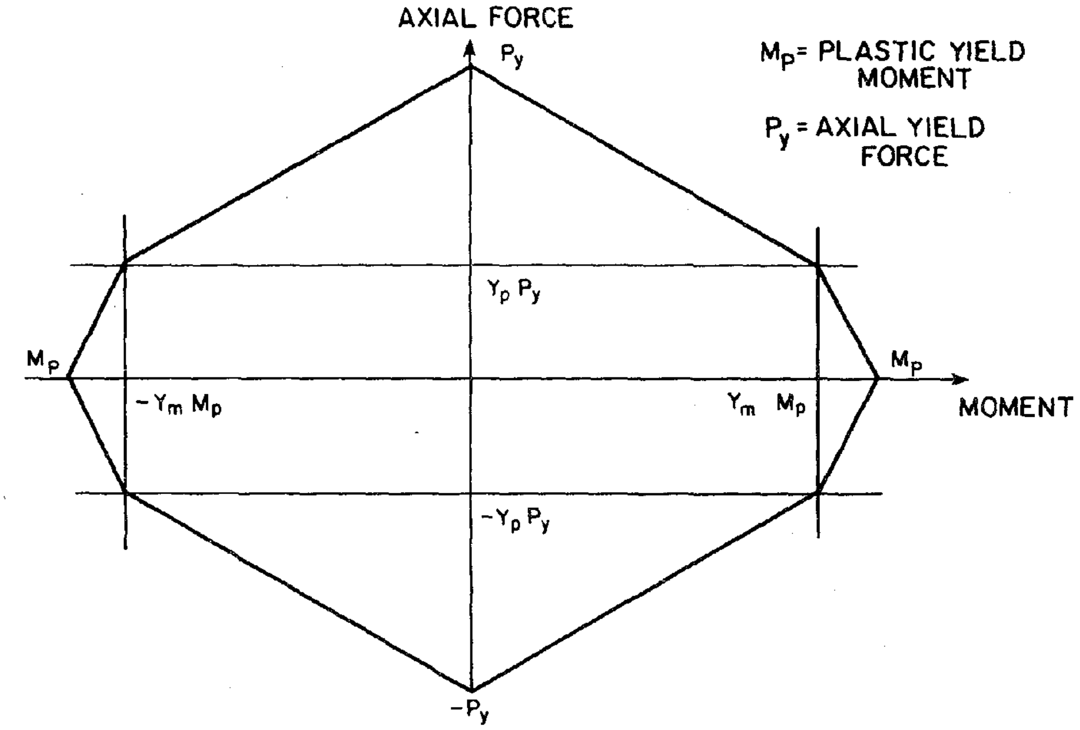

COLUMNS

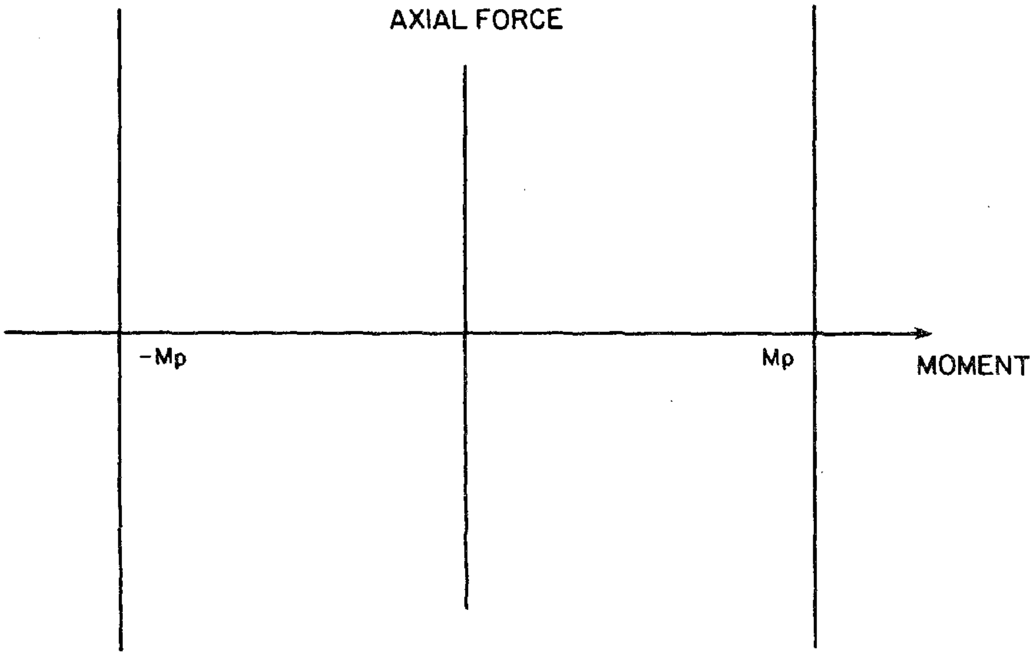

GIRDERS

FIGURE 9 : YIELD INTERACTION DIAGRAMS

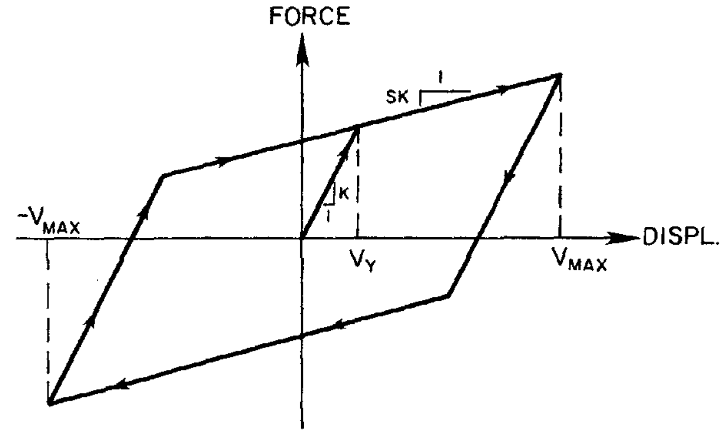

energy dissipated
in one cycle =
8(MU-1)(1-S)Ey
where
MU = Vmax/Vy
Ey = K(Vy**2)/2

$$\text{number of equivalent cycles at a ductility of MU} = \text{Nmu} = \frac{\text{energy dissipated}}{8(MU-1)(1-S)Ey}$$

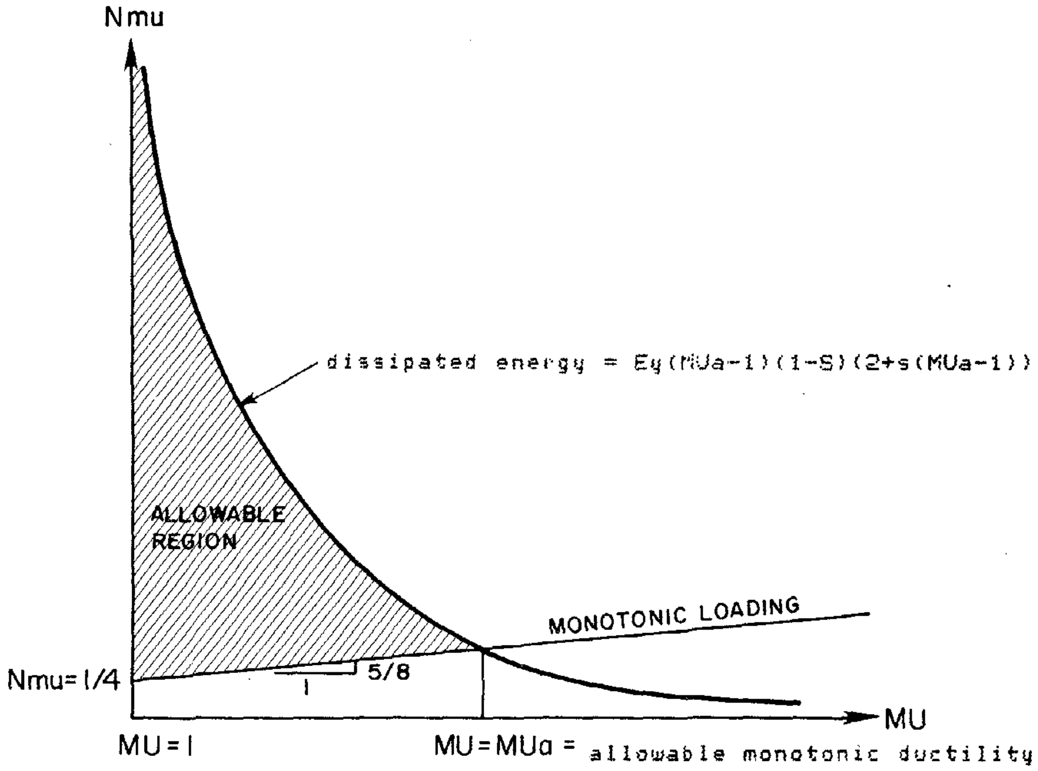

FIGURE 10 : CYCLES VS DUCTILITY

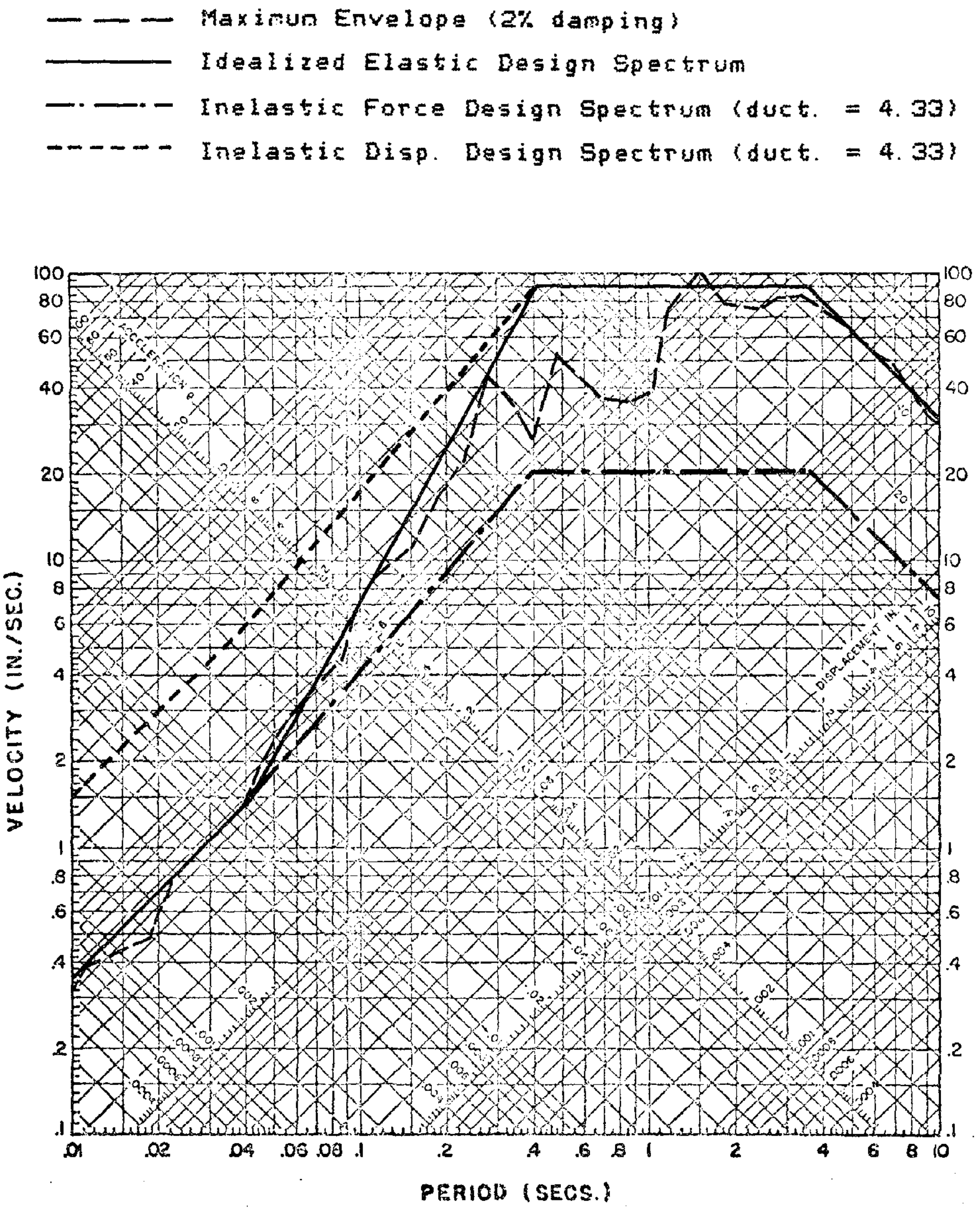

FIGURE 11 : CONSTRUCTION OF DESIGN SPECTRA

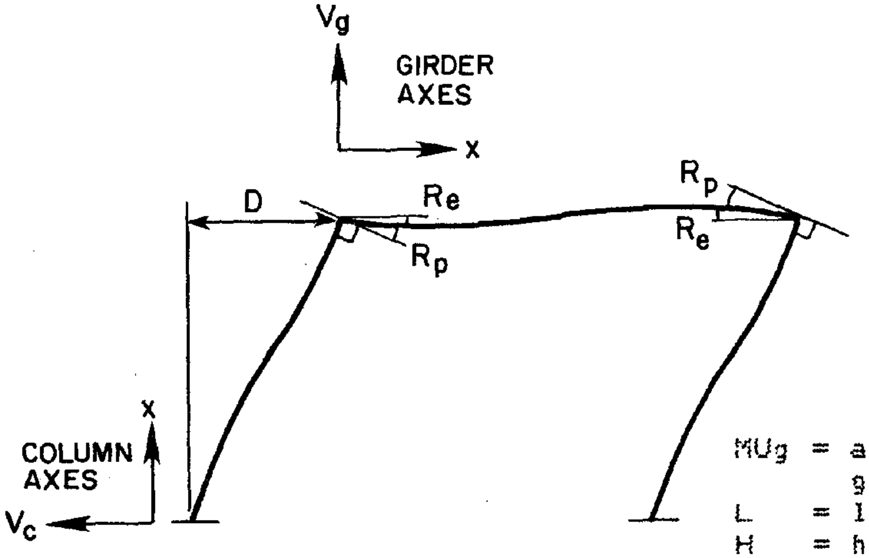

MUg = allowable girder ductility
L = length of girder
H = height of column
Ig = girder moment of inertia
Ic = column moment of inertia
My = yield moment for girders
E = modulus of elasticity

BOUNDARY CONDITIONS

girders: Vg(0) = 0 Vg(L) = 0 Vg''(L/2) = 0
columns: Vc(0) = 0 Vc''(H/2) = 0

AT YIELD IN GIRDERS

Vg'(0) = -Re
====> My = EIgVg''(0) = 6EIgRe/L
Vc''(H) = My/E/Ic Vc'(H) = -Re
====> Dy = -Vc(H) = HRe(1+IgH/Ic/L)

AT ALLOWABLE DUCTILITY IN GIRDERS

Vc''(H) = My/E/Ic Vc'(H) = -(Re+Rp) = -MUgRe
====> Dmax = -Vc(H) = HRe(MUg+IgH/Ic/L)

STORY DUCTILITY = Dmax/Dy = 1+(MUg-1)/(1+IgH/Ic/L)

FIGURE 12 : STORY DUCTILITY

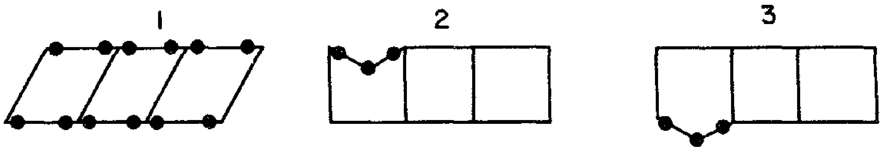

SINGLE MECHANISMS

DOUBLE MECHANISMS

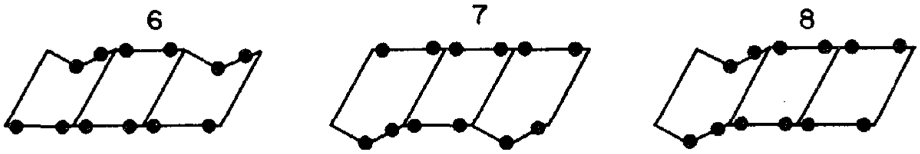

TRIPLE MECHANISMS

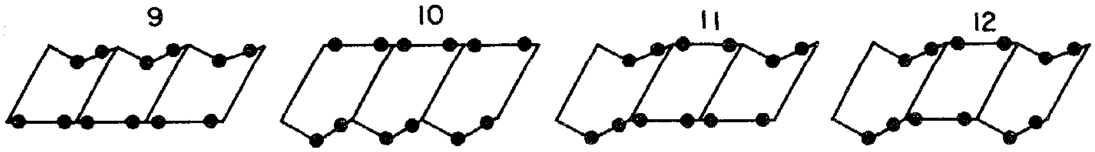

QUADRUPLE MECHANISMS

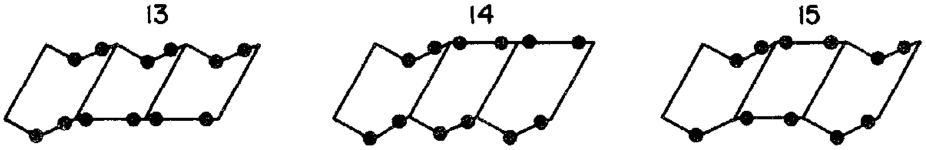

QUINTUPLE MECHANISMS

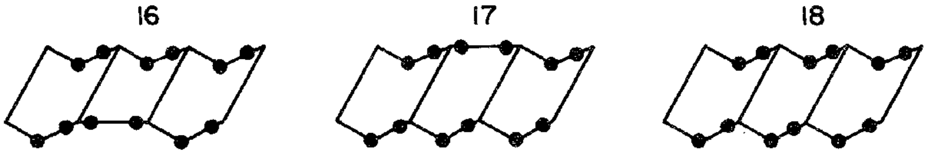

SEXTUPLE MECHANISMS

SEPTUPLE MECHANISMS

FIGURE 13 : NON-REDUNDANT STORY COLLAPSE MECHANISMS

		STARTING DESIGN	PRELIM DESIGN
MOMENTS OF INERTIA (in**4)	ext lower columns	210	216
	int lower columns	210	593
	ext upper columns	171	101
	int upper columns	171	340
	1st story girders	374	432
	2nd story girders	374	370
	3rd story girders	374	279
	4th story girders	300	97
NATURAL PERIODS (seconds)	1st	0. 967	0. 853
	2nd	0. 320	0. 304
	3rd	0. 186	0. 167
	4th	0. 134	0. 105
PSEUDO-ACCELERATION (g's)	1st	0. 332	0. 377
	2nd	0. 780	0. 773
	3rd	0. 712	0. 699
	4th	0. 674	0. 647
SHEAR FORCES (kips)	1st story	106. 5	113. 5
	2nd story	94. 2	101. 4
	3rd story	75. 4	82. 5
	4th story	48. 7	57. 1
GIRDER PLAST MOM CAPACITIES (kip-in)	1st story	2043	2270
	2nd story	2043	2028
	3rd story	2043	1650
	4th story	1740	765
COLUMN PLAST MOM CAPACITIES (kip-in)	ext lower	1568	1598
	int lower	1568	3333
	ext upper	1379	996
	int upper	1379	2116

FIGURE 14 : STARTING AND PRELIMINARY DESIGNS

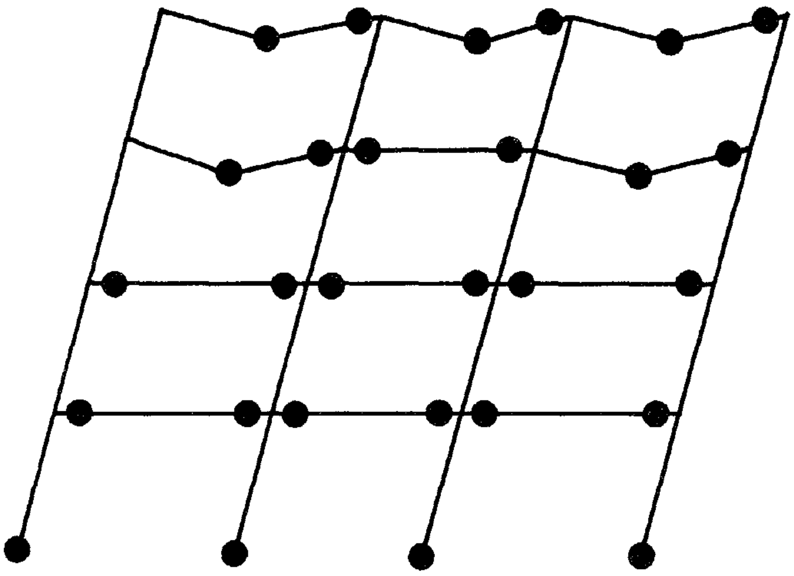

STARTING DESIGN

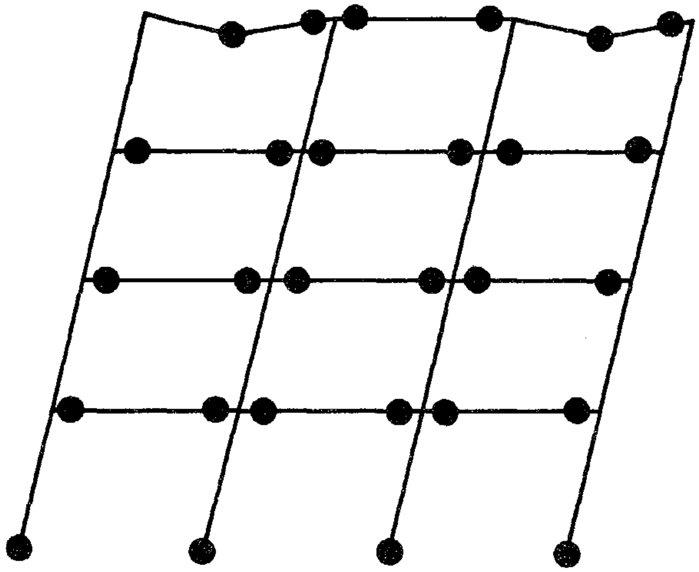

PRELIMINARY DESIGN

FIGURE 15 : COLLAPSE MECHANISMS

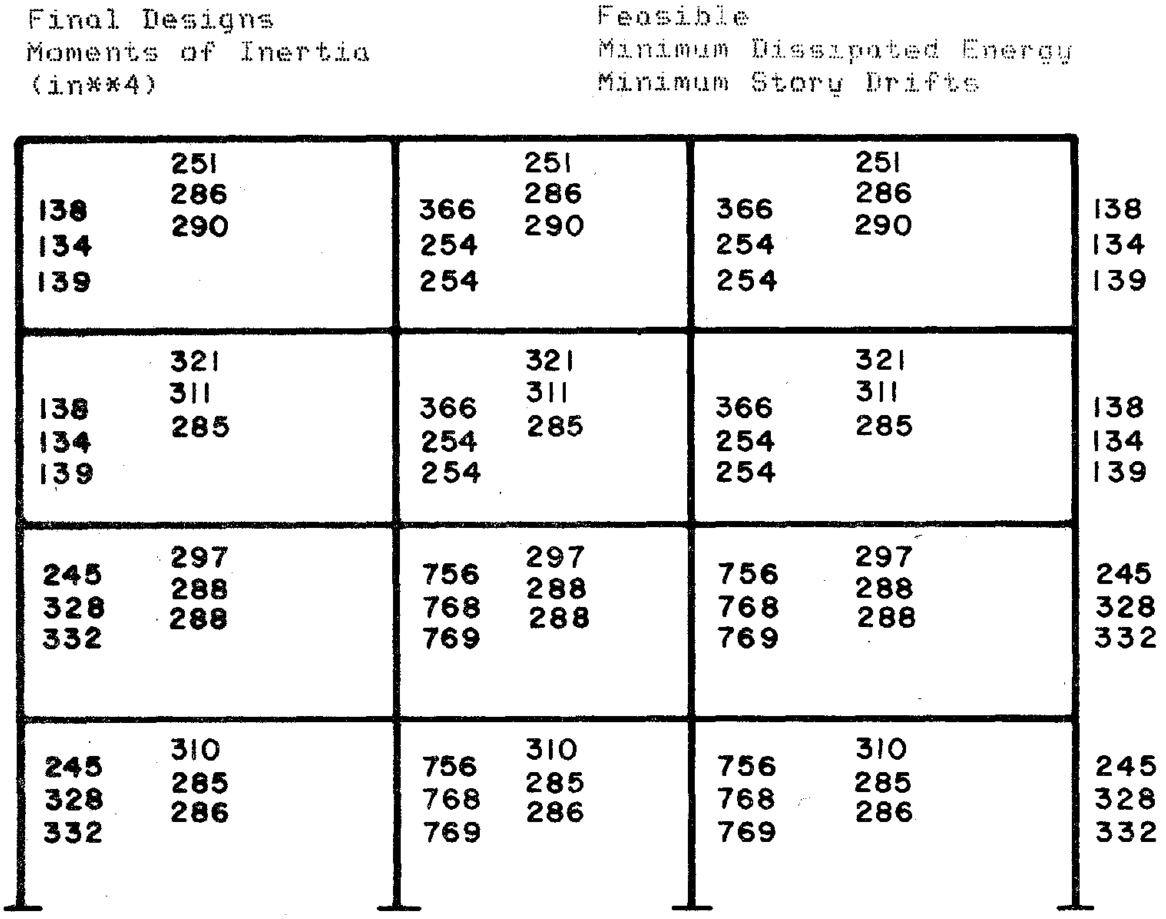

FINAL DESIGN	VOLUME (in**3)	SUM OF DRIFTS (.00001)	INELASTIC ENERGY (kip-in)	ITERATION CPU-TIME (hours)	CONSTRAINT FROM OTHER RECORDS
Feasible	48720	5.35	441	-	132%
Min Diss. Energy	48660	4.55	378	4.3	239%
Min Story Drifts	48530	4.41	371	2.1	204%

FIGURE 16 : COMPARISON OF FINAL DESIGNS

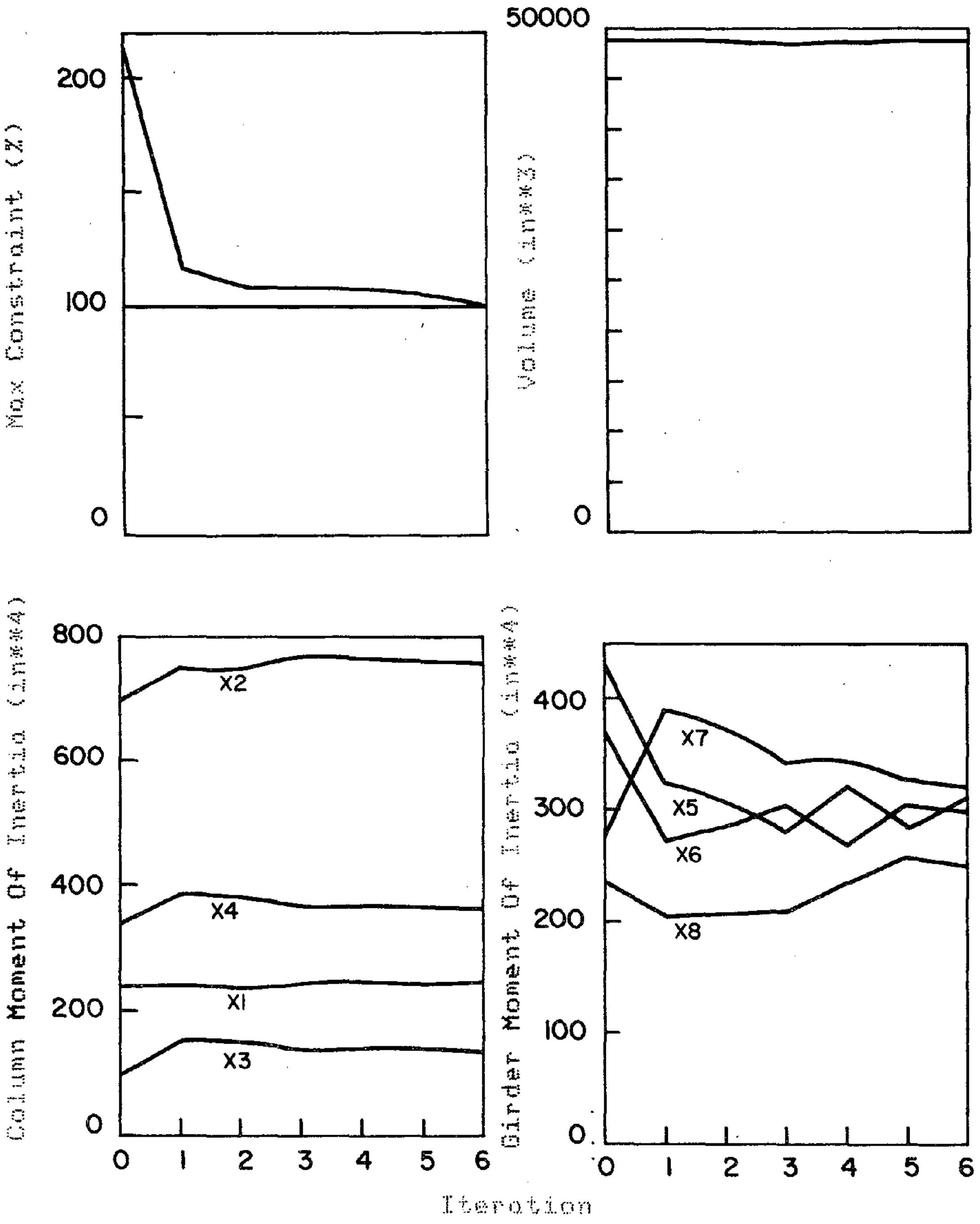

FIGURE 17 : ITERATION HISTORY FOR FEASIBLE DESIGN

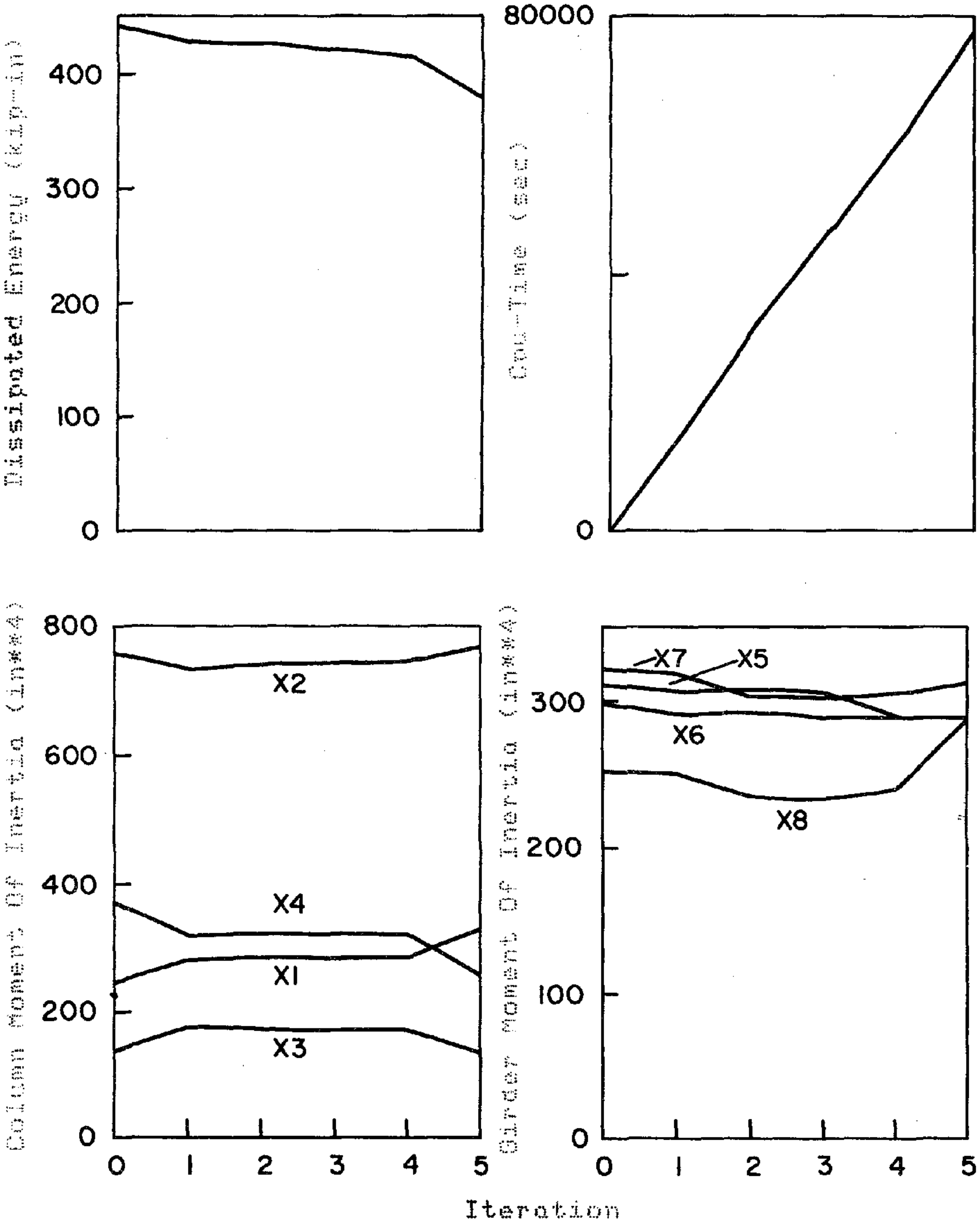

FIGURE 18 : ITERATION HISTORY FOR MIN DISSIPATED ENERGY DESIGN

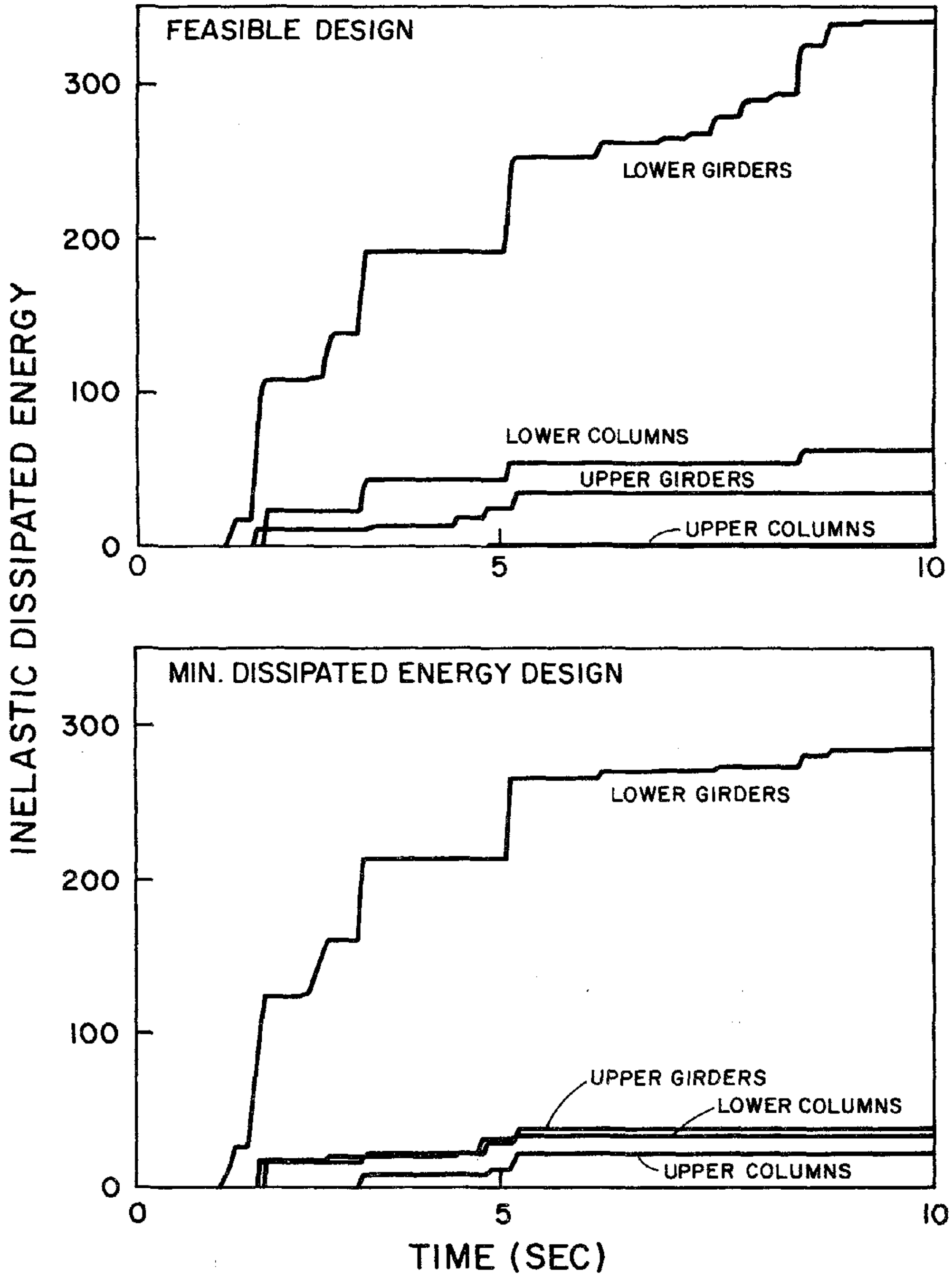

FIGURE 19 : DISSIPATED ENERGY DISTRIBUTION

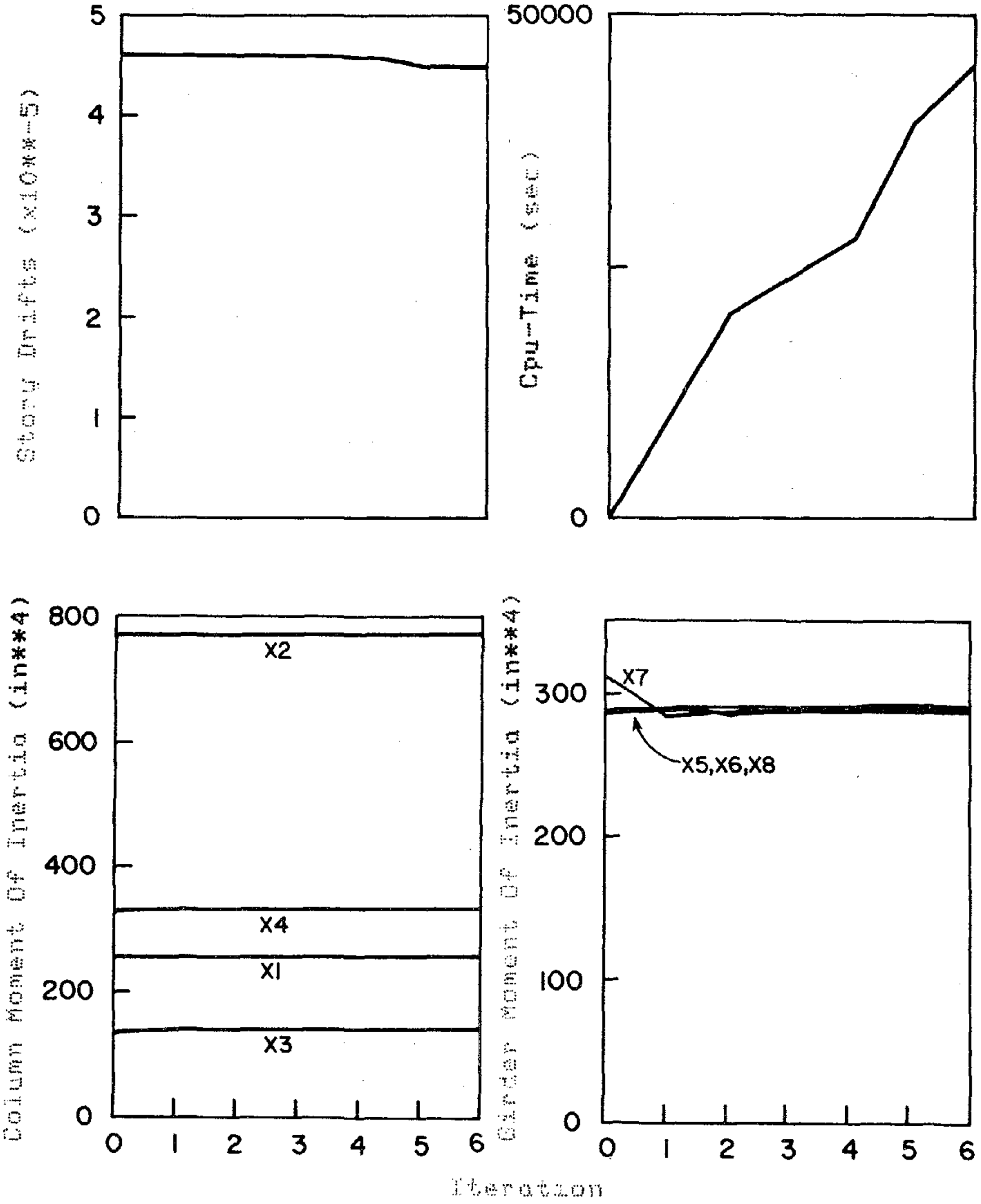

FIGURE 20 : ITERATION HISTORY FOR MIN STORY DRIFTS DESIGN

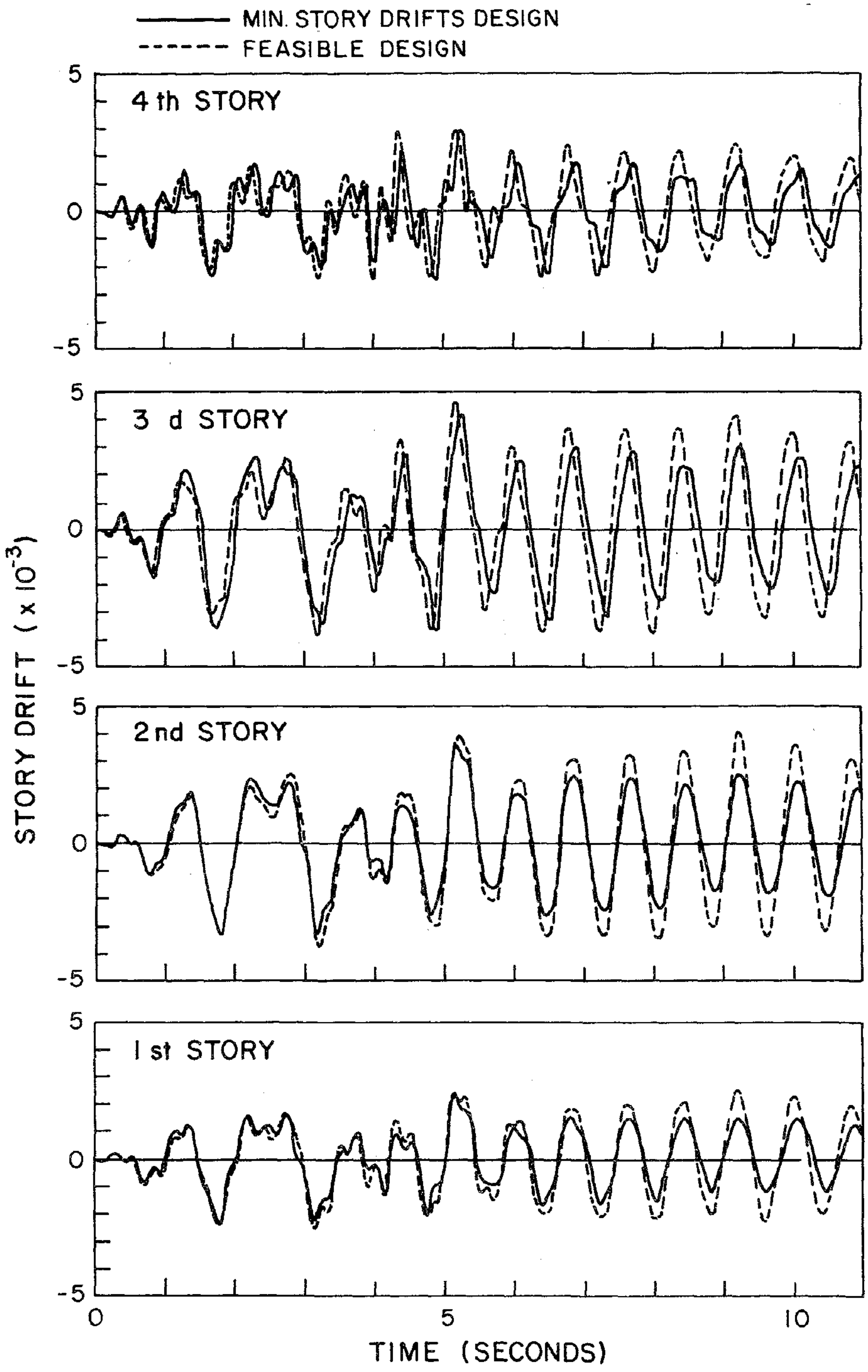

FIGURE 21 : MODERATE QUAKE STORY DRIFTS

APPENDIX 1 : RATTLE PROGRAM FOR PRELIMINARY DESIGN

Initialization

```
array unif(4),axial(4,2)
call massload (mass,unif,axial)
array inertia(8)
readmatrix inertia
:210 210 171 171 374 374 374 300
matop oldin = array(8) of 100000
array stiffness(20,20),periods(4),modes(4,4),pseudoacc(4),
    pseudodis(4), forces(4),girmom(4),colmom(4)
echo_to preliminary
```

Main Loop Of Program

```
repeat {
  printv inertia
  diff = 0
  for i = 1 to 8 diff = max(diff,abs(inertia(i)-oldin(i)))
  if (diff < 1) break
  matop oldin = inertia
  call assemble (inertia,stiffness)
  call eigenprob (stiffness,mass,periods,modes)
  printv periods
  call pseudo (periods,pseudoacc,pseudodis)
  printv pseudoacc
  call dynforce (pseudoacc,pseudodis,modes,mass,forces)
  printv forces
  call girder (forces,unif,girmom)
  printv girmom
  call column (girmom,inertia,axial,colmom)
  printv colmom
  call inertias (girmom,colmom,inertia)
  }
forever
echo_end
```

Procedure For Computing Mass, Gravity Loads, And Axial Forces

```
procedure massload (mass,unif,axial) {
  array unif(),axial(,)
  mass = 80*20*55/1000/386.088
  for i = 1 to 3 unif(i) = (80+1.4*40)*20/1000/12
  unif(4) = (80+1.4*20)*20/1000/12
  matop axial = array(4,2) of 0
  for i = 1 to 4
    for j = 1 to i {
      axial(j,1) = axial(j,1)+120*unif(i)
      axial(j,2) = axial(j,2)+210*unif(i)
      }
  }
```

Procedure For Formulating Element Stiffness Matrix

```
procedure elemstiff (iner,leng,kelem) {
  array kelem(,)
  fac = 12*29000*iner/leng**3
  kelem(1,1) = fac ; kelem(1,2) = -fac
  kelem(2,1) = -fac ; kelem(2,2) = fac
  fac = fac*leng/2
  kelem(1,3) = fac ; kelem(2,3) = -fac
  kelem(2,4) = -fac ; kelem(1,4) = fac
  kelem(3,1) = fac ; kelem(3,2) = -fac
  kelem(4,2) = -fac ; kelem(4,1) = fac
  fac = fac*leng/3
  kelem(3,4) = fac ; kelem(4,3) = fac
  kelem(3,3) = 2*fac ; kelem(4,4) = 2*fac
  }
```

Procedure For Including Element Stiffness Matrix Into Global Stiffness Matrix

```
procedure elemassem (kelem,elmap,stiffness) {
  array kelem(,),elmap(),stiffness(,)
  for i = 1 to 4 {
    ii = abs(elmap(i))
    if (ii == 0) next
    is = elmap(i)/ii
    for j = 1 to 4 {
      jj = abs(elmap(j))
      if (jj == 0) next
      js = elmap(j)/jj
      stiffness(ii,jj) =stiffness(ii,jj) +is*js*kelem(i,j)
      }
    }
  }
```

Procedure For Assembling Global Stiffness Matrix

```
procedure assemble (inertia,stiffness) {
  array inertia(),stiffness(,)
  array elmap(4),kelem(4,4)
  matop stiffness = array(20,20) of 0
  for i = 1 to 4 {
    leng = 10*12
    elmap(1) = -(i-1) ; elmap(2) = -i
    for j = 1 to 4 {
      elmap(4) = 4*i+j
      if (i == 1) elmap(3) = 0
      if (i != 1) elmap(3) = 4*(i-1)+j
      if (i <= 2) {
        if (j == 1 | j == 4) iner = inertia(1)
        if (j == 2 | j == 3) iner = inertia(2)
        }
      if (i >= 3) {
        if (j == 1 | j == 4) iner = inertia(3)
        if (j == 2 | j == 3) iner = inertia(4)
```

```
          }
        call elemstiff (iner,leng,kelem)
        call elemassem (kelem,elmap,stiffness)
        }
      elmap(1) = 0 ; elmap(2) = 0
      for j = 1 to 3 {
        elmap(3) = 4*i+j ; elmap(4) = 4*i+j+1
        if (j == 2) leng = 12*15
        if (j != 2) leng = 12*20
        iner = inertia(4+i)
        call elemstiff (iner,leng,kelem)
        call elemassem (kelem,elmap,stiffness)
        }
      }
  }
```

Procedure For Computing Periods And Mode Shapes

```
procedure eigenprob (stiffness,mass,periods,modes) {
  array stiffness(,), periods(), modes(,)
  matop mhi = identity(4)
  matop mhi = (1/sqrt(mass)) * mhi
  clip k11 = stiffness(1:4,1:4)
  clip k12 = stiffness(1:4,5:20)
  clip k22 = stiffness(5:20,5:20)
  matop a1 = inv(k22)
  matop a2 = a1 * k12'
  matop a3 = k12 * a2
  matop a4 = k11 - a3
  matop a5 = mhi * a4
  matop a6 = a5 * mhi
  matop periods,a7 = sym_eigen(a6)
  matop modes = mhi * a7
  for i = 1 to 4 periods(i) = TWOPI/sqrt(periods(i))
  }
```

Procedure For Finding Pseudo Accelerations And Displacements

```
procedure pseudo (periods,pseudoacc,pseudodis) {
  array periods(),pseudoacc(),pseudodis()
  per1 = .01; per2 = .04; per3 = .4; per4 = 3.4; per5 = 10.
  a1 = .55  ; a2 = .55  ; a3 = .81 ; a4 = .093 ; a5 = .012
  d1 = .0025; d2 = .039 ; d3 = 5.9 ; d4 = 50.  ; d5 = 50.
  ca1 = 0.    ; ca2 = .16812; ca3 = -1.0114; ca4 = -1.8981
  cd1 = 1.9817; cd2 = 2.1798; cd3 = .99860 ; cd4 = 0.
  for i = 1 to 4 {
    per = periods(i)
    if (per <= per2) {
      pseudoacc(i) = a1*(per/per1)**ca1
      pseudodis(i) = d1*(per/per1)**cd1
      }
    if (per > per2 & per <= per3) {
      pseudoacc(i) = a2*(per/per2)**ca2
      pseudodis(i) = d2*(per/per2)**cd2
```

```
      }
    if (per > per3 & per <= per4) {
      pseudoacc(i) = a3*(per/per3)**ca3
      pseudodis(i) = d3*(per/per3)**cd3
      }
    if (per > per4) {
      pseudoacc(i) = a4*(per/per4)**ca4
      pseudodis(i) = d4*(per/per4)**cd4
      }
    }
  }
```

Procedure For Computing Maximum Dynamic Story Shears

```
procedure dynforce (pseudoacc,pseudodis,modes,mass,forces){
  array pseudoacc(), pseudodis(), modes(,), forces()
  array disps(4)
  matop forc = (mass) * modes'
  matop disp = modes'
  matop one = array(4,1) of 1
  matop modefac = modes' * one
  matop modefac = (mass) * modefac
  for i = 1 to 4
    for j = 1 to 4 {
    disp(i,j) = disp(i,j)*modefac(i,1)*pseudodis(i)
    forc(i,j)=forc(i,j)*modefac(i,1)*pseudoacc(i)*386.088
    }
  for j = 3 downto 1
    for i = 1 to 4
      forc(i,j) = forc(i,j)+forc(i,j+1)
  for i = 1 to 4 {
    clip fvec = forc(,i)
    forces(i) = |fvec|
    clip dvec = disp(,i)
    disps(i) = |dvec|
    }
  odisp = 0
  for i = 1 to 4 {
    ndisp = disps(i)
    forces(i) = forces(i)+386.088*mass*(ndisp-odisp)/120
    odisp = ndisp
    }
  }
```

procedure for finding girder plastic moments of failure mechanism

```
procedure girder (forces,unif,girmom) {
  array forces(),unif(),girmom()
  array cost(2),coeff(19,2),rhs(19)
  cost(1) = 11 ; cost(2) = 11+1.2*32
  coeff(1,1) = 1 ; coeff(1,2) = 1
  coeff(2,1) = 1 ; coeff(2,2) = 0
  coeff(3,1) = 0 ; coeff(3,2) = 1
  coeff(4,1) = 4 ; coeff(4,2) = 3
```

```
coeff(5,1) = 3 ; coeff(5,2) = 4
coeff(6,1) = 5 ; coeff(6,2) = 3
coeff(7,1) = 3 ; coeff(7,2) = 5
coeff(8,1) = 1 ; coeff(8,2) = 1
coeff(9,1) = 2 ; coeff(9,2) = 1
coeff(10,1) = 1 ; coeff(10,2) = 2
coeff(11,1) = 5 ; coeff(11,2) = 4
coeff(12,1) = 4 ; coeff(12,2) = 5
coeff(13,1) = 3 ; coeff(13,2) = 2
coeff(14,1) = 2 ; coeff(14,2) = 3
coeff(15,1) = 1 ; coeff(15,2) = 1
coeff(16,1) = 6 ; coeff(16,2) = 5
coeff(17,1) = 5 ; coeff(17,2) = 6
coeff(18,1) = 1 ; coeff(18,2) = 1
coeff(19,1) = -1 ; coeff(19,2) = 1
for i = 1 to 4 {
  wt = unif(i)
  if (i == 4) {
    wt = 2*wt
    for j = 1 to 19 coeff(j,1) = 2*coeff(j,1)
    cost(1) = 2*cost(1)
    }
  if (i == 1) then wb = 0
  else wb = unif(i-1)
  s = forces(i)
  rhs(1) = 40*s
  rhs(2) = 3600*wt
  rhs(3) = 3600*wb
  rhs(4) = 120*s+7200*wt
  rhs(5) = 120*s+7200*wb
  rhs(6) = 120*s+14400*wt
  rhs(7) = 120*s+14400*wb
  rhs(8) = 30*s+1800*(wt+wb)
  rhs(9) = 40*s+6150*wt
  rhs(10) = 40*s+6150*wb
  rhs(11) = 120*s+14400*wt+7200*wb
  rhs(12) = 120*s+7200*wt+14400*wb
  rhs(13) = 60*s+9225*wt+3600*wb
  rhs(14) = 60*s+3600*wt+9225*wb
  rhs(15) = 24*s+2880*(wt+wb)
  rhs(16) = 120*s+18450*wt+14400*wb
  rhs(17) = 120*s+14400*wt+18450*wb
  rhs(18) = 20*s+3075*(wt+wb)
  rhs(19) = 0
  linprog var = argmin { cost'*x | coeff*x>=rhs }
  act1 = 1000 ; act2 = 1000 ; j1 = 0 ; j2 = 0
  matop active = coeff * var
  matop active = active - rhs
  for j = 1 to 19
    if (active(j) <= act2) {
      if (active(j) <= act1) {
        act2 = act1 ; act1 = active(j)
        j2 = j1 ; j1 = j
        }
```

```
        if (active(j) > act1) {
          act2 = active(j) ; j2 = j
          }
        }
    printf 'max constraint numbers = %i %i/n' j1 j2
    girmom(i) = var(1)
    if (i != 1)
      if (var(2) > girmom(i-1))
        girmom(i-1) = var(2)
    }
  }
```

Procedure For Computing Column Plastic Moduli

```
procedure column (girmom,inertia,axial,colmom) {
  array girmom(),inertia(),axial(,),colmom()
  array area(4)
  for i = 1 to 4 {
    if (inertia(i) > 429)
    then depth = 10.5*inertia(i)**0.0436
    else depth = 1.47*inertia(i)**0.368
    area(i) = inertia(i)/(0.39*depth**1.04)**2
    }
  m1 = 1.2*girmom(4) ; m2 = 0.6*girmom(3)
  c3 = max(m1,m2)
  if (axial(4,1) > 0.15*area(3)*36)
    m1 = 0.85*m1/(1-axial(4,1)/36/area(3))
  if (axial(3,1) > 0.15*area(3)*36)
    m2 = 0.85*m2/(1-axial(3,1)/36/area(3))
  colmom(3) = max(m1,m2)
  m1 = 2.4*girmom(4) ; m2 = 1.2*girmom(3)
  c4 = max(m1,m2)
  if (axial(4,2) > 0.15*area(4)*36)
    m1 = 0.85*m1/(1-axial(4,2)/36/area(4))
  if (axial(3,2) > 0.15*area(4)*36)
    m2 = 0.85*m2/(1-axial(3,2)/36/area(4))
  colmom(4) = max(m1,m2)
  m1 = 1.2*girmom(2)-c3 ; m2 = 0.6*girmom(1)
  if (axial(2,1) > 0.15*area(1)*36)
    m1 = 0.85*m1/(1-axial(2,1)/36/area(1))
  if (axial(1,1) > 0.15*area(1)*36)
    m2 = 0.85*m2/(1-axial(1,1)/36/area(1))
  colmom(1) = max(m1,m2,colmom(3))
  m1 = 2.4*girmom(2)-c4 ; m2 = 1.2*girmom(1)
  if (axial(2,2) > 0.15*area(2)*36)
    m1 = 0.85*m1/(1-axial(2,2)/36/area(2))
  if (axial(1,2) > 0.15*area(2)*36)
    m2 = 0.85*m2/(1-axial(1,2)/36/area(2))
  colmom(2) = max(m1,m2,colmom(4))
  }
```

Procedure For Computing Inertias From Plastic Moduli

```
procedure inertias (girmom,colmom,inertia) {
  array girmom(),colmom(),inertia()
  ac1 = 19.516; bc1 = .60256; cc1 = 36.735; dc1 = .63200
  ac2 = 2.3345; bc2 = .95291; cc2 = 5.1429; dc2 = .95640
  ag  = 7.3165; bg  = .75892; cg  = 20.301; dg  = .71300
  toler = .00001
  for i = 1 to 4 {
    inert = 200 ; pm = colmom(i)
    repeat {
      if (inert <= 429)
        {ac = ac1 ; bc = bc1 ; cc = cc1 ; dc = dc1}
      if (inert >  429)
        {ac = ac2 ; bc = bc2 ; cc = cc2 ; dc = dc2}
      pmt = ac*inert**bc+cc*inert**dc
      dpm = ac*bc*inert**(bc-1)+cc*dc*inert**(dc-1)
      dinert = (pm-pmt)/dpm
      inert = inert+dinert
      if (abs(dinert/inert) < toler) break
      }
    forever
    inertia(i) = inert
    }
  for i = 1 to 4 {
    inert = 200 ; pm = girmom(i)
    repeat {
      pmt = ag*inert**bg+cg*inert**dg
      dpm = ag*bg*inert**(bg-1)+cg*dg*inert**(dg-1)
      dinert = (pm-pmt)/dpm
      inert = inert+dinert
      if (abs(dinert/inert) < toler) break
      }
    forever
    inertia(4+i) = inert
    }
  }
```

APPENDIX 2 : PERCENTAGES OF ALLOWABLES FOR CONSTRAINTS ON PRELIMINARY DESIGN

Constraints Under Gravity Loads Only

|column axial force| < 0.5 * column failure force

element	
1	46%
2	56%
3	56%
4	46%
5	34%
6	42%
7	42%
8	34%
9	26%
10	38%
11	38%
12	26%
13	12%
14	17%
15	17%
16	12%

```
|column end moment| < 0.6 * column yield moment
element  node
   1       bot   17%
   1       top   33%
   2       bot    5%
   2       top   10%
   3       bot    5%
   3       top   10%
   4       bot   17%
   4       top   33%
   5       bot   46%
   5       top   49%
   6       bot   15%
   6       top   15%
   7       bot   15%
   7       top   15%
   8       bot   46%
   8       top   49%
   9       bot   44%
   9       top   48%
  10       bot   14%
  10       top   14%
  11       bot   14%
  11       top   14%
  12       bot   44%
  12       top   48%
  13       bot   73%
  13       top   98%
  14       bot   23%
  14       top   31%
  15       bot   23%
  15       top   31%
  16       bot   73%
  16       top   98%
```

```
    |girder end moment| < 0.6 * girder yield moment
    element  node
      17       lft   53%
      17       rht   75%
      18       lft   43%
      18       rht   43%
      19       lft   75%
      19       rht   53%
      20       lft   59%
      20       rht   85%
      21       lft   48%
      21       rht   48%
      22       lft   85%
      22       rht   59%
      23       lft   73%
***   23       rht  104%
      24       lft   58%
      24       rht   58%
***   25       lft  104%
      25       rht   73%
***   26       lft  128%
***   26       rht  190%
***   27       lft  105%
***   27       rht  105%
***   28       lft  190%
***   28       rht  128%
    |live load girder midspan deflection| < girder span / 240
    element
      17             10%
      18              0%
      19             10%
      20             11%
      21              0%
      22             11%
      23             14%
      24              1%
      25             14%
      26             36%
      27              1%
      28             36%
```

Constraints Under Combined Gravity And Moderate Quake Loads

|column end moment| < 1.0 * column yield moment

element	node	E1	E2	E3	E4	E5	E6
1	bot	57%	55%	46%	43%	45%	52%
1	top	46%	44%	40%	38%	41%	45%
2	bot	60%	62%	45%	53%	44%	64%
2	top	36%	37%	28%	33%	23%	41%
3	bot	65%	62%	51%	47%	50%	59%
3	top	39%	36%	32%	29%	33%	37%
4	bot	53%	54%	40%	48%	34%	56%
4	top	44%	44%	37%	41%	33%	47%
5	bot	61%	63%	53%	52%	51%	54%
5	top	62%	63%	55%	54%	53%	57%
6	bot	44%	46%	31%	40%	27%	43%
6	top	43%	43%	33%	39%	27%	42%
7	bot	47%	49%	38%	37%	34%	38%
7	top	45%	45%	38%	36%	35%	41%
8	bot	59%	61%	48%	55%	44%	58%
8	top	60%	61%	51%	56%	46%	59%
9	bot	55%	60%	50%	50%	47%	53%
9	top	61%	64%	50%	52%	49%	55%
10	bot	49%	53%	46%	42%	30%	47%
10	top	52%	54%	41%	45%	31%	48%
11	bot	49%	57%	43%	42%	38%	47%
11	top	54%	57%	40%	42%	37%	45%
12	bot	55%	58%	52%	49%	41%	53%
12	top	60%	61%	52%	54%	44%	57%
13	bot	63%	67%	66%	64%	62%	66%
13	top	76%	81%	78%	76%	75%	78%
14	bot	36%	37%	38%	40%	33%	42%
14	top	38%	41%	39%	39%	33%	42%
15	bot	34%	39%	39%	38%	34%	40%
15	top	38%	43%	40%	38%	37%	40%
16	bot	64%	66%	65%	66%	60%	68%
16	top	77%	79%	77%	77%	72%	79%

```
    |girder end moment| < 1.0 * girder yield moment
    element   node    E1    E2    E3    E4    E5    E6
      17       lft    70%   70%   61%   60%   59%   64%
      17       rht    82%   84%   70%   77%   65%   82%
      18       lft    79%   80%   67%   65%   65%   71%
      18       rht    76%   78%   59%   69%   53%   75%
      19       lft    85%   85%   76%   74%   74%   79%
      19       rht    67%   69%   56%   63%   51%   67%
      20       lft    74%   77%   63%   62%   61%   65%
      20       rht    89%   92%   76%   83%   71%   86%
      21       lft    84%   88%   68%   67%   65%   71%
      21       rht    81%   84%   62%   73%   56%   77%
      22       lft    91%   94%   80%   79%   78%   82%
      22       rht    72%   74%   59%   66%   54%   69%
      23       lft    72%   79%   69%   68%   66%   71%
      23       rht    93%   97%   92%   89%   80%   93%
      24       lft    77%   88%   74%   72%   69%   76%
      24       rht    77%   83%   75%   71%   59%   76%
      25       lft    93%  101%   91%   90%   88%   93%
      25       rht    71%   75%   70%   67%   59%   71%
***   26       lft   100%  105%  102%   99%   98%  102%
***   26       rht   137%  140%  138%  139%  131%  141%
***   27       lft    95%  103%   98%   95%   92%   98%
      27       rht    95%   99%   96%   97%   87%  100%
***   28       lft   137%  143%  140%  137%  135%  140%
***   28       rht   100%  103%  100%  101%   94%  103%
    |story drift| < 1/200
    story             E1    E2    E3    E4    E5    E6
       1              61%   59%   47%   49%   46%   59%
       2              87%   91%   66%   71%   60%   78%
***    3              93%  106%   72%   73%   63%   82%
       4              69%   87%   73%   69%   61%   77%
    |absolute floor acceleration| < g/2
    floor             E1    E2    E3    E4    E5    E6
       1              29%   26%   34%   33%   31%   40%
       2              38%   40%   46%   46%   38%   61%
       3              56%   49%   45%   48%   37%   52%
       4              56%   67%   62%   62%   51%   68%
```

Constraints Under Combined Gravity And Severe Quake Loads

```
   column end energy dissipation < ductility=3 dissipation
   element  node   E1    E2    E3    E4    E5    E6
***   1     bot   85%   68%    7%   22%   31%  131%
      1     top    0%    0%    0%    0%    0%    0%
***   2     bot  280%  337%   30%  199%   79%  370%
      2     top    0%    0%    0%    0%    0%    0%
***   3     bot  276%  343%   35%  205%   84%  377%
      3     top    0%    0%    0%    0%    0%    0%
***   4     bot   96%   58%    0%   10%   17%  120%
      4     top    0%    0%    0%    0%    0%    0%
      5     bot    0%    0%    0%    0%    0%    0%
      5     top    0%    0%    0%    0%    0%    0%
      6     bot    0%    0%    0%    0%    0%    0%
      6     top    0%    0%    0%    0%    0%    0%
      7     bot    0%    0%    0%    0%    0%    0%
      7     top    0%    0%    0%    0%    0%    0%
      8     bot    0%    0%    0%    0%    0%    0%
      8     top    0%    0%    0%    0%    0%    0%
      9     bot    0%    0%    0%    0%    0%    0%
      9     top    0%   10%    0%    0%    0%    6%
     10     bot    4%   58%    4%    0%    0%    7%
     10     top   24%   36%    0%    0%    0%    3%
     11     bot   13%   37%    0%    0%    0%    0%
     11     top    0%   42%    0%    0%    0%   16%
     12     bot    0%   11%    0%    0%    0%    0%
     12     top    6%    0%    0%    0%    0%    0%
     13     bot    0%    0%    0%    0%    0%    0%
     13     top    0%    0%    0%    0%    0%    0%
     14     bot    0%    0%    0%    0%    0%    0%
     14     top    0%    0%    0%    0%    0%    0%
     15     bot    0%    0%    0%    0%    0%    0%
     15     top    0%    0%    0%    0%    0%    0%
     16     bot    0%    0%    0%    0%    0%    0%
     16     top    0%    0%    0%    0%    0%    0%
```

```
   girder end energy dissipation < ductility=6 dissipation
   element  node   E1   E2   E3   E4   E5   E6
     17     lft     7%  15%   7%   9%   9%  19%
     17     rht    20%  10%   0%   6%   0%   7%
     18     lft    26%  25%  15%  18%  17%  39%
     18     rht    33%  26%   1%  11%   0%  13%
     19     lft     9%  16%  11%  11%  13%  22%
     19     rht    18%   8%   0%   4%   0%   6%
     20     lft    14%  23%  13%  10%  11%  18%
     20     rht    19%  17%   0%   9%   0%  10%
     21     lft    42%  49%  22%  19%  21%  41%
     21     rht    38%  69%   0%  16%   3%  19%
     22     lft    15%  26%  16%  13%  15%  20%
     22     rht    17%  16%   0%   7%   0%   9%
     23     lft    15%  13%   8%   7%   8%  10%
     23     rht    10%  28%   9%  10%   4%   9%
     24     lft    27%  40%  18%  15%  17%  22%
     24     rht    15%  45%  12%  12%   3%  14%
     25     lft    18%  16%  14%  11%  14%  14%
     25     rht     6%  25%   4%   4%   0%   4%
     26     lft    30%  27%  31%  31%  31%  35%
     26     rht    29%  41%  31%  35%  28%  34%
     27     lft    27%  22%  26%  26%  26%  31%
     27     rht    18%  35%  21%  26%  17%  24%
     28     lft    35%  31%  36%  35%  35%  39%
     28     rht    24%  37%  27%  31%  24%  31%
  |structure sway| < 1/100
                   E1   E2   E3   E4   E5   E6
***                91%  97%  89%  78%  93% 103%
```

APPENDIX 3 : PERCENTAGES OF ALLOWABLES FOR CONSTRAINTS ON FEASIBLE DESIGN

Constraints Under Gravity Loads Only

$|\text{column axial force}| < 0.5 * \text{column failure force}$

element	
1	45%
2	45%
3	45%
4	45%
5	33%
6	33%
7	33%
8	33%
9	24%
10	38%
11	38%
12	24%
13	11%
14	17%
15	17%
16	11%

```
|column end moment| < 0.6 * column yield moment
element  node
   1       bot   18%
   1       top   34%
   2       bot    4%
   2       top    8%
   3       bot    4%
   3       top    8%
   4       bot   18%
   4       top   34%
   5       bot   45%
   5       top   46%
   6       bot   11%
   6       top   12%
   7       bot   11%
   7       top   12%
   8       bot   45%
   8       top   46%
   9       bot   42%
   9       top   45%
  10       bot   13%
  10       top   14%
  11       bot   13%
  11       top   14%
  12       bot   42%
  12       top   45%
  13       bot   56%
  13       top   68%
  14       bot   21%
  14       top   27%
  15       bot   21%
  15       top   27%
  16       bot   56%
  16       top   68%
```

```
¦girder end moment¦ ≤ 0.6 * girder yield moment
element  node
  17       lft   73%
  17       rht   96%
  18       lft   53%
  18       rht   53%
  19       lft   96%
  19       rht   73%
  20       lft   75%
  20       rht   99%
  21       lft   55%
  21       rht   55%
  22       lft   99%
  22       rht   75%
  23       lft   67%
  23       rht   94%
  24       lft   53%
  24       rht   53%
  25       lft   94%
  25       rht   67%
  26       lft   54%
  26       rht   95%
  27       lft   56%
  27       rht   56%
  28       lft   95%
  28       rht   54%
¦live load girder midspan deflection¦ ≤ girder span / 240
element
  17             11%
  18              1%
  19             11%
  20             12%
  21              1%
  22             12%
  23             12%
  24              0%
  25             12%
  26             18%
  27              2%
  28             18%
```

Constraints Under Combined Gravity And Moderate Quake Loads

|column end moment| < 1.0 * column yield moment

element	node	E1	E2	E3	E4	E5	E6
1	bot	52%	55%	45%	57%	49%	46%
1	top	38%	39%	36%	43%	38%	36%
2	bot	47%	53%	39%	57%	43%	45%
2	top	20%	22%	19%	27%	14%	20%
3	bot	52%	55%	44%	58%	48%	44%
3	top	22%	23%	20%	28%	23%	20%
4	bot	48%	53%	42%	56%	31%	46%
4	top	36%	38%	34%	42%	30%	36%
5	bot	55%	60%	50%	50%	48%	51%
5	top	55%	56%	50%	57%	52%	52%
6	bot	33%	36%	24%	30%	21%	32%
6	top	31%	34%	27%	35%	20%	30%
7	bot	34%	39%	28%	27%	26%	29%
7	top	33%	34%	29%	37%	31%	30%
8	bot	54%	58%	46%	51%	42%	53%
8	top	53%	56%	48%	56%	42%	52%
9	bot	52%	59%	45%	51%	44%	49%
9	top	59%	67%	50%	51%	47%	54%
10	bot	42%	50%	37%	43%	29%	47%
10	top	51%	60%	39%	46%	31%	54%
11	bot	44%	54%	35%	45%	34%	41%
11	top	54%	64%	41%	43%	38%	47%
12	bot	50%	56%	45%	50%	40%	54%
12	top	57%	63%	48%	54%	42%	59%
13	bot	48%	51%	49%	58%	49%	51%
13	top	61%	65%	58%	69%	59%	60%
14	bot	29%	32%	34%	39%	27%	36%
14	top	40%	46%	40%	47%	34%	45%
15	bot	29%	33%	31%	44%	31%	34%
15	top	42%	48%	38%	52%	40%	41%
16	bot	48%	50%	51%	55%	46%	53%
16	top	59%	64%	59%	64%	55%	63%

```
    |girder end moment| < 1.0 * girder yield moment
    element   node    E1    E2    E3    E4    E5    E6
      17      lft     85%   88%   77%   85%   79%   78%
***   17      rht     97%  101%   87%   98%   79%   95%
      18      lft     89%   94%   78%   89%   81%   80%
      18      rht     85%   92%   73%   88%   61%   83%
***   19      lft     99%  103%   91%   99%   93%   93%
      19      rht     82%   87%   73%   84%   65%   80%
      20      lft     89%   96%   77%   76%   74%   80%
***   20      rht    101%  107%   86%   95%   82%  100%
***   21      lft     93%  104%   77%   76%   73%   81%
      21      rht     90%   98%   70%   82%   63%   88%
***   22      lft    103%  111%   91%   91%   89%   95%
      22      rht     86%   92%   72%   81%   67%   85%
      23      lft     71%   78%   61%   71%   63%   66%
      23      rht     86%   92%   80%   85%   74%   89%
      24      lft     74%   84%   60%   75%   64%   68%
      24      rht     71%   80%   63%   71%   55%   75%
      25      lft     88%   95%   78%   88%   80%   83%
      25      rht     69%   75%   63%   68%   57%   72%
      26      lft     48%   52%   46%   54%   47%   48%
      26      rht     72%   76%   72%   76%   68%   75%
      27      lft     56%   60%   52%   64%   54%   55%
      27      rht     54%   59%   54%   60%   49%   58%
      28      lft     73%   77%   71%   79%   72%   73%
      28      rht     47%   50%   47%   51%   44%   50%
    |story drift| < 1/200
    story             E1    E2    E3    E4    E5    E6
       1              58%   61%   48%   62%   52%   50%
***    2              90%  102%   70%   77%   70%   81%
***    3              95%  114%   64%   78%   62%   93%
       4              57%   69%   49%   72%   49%   61%
    |floor acceleration| < g/2
    floor             E1    E2    E3    E4    E5    E6
       1              23%   25%   33%   50%   38%   34%
       2              40%   47%   60%   90%   59%   57%
       3              45%   52%   40%   46%   39%   44%
       4              60%   74%   64%   96%   60%   74%
```

Constraints Under Combined Gravity And Severe Quake Loads

```
     column end energy dissipation < ductility=3 dissipation
     element  node   E1    E2    E3    E4    E5    E6
        1      bot   19%    7%   29%   24%   53%   50%
        1      top    0%    0%    0%    0%    0%    0%
        2      bot   68%   56%   41%  103%   72%   93%
        2      top    0%    0%    0%    0%    0%    0%
        3      bot   65%   52%   45%   99%   76%   96%
        3      top    0%    0%    0%    0%    0%    0%
        4      bot   28%   12%   17%   36%   43%   40%
        4      top    0%    0%    0%    0%    0%    0%
        5      bot    0%    0%    0%    0%    0%    0%
        5      top    0%    0%    0%    0%    0%    0%
        6      bot    0%    0%    0%    0%    0%    0%
        6      top    0%    0%    0%    0%    0%    0%
        7      bot    0%    0%    0%    0%    0%    0%
        7      top    0%    0%    0%    0%    0%    0%
        8      bot    0%    0%    0%    0%    0%    0%
        8      top    0%    0%    0%    0%    0%    0%
        9      bot    0%    0%    0%    0%    0%    0%
        9      top    0%   18%    0%    0%    0%    0%
       10      bot    0%    0%    2%    1%    0%    0%
***    10      top   19%  108%    0%    0%    0%    1%
       11      bot    0%    0%    0%    0%    0%    0%
***    11      top    7%  105%    0%    4%    4%   12%
       12      bot    0%    0%    0%    0%    0%    0%
       12      top    0%    0%    0%    0%    0%    0%
       13      bot    0%    0%    0%    0%    0%    0%
       13      top    0%    0%    0%   18%    0%    0%
       14      bot    0%    0%    0%    0%    0%    0%
       14      top    0%    0%    0%    0%    0%    0%
       15      bot    0%    0%    0%    0%    0%    0%
       15      top    0%    0%    0%    0%    0%    0%
       16      bot    0%    0%    0%    0%    0%    0%
       16      top    0%    0%    0%    0%    0%    0%
```

```
girder end energy dissipation < ductility=6 dissipation
element  node   E1   E2   E3   E4   E5   E6
   17     lft   26%  26%  22%  22%  25%  31%
   17     rht   28%  28%   7%  21%   4%  22%
   18     lft   58%  71%  34%  58%  36%  81%
   18     rht   61%  85%   7%  54%   4%  59%
   19     lft   27%  27%  24%  23%  26%  32%
   19     rht   27%  27%   5%  19%   2%  21%
   20     lft   30%  37%  22%  20%  25%  29%
   20     rht   36%  46%   3%  20%   8%  26%
***   21     lft   82% 122%  28%  39%  35%  97%
***   21     rht   89% 132%   2%  21%  14%  81%
   22     lft   32%  40%  23%  21%  27%  30%
   22     rht   33%  42%   2%  19%   7%  26%
   23     lft    8%  18%   3%   9%   5%   7%
   23     rht    9%  14%   5%  11%   1%   7%
   24     lft   15%  20%  10%  15%  10%  12%
   24     rht   12%  23%   6%  14%   0%  10%
   25     lft   11%  16%   9%  11%  10%  10%
   25     rht    7%  12%   2%   9%   0%   5%
   26     lft    0%   0%   0%   0%   0%   0%
   26     rht    0%   1%   0%   1%   0%   0%
   27     lft    0%   0%   0%   5%   0%   0%
   27     rht    0%   0%   0%   0%   0%   0%
   28     lft    0%   0%   0%   6%   0%   0%
   28     rht    0%   0%   0%   0%   0%   0%
|structure sway| < 1/100
                E1   E2   E3   E4   E5   E6
                94% 100%  87%  79%  97%  99%
```

APPENDIX 4 : PERCENTAGES OF ALLOWABLES FOR CONSTRAINTS ON MINIMUM DISSIPATED ENERGY DESIGN

Constraints Under Gravity Loads Only

|column axial force| < 0.5 * column failure force

element	
1	43%
2	44%
3	44%
4	43%
5	31%
6	33%
7	33%
8	31%
9	25%
10	41%
11	41%
12	25%
13	11%
14	19%
15	19%
16	11%

```
|column end moment| < 0.6 * column yield moment
element  node
   1       bot   16%
   1       top   30%
   2       bot    3%
   2       top    7%
   3       bot    3%
   3       top    7%
   4       bot   16%
   4       top   30%
   5       bot   40%
   5       top   42%
   6       bot   11%
   6       top   12%
   7       bot   11%
   7       top   12%
   8       bot   40%
   8       top   42%
   9       bot   40%
   9       top   46%
  10       bot   13%
  10       top   16%
  11       bot   13%
  11       top   16%
  12       bot   40%
  12       top   46%
  13       bot   58%
  13       top   68%
  14       bot   24%
  14       top   29%
  15       bot   24%
  15       top   29%
  16       bot   58%
  16       top   68%
```

```
¦girder end moment¦ < 0.6 * girder yield moment
element  node
  17       lft   83%
  17       rht   99%
  18       lft   56%
  18       rht   56%
  19       lft   99%
  19       rht   83%
  20       lft   80%
  20       rht   99%
  21       lft   56%
  21       rht   56%
  22       lft   99%
  22       rht   80%
  23       lft   69%
  23       rht   94%
  24       lft   55%
  24       rht   55%
  25       lft   94%
  25       rht   69%
  26       lft   48%
  26       rht   84%
  27       lft   54%
  27       rht   54%
  28       lft   84%
  28       rht   48%
¦live load girder midspan deflection¦ < girder span / 240
element
  17             11%
  18              2%
  19             11%
  20             11%
  21              1%
  22             11%
  23             13%
  24              0%
  25             13%
  26             18%
  27              3%
  28             18%
```

<u>Constraints Under Combined Gravity And Moderate Quake Loads</u>

|column end moment| < 1.0 * column yield moment

element	node	E1	E2	E3	E4	E5	E6
1	bot	55%	48%	43%	51%	48%	43%
1	top	32%	30%	29%	32%	31%	29%
2	bot	50%	44%	37%	49%	42%	41%
2	top	19%	17%	16%	20%	14%	16%
3	bot	54%	47%	41%	50%	46%	41%
3	top	21%	18%	17%	21%	20%	17%
4	bot	51%	46%	38%	50%	31%	43%
4	top	31%	29%	27%	32%	25%	28%
5	bot	50%	47%	43%	45%	42%	43%
5	top	50%	48%	45%	49%	47%	45%
6	bot	33%	34%	23%	29%	20%	27%
6	top	33%	31%	25%	32%	21%	29%
7	bot	35%	32%	27%	29%	26%	26%
7	top	35%	32%	28%	33%	31%	28%
8	bot	49%	49%	39%	44%	37%	44%
8	top	48%	46%	42%	48%	39%	45%
9	bot	58%	52%	45%	50%	46%	49%
9	top	66%	59%	52%	57%	49%	53%
10	bot	57%	57%	41%	48%	32%	48%
10	top	66%	66%	45%	54%	37%	54%
11	bot	60%	50%	41%	48%	41%	47%
11	top	69%	58%	48%	55%	45%	50%
12	bot	56%	56%	46%	50%	39%	50%
12	top	64%	64%	50%	56%	45%	55%
13	bot	51%	50%	49%	52%	49%	48%
13	top	65%	62%	58%	62%	60%	59%
14	bot	38%	41%	35%	37%	36%	39%
14	top	51%	53%	42%	48%	42%	49%
15	bot	41%	38%	36%	40%	37%	34%
15	top	54%	49%	43%	49%	46%	44%
16	bot	50%	52%	49%	50%	50%	51%
16	top	63%	65%	58%	61%	57%	62%

```
    ¦girder  end  moment¦  < 1.0  * girder  yield  moment
    element   node    E1    E2    E3    E4    E5    E6
      17       lft    96%   90%   84%   91%   87%   83%
***   17       rht   103%  100%   89%   99%   82%   94%
      18       lft    96%   88%   79%   88%   83%   78%
      18       rht    92%   87%   72%   87%   64%   80%
***   19       lft   106%  100%   94%  100%   97%   93%
      19       rht    93%   90%   79%   89%   72%   84%
      20       lft    97%   90%   81%   85%   80%   81%
***   20       rht   105%  105%   86%   96%   83%   94%
      21       lft    98%   89%   77%   82%   76%   76%
      21       rht    94%   94%   69%   83%   65%   80%
***   22       lft   108%  101%   92%   96%   91%   92%
      22       rht    94%   94%   75%   85%   72%   83%
      23       lft    78%   71%   63%   69%   66%   67%
      23       rht    90%   90%   78%   84%   73%   85%
      24       lft    79%   70%   60%   68%   64%   65%
      24       rht    76%   76%   61%   69%   54%   69%
      25       lft    92%   85%   78%   84%   81%   82%
      25       rht    75%   76%   63%   69%   58%   70%
      26       lft    46%   44%   41%   44%   42%   41%
      26       rht    66%   67%   62%   65%   62%   66%
      27       lft    54%   51%   47%   51%   49%   48%
      27       rht    52%   53%   47%   50%   46%   51%
      28       lft    68%   65%   63%   66%   64%   63%
      28       rht    45%   46%   41%   43%   40%   44%
    ¦story  drift¦  < 1/200
    story             E1    E2    E3    E4    E5    E6
       1              62%   54%   46%   56%   51%   46%
       2              98%   88%   69%   80%   72%   72%
***    3             115%  109%   70%   87%   70%   86%
       4              70%   67%   46%   58%   52%   59%
    ¦absolute  floor  acceleration¦  < g/2
    floor             E1    E2    E3    E4    E5    E6
       1              27%   27%   30%   32%   35%   34%
       2              43%   41%   45%   64%   59%   44%
       3              52%   51%   40%   45%   41%   41%
       4              70%   70%   53%   65%   57%   64%
```

Constraints Under Combined Gravity And Severe Quake Loads

```
    column end energy dissipation < ductility=3 dissipation
    element  node   E1    E2    E3    E4    E5    E6
       1      bot    6%    0%   18%   10%   57%   31%
       1      top    0%    0%    0%    0%    0%    0%
       2      bot   27%    8%   23%   37%   68%   43%
       2      top    0%    0%    0%    0%    0%    0%
       3      bot   25%    4%   26%   32%   71%   46%
       3      top    0%    0%    0%    0%    0%    0%
       4      bot   11%    0%    8%    7%   49%   26%
       4      top    0%    0%    0%    0%    0%    0%
       5      bot    0%    0%    0%    0%    0%    0%
       5      top    0%    0%    0%    0%    0%    0%
       6      bot    0%    0%    0%    0%    0%    0%
       6      top    0%    0%    0%    0%    0%    0%
       7      bot    0%    0%    0%    0%    0%    0%
       7      top    0%    0%    0%    0%    0%    0%
       8      bot    0%    0%    0%    0%    0%    0%
       8      top    0%    0%    0%    0%    0%    0%
       9      bot    0%    0%    0%    0%    0%    0%
       9      top    8%    0%    0%    0%    7%    7%
      10      bot    0%   22%   13%    0%    0%    0%
***   10      top  229%  239%    0%   31%   15%   61%
      11      bot    0%   22%    5%    0%    0%    0%
***   11      top  227%  220%   17%   43%   34%   81%
      12      bot    0%    0%    0%    0%    0%    0%
      12      top   13%   14%    0%    0%    0%    0%
      13      bot    0%    0%    0%    0%    0%    0%
      13      top    0%    0%    0%    0%    0%    0%
      14      bot    0%    0%    0%    0%    0%    0%
      14      top    0%    0%    0%    0%    0%    0%
      15      bot    0%    0%    0%    0%    0%    0%
      15      top    0%    0%    0%    0%    8%    0%
      16      bot    0%    0%    0%    0%    0%    0%
      16      top    0%    0%    0%    0%    0%    0%
```

```
   girder end energy dissipation < ductility=6 dissipation
   element  node   E1   E2   E3   E4   E5   E6
     17      lft   26%  23%  24%  27%  28%  32%
     17      rht   30%  28%   6%  23%   3%  21%
     18      lft   49%  45%  30%  46%  35%  61%
     18      rht   58%  59%   5%  49%   0%  40%
     19      lft   27%  23%  25%  28%  28%  32%
     19      rht   29%  27%   5%  22%   2%  20%
     20      lft   33%  28%  25%  22%  26%  35%
     20      rht   39%  36%   2%  20%   4%  24%
     21      lft   80%  79%  31%  42%  32%  71%
     21      rht   92%  96%   0%  31%   1%  51%
     22      lft   32%  28%  25%  23%  26%  34%
     22      rht   40%  37%   1%  20%   3%  24%
     23      lft   10%  14%   3%   5%   9%  11%
     23      rht    9%  11%   4%   8%   3%   7%
     24      lft   10%  12%   5%   6%  11%  13%
     24      rht    8%  11%   3%   8%   2%   6%
     25      lft   11%  13%   6%   6%  10%  12%
     25      rht    9%  10%   2%   6%   0%   5%
     26      lft    0%   0%   0%   0%   0%   0%
     26      rht    0%   0%   0%   0%   0%   0%
     27      lft    0%   0%   0%   0%   0%   0%
     27      rht    0%   0%   0%   0%   0%   0%
     28      lft    0%   0%   0%   0%   0%   0%
     28      rht    0%   0%   0%   0%   0%   0%
   ¦structure sway¦ < 1/100
                   E1   E2   E3   E4   E5   E6
*4*                97%  96%  88%  78% 103% 100%
```

APPENDIX 5 : PERCENTAGES OF ALLOWABLES FOR CONSTRAINTS ON MINIMUM STORY DRIFT DESIGN

Constraints Under Gravity Loads Only

|column axial force| < 0.5 * column failure force

1	42%
2	44%
3	44%
4	42%
5	31%
6	33%
7	33%
8	31%
9	25%
10	41%
11	41%
12	25%
13	11%
14	19%
15	19%
16	11%

```
|column end moment| < 0.6 * column yield moment
element  node
   1       bot   16%
   1       top   30%
   2       bot    3%
   2       top    7%
   3       bot    3%
   3       top    7%
   4       bot   16%
   4       top   30%
   5       bot   39%
   5       top   42%
   6       bot   11%
   6       top   12%
   7       bot   11%
   7       top   12%
   8       bot   39%
   8       top   42%
   9       bot   40%
   9       top   46%
  10       bot   13%
  10       top   16%
  11       bot   13%
  11       top   16%
  12       bot   40%
  12       top   46%
  13       bot   58%
  13       top   67%
  14       bot   24%
  14       top   29%
  15       bot   24%
  15       top   29%
  16       bot   58%
  16       top   67%
```

```
|girder end moment| < 0.6 * girder yield moment
element  node
  17      lft   83%
  17      rht   99%
  18      lft   56%
  18      rht   56%
  19      lft   99%
  19      rht   83%
  20      lft   80%
  20      rht   99%
  21      lft   56%
  21      rht   56%
  22      lft   99%
  22      rht   80%
  23      lft   75%
  23      rht  100%
  24      lft   58%
  24      rht   58%
  25      lft  100%
  25      rht   75%
  26      lft   48%
  26      rht   83%
  27      lft   53%
  27      rht   53%
  28      lft   83%
  28      rht   48%
|live load girder midspan deflection| < girder span / 240
element
  17            11%
  18             2%
  19            11%
  20            11%
  21             1%
  22            11%
  23            14%
  24             0%
  25            14%
  26            17%
  27             3%
  28            17%
```

Constraints Under Combined Gravity And Moderate Quake Loads

¦column end moment¦ < 1.0 * column yield moment

element	node	E1	E2	E3	E4	E5	E6
1	bot	56%	49%	43%	50%	48%	43%
1	top	32%	29%	29%	31%	31%	29%
2	bot	51%	44%	36%	48%	42%	40%
2	top	19%	17%	15%	20%	15%	16%
3	bot	55%	47%	41%	49%	46%	40%
3	top	21%	18%	17%	20%	20%	17%
4	bot	52%	46%	38%	49%	31%	43%
4	top	31%	28%	27%	31%	26%	28%
5	bot	50%	47%	43%	45%	42%	42%
5	top	49%	47%	44%	48%	47%	44%
6	bot	34%	34%	23%	29%	20%	27%
6	top	33%	31%	25%	31%	21%	29%
7	bot	36%	32%	27%	29%	26%	26%
7	top	35%	32%	28%	33%	31%	28%
8	bot	48%	48%	39%	44%	37%	43%
8	top	48%	46%	42%	47%	38%	44%
9	bot	59%	50%	45%	51%	46%	49%
9	top	66%	58%	52%	57%	49%	52%
10	bot	57%	56%	41%	48%	33%	47%
10	top	66%	65%	44%	54%	37%	52%
11	bot	61%	47%	41%	49%	42%	46%
11	top	69%	57%	47%	55%	44%	49%
12	bot	57%	56%	46%	50%	40%	50%
12	top	64%	63%	49%	56%	45%	54%
13	bot	50%	49%	49%	51%	49%	47%
13	top	65%	62%	57%	62%	59%	58%
14	bot	37%	40%	34%	37%	36%	37%
14	top	51%	53%	42%	48%	42%	48%
15	bot	39%	38%	35%	40%	36%	34%
15	top	54%	49%	43%	50%	46%	44%
16	bot	49%	50%	48%	49%	50%	49%
16	top	63%	64%	57%	61%	57%	61%

```
    |girder end moment| < 1.0 * girder yield moment
    element  node    E1   E2   E3   E4   E5   E6
      17      lft    97%  91%  83%  90%  87%  83%
***   17      rht   103% 100%  88%  99%  82%  94%
      18      lft    96%  88%  78%  87%  83%  78%
      18      rht    92%  88%  72%  86%  63%  79%
***   19      lft   107% 100%  93% 100%  96%  93%
      19      rht    93%  90%  78%  89%  72%  84%
      20      lft    98%  91%  82%  86%  81%  81%
***   20      rht   106% 105%  86%  97%  83%  93%
      21      lft    99%  89%  77%  83%  76%  77%
      21      rht    95%  94%  69%  83%  64%  79%
***   22      lft   109% 101%  92%  97%  91%  92%
      22      rht    95%  95%  75%  86%  72%  83%
      23      lft    83%  75%  67%  74%  70%  71%
      23      rht    95%  95%  83%  89%  77%  89%
      24      lft    83%  73%  63%  72%  67%  68%
      24      rht    80%  80%  64%  72%  57%  72%
      25      lft    98%  90%  82%  89%  85%  86%
      25      rht    81%  81%  68%  75%  62%  74%
      26      lft    46%  44%  41%  44%  42%  42%
      26      rht    66%  67%  62%  64%  62%  64%
      27      lft    53%  50%  47%  51%  48%  48%
      27      rht    52%  53%  46%  50%  46%  50%
      28      lft    67%  65%  62%  65%  63%  63%
      28      rht    45%  46%  41%  44%  41%  44%
    |story drift| < 1/200
    story           E1   E2   E3   E4   E5   E6
       1             63%  54%  46%  55%  51%  45%
       2             99%  89%  69%  80%  72%  70%
***    3            118% 110%  70%  89%  70%  85%
       4             71%  69%  47%  60%  53%  59%
    |floor acceleration| < g/2
    floor           E1   E2   E3   E4   E5   E6
       1             28%  26%  28%  31%  38%  34%
       2             43%  40%  42%  61%  58%  45%
       3             51%  51%  40%  45%  42%  39%
       4             69%  69%  52%  65%  57%  61%
```

Constraints Under Combined Gravity And Severe Quake Loads

```
   column end energy dissipation < ductility=3 dissipation
   element  node    E1    E2    E3    E4    E5    E6
      1      bot     7%    0%   15%    6%   54%   28%
      1      top     0%    0%    0%    0%    0%    0%
      2      bot    26%    9%   19%   25%   64%   39%
      2      top     0%    0%    0%    0%    0%    0%
      3      bot    24%    8%   23%   21%   68%   43%
      3      top     0%    0%    0%    0%    0%    0%
      4      bot    11%    0%    5%    3%   46%   23%
      4      top     0%    0%    0%    0%    0%    0%
      5      bot     0%    0%    0%    0%    0%    0%
      5      top     0%    0%    0%    0%    0%    0%
      6      bot     0%    0%    0%    0%    0%    0%
      6      top     0%    0%    0%    0%    0%    0%
      7      bot     0%    0%    0%    0%    0%    0%
      7      top     0%    0%    0%    0%    0%    0%
      8      bot     0%    0%    0%    0%    0%    0%
      8      top     0%    0%    0%    0%    0%    0%
      9      bot     0%    0%    0%    0%    0%    0%
      9      top     4%    0%    0%    0%    0%    0%
     10      bot     0%   19%    6%    0%    1%    0%
***  10      top   204%  170%    0%   24%   13%   47%
     11      bot     0%   19%    0%    0%    0%    0%
***  11      top   195%  151%   14%   27%   29%   66%
     12      bot     0%    0%    0%    0%    0%    0%
     12      top     5%    3%    0%    0%    0%    0%
     13      bot     0%    0%    0%    0%    0%    0%
     13      top     0%    0%    0%    0%    0%    0%
     14      bot     0%    0%    0%    0%    0%    0%
     14      top     0%    1%    0%    0%    0%    0%
     15      bot     0%    0%    0%    0%    0%    0%
     15      top     0%    0%    0%    0%   10%    0%
     16      bot     0%    0%    0%    0%    0%    0%
     16      top     0%    0%    0%    0%    0%    0%
```

```
   girder end energy dissipation ≤ ductility=6 dissipation
   element  node   E1   E2   E3   E4   E5   E6
     17      lft   26%  23%  23%  26%  28%  31%
     17      rht   30%  29%   5%  23%   3%  21%
     18      lft   48%  45%  30%  43%  34%  57%
     18      rht   57%  60%   4%  48%   0%  38%
     19      lft   27%  24%  25%  27%  28%  31%
     19      rht   29%  28%   4%  22%   1%  20%
     20      lft   33%  27%  26%  23%  26%  34%
     20      rht   40%  35%   2%  22%   3%  24%
     21      lft   84%  75%  31%  42%  31%  66%
     21      rht   96%  95%   0%  34%   0%  46%
     22      lft   33%  27%  25%  23%  26%  34%
     22      rht   42%  36%   1%  22%   2%  23%
     23      lft   14%  17%   6%  10%  14%  16%
     23      rht   12%  15%   6%  11%   6%  11%
     24      lft   12%  15%   7%   9%  13%  16%
     24      rht   12%  15%   4%  11%   5%   9%
     25      lft   14%  16%   8%  10%  13%  15%
     25      rht   14%  16%   4%  10%   4%  10%
     26      lft    0%   0%   0%   0%   0%   0%
     26      rht    0%   0%   0%   0%   0%   0%
     27      lft    0%   0%   0%   0%   0%   0%
     27      rht    0%   0%   0%   0%   0%   0%
     28      lft    0%   0%   0%   0%   0%   0%
     28      rht    0%   0%   0%   0%   0%   0%
   |structure sway| ≤ 1/100
                   E1   E2   E3   E4   E5   E6
***                98%  97%  88%  76%  105% 99%
```

EARTHQUAKE ENGINEERING RESEARCH CENTER REPORTS

NOTE: Numbers in parenthesis are Accession Numbers assigned by the National Technical Information Service; these are followed by a price code. Copies of the reports may be ordered from the National Technical Information Service, 5285 Port Royal Road, Springfield, Virginia, 22161. Accession Numbers should be quoted on orders for reports (PB --- ---) and remittance must accompany each order. Reports without this information were not available at time of printing. Upon request, EERC will mail inquirers this information when it becomes available.

EERC 67-1 "Feasibility Study Large-Scale Earthquake Simulator Facility," by J. Penzien, J.G. Bouwkamp, R.W. Clough and D. Rea - 1967 (PB 187 905)A07

EERC 68-1 Unassigned

EERC 68-2 "Inelastic Behavior of Beam-to-Column Subassemblages Under Repeated Loading," by V.V. Bertero - 1968 (PB 184 888)A05

EERC 68-3 "A Graphical Method for Solving the Wave Reflection-Refraction Problem," by H.D. McNiven and Y. Mengi - 1968 (PB 187 943)A03

EERC 68-4 "Dynamic Properties of McKinley School Buildings," by D. Rea, J.G. Bouwkamp and R.W. Clough - 1968 (PB 187 902)A07

EERC 68-5 "Characteristics of Rock Motions During Earthquakes," by H.B. Seed, I.M. Idriss and F.W. Kiefer - 1968 (PB 188 338)A03

EERC 69-1 "Earthquake Engineering Research at Berkeley," - 1969 (PB 187 906)A11

EERC 69-2 "Nonlinear Seismic Response of Earth Structures," by M. Dibaj and J. Penzien - 1969 (PB 187 904)A08

EERC 69-3 "Probabilistic Study of the Behavior of Structures During Earthquakes," by R. Ruiz and J. Penzien - 1969 (PB 187 886)A06

EERC 69-4 "Numerical Solution of Boundary Value Problems in Structural Mechanics by Reduction to an Initial Value Formulation," by N. Distefano and J. Schujman - 1969 (PB 187 942)A02

EERC 69-5 "Dynamic Programming and the Solution of the Biharmonic Equation," by N. Distefano - 1969 (PB 187 941)A03

EERC 69-6 "Stochastic Analysis of Offshore Tower Structures," by A.K. Malhotra and J. Penzien - 1969 (PB 187 903)A09

EERC 69-7 "Rock Motion Accelerograms for High Magnitude Earthquakes," by H.B. Seed and I.M. Idriss - 1969 (PB 187 940)A02

EERC 69-8 "Structural Dynamics Testing Facilities at the University of California, Berkeley," by R.M. Stephen, J.G. Bouwkamp, R.W. Clough and J. Penzien - 1969 (PB 189 111)A04

EERC 69-9 "Seismic Response of Soil Deposits Underlain by Sloping Rock Boundaries," by H. Dezfulian and H.B. Seed 1969 (PB 189 114)A03

EERC 69-10 "Dynamic Stress Analysis of Axisymmetric Structures Under Arbitrary Loading," by S. Ghosh and E.L. Wilson 1969 (PB 189 026)A10

EERC 69-11 "Seismic Behavior of Multistory Frames Designed by Different Philosophies," by J.C. Anderson and V. V. Bertero - 1969 (PB 190 662)A10

EERC 69-12 "Stiffness Degradation of Reinforcing Concrete Members Subjected to Cyclic Flexural Moments," by V.V. Bertero, B. Bresler and H. Ming Liao - 1969 (PB 202 942)A07

EERC 69-13 "Response of Non-Uniform Soil Deposits to Travelling Seismic Waves," by H. Dezfulian and H.B. Seed - 1969 (PB 191 023)A03

EERC 69-14 "Damping Capacity of a Model Steel Structure," by D. Rea, R.W. Clough and J.G. Bouwkamp - 1969 (PB 190 663)A06

EERC 69-15 "Influence of Local Soil Conditions on Building Damage Potential during Earthquakes," by H.B. Seed and I.M. Idriss - 1969 (PB 191 036)A03

EERC 69-16 "The Behavior of Sands Under Seismic Loading Conditions," by M.L. Silver and H.B. Seed - 1969 (AD 714 982)A07

EERC 70-1 "Earthquake Response of Gravity Dams," by A.K. Chopra - 1970 (AD 709 640)A03

EERC 70-2 "Relationships between Soil Conditions and Building Damage in the Caracas Earthquake of July 29, 1967," by H.B. Seed, I.M. Idriss and H. Dezfulian - 1970 (PB 195 762)A05

EERC 70-3 "Cyclic Loading of Full Size Steel Connections," by E.P. Popov and R.M. Stephen - 1970 (PB 213 545)A04

EERC 70-4 "Seismic Analysis of the Charaima Building, Caraballeda, Venezuela," by Subcommittee of the SEAONC Research Committee: V.V. Bertero, P.F. Fratessa, S.A. Mahin, J.H. Sexton, A.C. Scordelis, E.L. Wilson, L.A. Wyllie, H.B. Seed and J. Penzien, Chairman - 1970 (PB 201 455)A06

EERC 70-5 "A Computer Program for Earthquake Analysis of Dams," by A.K. Chopra and P. Chakrabarti - 1970 (AD 723 994)A05

EERC 70-6 "The Propagation of Love Waves Across Non-Horizontally Layered Structures," by J. Lysmer and L.A. Drake 1970 (PB 197 896)A03

EERC 70-7 "Influence of Base Rock Characteristics on Ground Response," by J. Lysmer, H.B. Seed and P.B. Schnabel 1970 (PB 197 897)A03

EERC 70-8 "Applicability of Laboratory Test Procedures for Measuring Soil Liquefaction Characteristics under Cyclic Loading," by H.B. Seed and W.H. Peacock - 1970 (PB 198 016)A03

EERC 70-9 "A Simplified Procedure for Evaluating Soil Liquefaction Potential," by H.B. Seed and I.M. Idriss - 1970 (PB 198 009)A03

EERC 70-10 "Soil Moduli and Damping Factors for Dynamic Response Analysis," by H.B. Seed and I.M. Idriss - 1970 (PB 197 869)A03

EERC 71-1 "Koyna Earthquake of December 11, 1967 and the Performance of Koyna Dam," by A.K. Chopra and P. Chakrabarti 1971 (AD 731 496)A06

EERC 71-2 "Preliminary In-Situ Measurements of Anelastic Absorption in Soils Using a Prototype Earthquake Simulator," by R.D. Borcherdt and P.W. Rodgers - 1971 (PB 201 454)A03

EERC 71-3 "Static and Dynamic Analysis of Inelastic Frame Structures," by F.L. Porter and G.H. Powell - 1971 (PB 210 135)A06

EERC 71-4 "Research Needs in Limit Design of Reinforced Concrete Structures," by V.V. Bertero - 1971 (PB 202 943)A04

EERC 71-5 "Dynamic Behavior of a High-Rise Diagonally Braced Steel Building," by D. Rea, A.A. Shah and J.G. Bouwkamp 1971 (PB 203 584)A06

EERC 71-6 "Dynamic Stress Analysis of Porous Elastic Solids Saturated with Compressible Fluids," by J. Ghaboussi and E. L. Wilson - 1971 (PB 211 396)A06

EERC 71-7 "Inelastic Behavior of Steel Beam-to-Column Subassemblages," by H. Krawinkler, V.V. Bertero and E.P. Popov 1971 (PB 211 335)A14

EERC 71-8 "Modification of Seismograph Records for Effects of Local Soil Conditions," by P. Schnabel, H.B. Seed and J. Lysmer - 1971 (PB 214 450)A03

EERC 72-1 "Static and Earthquake Analysis of Three Dimensional Frame and Shear Wall Buildings," by E.L. Wilson and H.H. Dovey - 1972 (PB 212 904)A05

EERC 72-2 "Accelerations in Rock for Earthquakes in the Western United States," by P.B. Schnabel and H.B. Seed - 1972 (PB 213 100)A03

EERC 72-3 "Elastic-Plastic Earthquake Response of Soil-Building Systems," by T. Minami - 1972 (PB 214 868)A08

EERC 72-4 "Stochastic Inelastic Response of Offshore Towers to Strong Motion Earthquakes," by M.K. Kaul - 1972 (PB 215 713)A05

EERC 72-5 "Cyclic Behavior of Three Reinforced Concrete Flexural Members with High Shear," by E.P. Popov, V.V. Bertero and H. Krawinkler - 1972 (PB 214 555)A05

EERC 72-6 "Earthquake Response of Gravity Dams Including Reservoir Interaction Effects," by P. Chakrabarti and A.K. Chopra - 1972 (AD 762 330)A08

EERC 72-7 "Dynamic Properties of Pine Flat Dam," by D. Rea, C.Y. Liaw and A.K. Chopra - 1972 (AD 763 928)A05

EERC 72-8 "Three Dimensional Analysis of Building Systems," by E.L. Wilson and H.H. Dovey - 1972 (PB 222 438)A06

EERC 72-9 "Rate of Loading Effects on Uncracked and Repaired Reinforced Concrete Members," by S. Mahin, V.V. Bertero, D. Rea and M. Atalay - 1972 (PB 224 520)A08

EERC 72-10 "Computer Program for Static and Dynamic Analysis of Linear Structural Systems," by E.L. Wilson, K.-J. Bathe, J.E. Peterson and H.H.Dovey - 1972 (PB 220 437)A04

EERC 72-11 "Literature Survey - Seismic Effects on Highway Bridges," by T. Iwasaki, J. Penzien and R.W. Clough - 1972 (PB 215 613)A19

EERC 72-12 "SHAKE-A Computer Program for Earthquake Response Analysis of Horizontally Layered Sites," by P.B. Schnabel and J. Lysmer - 1972 (PB 220 207)A06

EERC 73-1 "Optimal Seismic Design of Multistory Frames," by V.V. Bertero and H. Kamil - 1973

EERC 73-2 "Analysis of the Slides in the San Fernando Dams During the Earthquake of February 9, 1971," by H.B. Seed, K.L. Lee, I.M. Idriss and F. Makdisi - 1973 (PB 223 402)A14

EERC 73-3 "Computer Aided Ultimate Load Design of Unbraced Multistory Steel Frames," by M.B. El-Hafez and G.H. Powell 1973 (PB 248 315)A09

EERC 73-4 "Experimental Investigation into the Seismic Behavior of Critical Regions of Reinforced Concrete Components as Influenced by Moment and Shear," by M. Celebi and J. Penzien - 1973 (PB 215 884)A09

EERC 73-5 "Hysteretic Behavior of Epoxy-Repaired Reinforced Concrete Beams," by M. Celebi and J. Penzien - 1973 (PB 239 568)A03

EERC 73-6 "General Purpose Computer Program for Inelastic Dynamic Response of Plane Structures," by A. Kanaan and G.H. Powell - 1973 (PB 221 260)A08

EERC 73-7 "A Computer Program for Earthquake Analysis of Gravity Dams Including Reservoir Interaction," by P. Chakrabarti and A.K. Chopra - 1973 (AD 766 271)A04

EERC 73-8 "Behavior of Reinforced Concrete Deep Beam-Column Subassemblages Under Cyclic Loads," by O. Küstü and J.G. Bouwkamp - 1973 (PB 246 117)A12

EERC 73-9 "Earthquake Analysis of Structure-Foundation Systems," by A.K. Vaish and A.K. Chopra - 1973 (AD 766 272)A07

EERC 73-10 "Deconvolution of Seismic Response for Linear Systems," by R.B. Reimer - 1973 (PB 227 179)A08

EERC 73-11 "SAP IV: A Structural Analysis Program for Static and Dynamic Response of Linear Systems," by K.-J. Bathe, E.L. Wilson and F.E. Peterson - 1973 (PB 221 967)A09

EERC 73-12 "Analytical Investigations of the Seismic Response of Long, Multiple Span Highway Bridges," by W.S. Tseng and J. Penzien - 1973 (PB 227 816)A10

EERC 73-13 "Earthquake Analysis of Multi-Story Buildings Including Foundation Interaction," by A.K. Chopra and J.A. Gutierrez - 1973 (PB 222 970)A03

EERC 73-14 "ADAP: A Computer Program for Static and Dynamic Analysis of Arch Dams," by R.W. Clough, J.M. Raphael and S. Mojtahedi - 1973 (PB 223 763)A09

EERC 73-15 "Cyclic Plastic Analysis of Structural Steel Joints," by R.B. Pinkney and R.W. Clough - 1973 (PB 226 843)A08

EERC 73-16 "QUAD-4: A Computer Program for Evaluating the Seismic Response of Soil Structures by Variable Damping Finite Element Procedures," by I.M. Idriss, J. Lysmer, R. Hwang and H.B. Seed - 1973 (PB 229 424)A05

EERC 73-17 "Dynamic Behavior of a Multi-Story Pyramid Shaped Building," by R.M. Stephen, J.P. Hollings and J.G. Bouwkamp - 1973 (PB 240 718)A06

EERC 73-18 "Effect of Different Types of Reinforcing on Seismic Behavior of Short Concrete Columns," by V.V. Bertero, J. Hollings, O. Küstü, R.M. Stephen and J.G. Bouwkamp - 1973

EERC 73-19 "Olive View Medical Center Materials Studies, Phase I," by B. Bresler and V.V. Bertero - 1973 (PB 235 986)A06

EERC 73-20 "Linear and Nonlinear Seismic Analysis Computer Programs for Long Multiple-Span Highway Bridges," by W.S. Tseng and J. Penzien - 1973

EERC 73-21 "Constitutive Models for Cyclic Plastic Deformation of Engineering Materials," by J.M. Kelly and P.P. Gillis 1973 (PB 226 024)A03

EERC 73-22 "DRAIN - 2D User's Guide," by G.H. Powell - 1973 (PB 227 016)A05

EERC 73-23 "Earthquake Engineering at Berkeley - 1973," (PB 226 033)A11

EERC 73-24 Unassigned

EERC 73-25 "Earthquake Response of Axisymmetric Tower Structures Surrounded by Water," by C.Y. Liaw and A.K. Chopra 1973 (AD 773 052)A09

EERC 73-26 "Investigation of the Failures of the Olive View Stairtowers During the San Fernando Earthquake and Their Implications on Seismic Design," by V.V. Bertero and R.G. Collins - 1973 (PB 235 106)A13

EERC 73-27 "Further Studies on Seismic Behavior of Steel Beam-Column Subassemblages," by V.V. Bertero, H. Krawinkler and E.P. Popov - 1973 (PB 234 172)A06

EERC 74-1 "Seismic Risk Analysis," by C.S. Oliveira - 1974 (PB 235 920)A06

EERC 74-2 "Settlement and Liquefaction of Sands Under Multi-Directional Shaking," by R. Pyke, C.K. Chan and H.B. Seed 1974

EERC 74-3 "Optimum Design of Earthquake Resistant Shear Buildings," by D. Ray, K.S. Pister and A.K. Chopra - 1974 (PB 231 172)A06

EERC 74-4 "LUSH - A Computer Program for Complex Response Analysis of Soil-Structure Systems," by J. Lysmer, T. Udaka, H.B. Seed and R. Hwang - 1974 (PB 236 796)A05

EERC 74-5 "Sensitivity Analysis for Hysteretic Dynamic Systems: Applications to Earthquake Engineering," by D. Ray 1974 (PB 233 213)A06

EERC 74-6 "Soil Structure Interaction Analyses for Evaluating Seismic Response," by H.B. Seed, J. Lysmer and R. Hwang 1974 (PB 236 519)A04

EERC 74-7 Unassigned

EERC 74-8 "Shaking Table Tests of a Steel Frame - A Progress Report," by R.W. Clough and D. Tang - 1974 (PB 240 869)A03

EERC 74-9 "Hysteretic Behavior of Reinforced Concrete Flexural Members with Special Web Reinforcement," by V.V. Bertero, E.P. Popov and T.Y. Wang - 1974 (PB 236 797)A07

EERC 74-10 "Applications of Reliability-Based, Global Cost Optimization to Design of Earthquake Resistant Structures," by E. Vitiello and K.S. Pister - 1974 (PB 237 231)A06

EERC 74-11 "Liquefaction of Gravelly Soils Under Cyclic Loading Conditions," by R.T. Wong, H.B. Seed and C.K. Chan 1974 (PB 242 042)A03

EERC 74-12 "Site-Dependent Spectra for Earthquake-Resistant Design," by H.B. Seed, C. Ugas and J. Lysmer - 1974 (PB 240 953)A03

EERC 74-13 "Earthquake Simulator Study of a Reinforced Concrete Frame," by P. Hidalgo and R.W. Clough - 1974 (PB 241 944)A13

EERC 74-14 "Nonlinear Earthquake Response of Concrete Gravity Dams," by N. Pal - 1974 (AD/A 006 583)A06

EERC 74-15 "Modeling and Identification in Nonlinear Structural Dynamics - I. One Degree of Freedom Models," by N. Distefano and A. Rath - 1974 (PB 241 548)A06

EERC 75-1 "Determination of Seismic Design Criteria for the Dumbarton Bridge Replacement Structure, Vol. I: Description, Theory and Analytical Modeling of Bridge and Parameters," by F. Baron and S.-H. Pang - 1975 (PB 259 407)A15

EERC 75-2 "Determination of Seismic Design Criteria for the Dumbarton Bridge Replacement Structure, Vol. II: Numerical Studies and Establishment of Seismic Design Criteria," by F. Baron and S.-H. Pang - 1975 (PB 259 408)A11 (For set of EERC 75-1 and 75-2 (PB 259 406))

EERC 75-3 "Seismic Risk Analysis for a Site and a Metropolitan Area," by C.S. Oliveira - 1975 (PB 248 134)A09

EERC 75-4 "Analytical Investigations of Seismic Response of Short, Single or Multiple-Span Highway Bridges," by M.-C. Chen and J. Penzien - 1975 (PB 241 454)A09

EERC 75-5 "An Evaluation of Some Methods for Predicting Seismic Behavior of Reinforced Concrete Buildings," by S.A. Mahin and V.V. Bertero - 1975 (PB 246 306)A16

EERC 75-6 "Earthquake Simulator Study of a Steel Frame Structure, Vol. I: Experimental Results," by R.W. Clough and D.T. Tang - 1975 (PB 243 981)A13

EERC 75-7 "Dynamic Properties of San Bernardino Intake Tower," by D. Rea, C.-Y. Liaw and A.K. Chopra - 1975 (AD/A008 406) A05

EERC 75-8 "Seismic Studies of the Articulation for the Dumbarton Bridge Replacement Structure, Vol. I: Description, Theory and Analytical Modeling of Bridge Components," by F. Baron and R.E. Hamati - 1975 (PB 251 539)A07

EERC 75-9 "Seismic Studies of the Articulation for the Dumbarton Bridge Replacement Structure, Vol. 2: Numerical Studies of Steel and Concrete Girder Alternates," by F. Baron and R.E. Hamati - 1975 (PB 251 540)A10

EERC 75-10 "Static and Dynamic Analysis of Nonlinear Structures," by D.P. Mondkar and G.H. Powell - 1975 (PB 242 434)A08

EERC 75-11 "Hysteretic Behavior of Steel Columns," by E.P. Popov, V.V. Bertero and S. Chandramouli - 1975 (PB 252 365)A11

EERC 75-12 "Earthquake Engineering Research Center Library Printed Catalog," - 1975 (PB 243 711)A26

EERC 75-13 "Three Dimensional Analysis of Building Systems (Extended Version)," by E.L. Wilson, J.P. Hollings and H.H. Dovey - 1975 (PB 243 989)A07

EERC 75-14 "Determination of Soil Liquefaction Characteristics by Large-Scale Laboratory Tests," by P. De Alba, C.K. Chan and H.B. Seed - 1975 (NUREG 0027)A08

EERC 75-15 "A Literature Survey - Compressive, Tensile, Bond and Shear Strength of Masonry," by R.L. Mayes and R.W. Clough - 1975 (PB 246 292)A10

EERC 75-16 "Hysteretic Behavior of Ductile Moment Resisting Reinforced Concrete Frame Components," by V.V. Bertero and E.P. Popov - 1975 (PB 246 388)A05

EERC 75-17 "Relationships Between Maximum Acceleration, Maximum Velocity, Distance from Source, Local Site Conditions for Moderately Strong Earthquakes," by H.B. Seed, R. Murarka, J. Lysmer and I.M. Idriss - 1975 (PB 248 172)A03

EERC 75-18 "The Effects of Method of Sample Preparation on the Cyclic Stress-Strain Behavior of Sands," by J. Mulilis, C.K. Chan and H.B. Seed - 1975 (Summarized in EERC 75-28)

EERC 75-19 "The Seismic Behavior of Critical Regions of Reinforced Concrete Components as Influenced by Moment, Shear and Axial Force," by M.B. Atalay and J. Penzien - 1975 (PB 258 842)A11

EERC 75-20 "Dynamic Properties of an Eleven Story Masonry Building," by R.M. Stephen, J.P. Hollings, J.G. Bouwkamp and D. Jurukovski - 1975 (PB 246 945)A04

EERC 75-21 "State-of-the-Art in Seismic Strength of Masonry - An Evaluation and Review," by R.L. Mayes and R.W. Clough 1975 (PB 249 040)A07

EERC 75-22 "Frequency Dependent Stiffness Matrices for Viscoelastic Half-Plane Foundations," by A.K. Chopra, P. Chakrabarti and G. Dasgupta - 1975 (PB 248 121)A07

EERC 75-23 "Hysteretic Behavior of Reinforced Concrete Framed Walls," by T.Y. Wong, V.V. Bertero and E.P. Popov - 1975

EERC 75-24 "Testing Facility for Subassemblages of Frame-Wall Structural Systems," by V.V. Bertero, E.P. Popov and T. Endo - 1975

EERC 75-25 "Influence of Seismic History on the Liquefaction Characteristics of Sands," by H.B. Seed, K. Mori and C.K. Chan - 1975 (Summarized in EERC 75-28)

EERC 75-26 "The Generation and Dissipation of Pore Water Pressures during Soil Liquefaction," by H.B. Seed, P.P. Martin and J. Lysmer - 1975 (PB 252 648)A03

EERC 75-27 "Identification of Research Needs for Improving Aseismic Design of Building Structures," by V.V. Bertero 1975 (PB 248 136)A05

EERC 75-28 "Evaluation of Soil Liquefaction Potential during Earthquakes," by H.B. Seed, I. Arango and C.K. Chan - 1975 (NUREG 0026)A13

EERC 75-29 "Representation of Irregular Stress Time Histories by Equivalent Uniform Stress Series in Liquefaction Analyses," by H.B. Seed, I.M. Idriss, F. Makdisi and N. Banerjee - 1975 (PB 252 635)A03

EERC 75-30 "FLUSH - A Computer Program for Approximate 3-D Analysis of Soil-Structure Interaction Problems," by J. Lysmer, T. Udaka, C.-F. Tsai and H.B. Seed - 1975 (PB 259 332)A07

EERC 75-31 "ALUSH - A Computer Program for Seismic Response Analysis of Axisymmetric Soil-Structure Systems," by E. Berger, J. Lysmer and H.B. Seed - 1975

EERC 75-32 "TRIP and TRAVEL - Computer Programs for Soil-Structure Interaction Analysis with Horizontally Travelling Waves," by T. Udaka, J. Lysmer and H.B. Seed - 1975

EERC 75-33 "Predicting the Performance of Structures in Regions of High Seismicity," by J. Penzien - 1975 (PB 248 130)A03

EERC 75-34 "Efficient Finite Element Analysis of Seismic Structure - Soil - Direction," by J. Lysmer, H.B. Seed, T. Udaka, R.N. Hwang and C.-F. Tsai - 1975 (PB 253 570)A03

EERC 75-35 "The Dynamic Behavior of a First Story Girder of a Three-Story Steel Frame Subjected to Earthquake Loading," by R.W. Clough and L.-Y. Li - 1975 (PB 248 841)A05

EERC 75-36 "Earthquake Simulator Study of a Steel Frame Structure, Volume II - Analytical Results," by D.T. Tang - 1975 (PB 252 926)A10

EERC 75-37 "ANSR-I General Purpose Computer Program for Analysis of Non-Linear Structural Response," by D.P. Mondkar and G.H. Powell - 1975 (PB 252 386)A08

EERC 75-38 "Nonlinear Response Spectra for Probabilistic Seismic Design and Damage Assessment of Reinforced Concrete Structures," by M. Murakami and J. Penzien - 1975 (PB 259 530)A05

EERC 75-39 "Study of a Method of Feasible Directions for Optimal Elastic Design of Frame Structures Subjected to Earthquake Loading," by N.D. Walker and K.S. Pister - 1975 (PB 257 781)A06

EERC 75-40 "An Alternative Representation of the Elastic-Viscoelastic Analogy," by G. Dasgupta and J.L. Sackman - 1975 (PB 252 173)A03

EERC 75-41 "Effect of Multi-Directional Shaking on Liquefaction of Sands," by H.B. Seed, R. Pyke and G.R. Martin - 1975 (PB 258 781)A03

EERC 76-1 "Strength and Ductility Evaluation of Existing Low-Rise Reinforced Concrete Buildings - Screening Method," by T. Okada and B. Bresler - 1976 (PB 257 906)A11

EERC 76-2 "Experimental and Analytical Studies on the Hysteretic Behavior of Reinforced Concrete Rectangular and T-Beams," by S.-Y.M. Ma, E.P. Popov and V.V. Bertero - 1976 (PB 260 843)A12

EERC 76-3 "Dynamic Behavior of a Multistory Triangular-Shaped Building," by J. Petrovski, R.M. Stephen, E. Gartenbaum and J.G. Bouwkamp - 1976 (PB 273 279)A07

EERC 76-4 "Earthquake Induced Deformations of Earth Dams," by N. Serff, H.B. Seed, F.I. Makdisi & C.-Y. Chang - 1976 (PB 292 065)A08

EERC 76-5 "Analysis and Design of Tube-Type Tall Building Structures," by H. de Clercq and G.H. Powell - 1976 (PB 252 220) A10

EERC 76-6 "Time and Frequency Domain Analysis of Three-Dimensional Ground Motions, San Fernando Earthquake," by T. Kubo and J. Penzien (PB 260 556)A11

EERC 76-7 "Expected Performance of Uniform Building Code Design Masonry Structures," by R.L. Mayes, Y. Omote, S.W. Chen and R.W. Clough - 1976 (PB 270 098)A05

EERC 76-8 "Cyclic Shear Tests of Masonry Piers, Volume 1 - Test Results," by R.L. Mayes, Y. Omote, R.W. Clough - 1976 (PB 264 424)A06

EERC 76-9 "A Substructure Method for Earthquake Analysis of Structure - Soil Interaction," by J.A. Gutierrez and A.K. Chopra - 1976 (PB 257 783)A08

EERC 76-10 "Stabilization of Potentially Liquefiable Sand Deposits using Gravel Drain Systems," by H.B. Seed and J.R. Booker - 1976 (PB 258 820)A04

EERC 76-11 "Influence of Design and Analysis Assumptions on Computed Inelastic Response of Moderately Tall Frames," by G.H. Powell and D.G. Row - 1976 (PB 271 409)A06

EERC 76-12 "Sensitivity Analysis for Hysteretic Dynamic Systems: Theory and Applications," by D. Ray, K.S. Pister and E. Polak - 1976 (PB 262 859)A04

EERC 76-13 "Coupled Lateral Torsional Response of Buildings to Ground Shaking," by C.L. Kan and A.K. Chopra - 1976 (PB 257 907)A09

EERC 76-14 "Seismic Analyses of the Banco de America," by V.V. Bertero, S.A. Mahin and J.A. Hollings - 1976

EERC 76-15 "Reinforced Concrete Frame 2: Seismic Testing and Analytical Correlation," by R.W. Clough and J. Gidwani - 1976 (PB 261 323)A08

EERC 76-16 "Cyclic Shear Tests of Masonry Piers, Volume 2 - Analysis of Test Results," by R.L. Mayes, Y. Omote and R.W. Clough - 1976

EERC 76-17 "Structural Steel Bracing Systems: Behavior Under Cyclic Loading," by E.P. Popov, K. Takanashi and C.W. Roeder - 1976 (PB 260 715)A05

EERC 76-18 "Experimental Model Studies on Seismic Response of High Curved Overcrossings," by D. Williams and W.G. Godden - 1976 (PB 269 548)A08

EERC 76-19 "Effects of Non-Uniform Seismic Disturbances on the Dumbarton Bridge Replacement Structure," by F. Baron and R.E. Hamati - 1976 (PB 282 981)A16

EERC 76-20 "Investigation of the Inelastic Characteristics of a Single Story Steel Structure Using System Identification and Shaking Table Experiments," by V.C. Matzen and H.D. McNiven - 1976 (PB 258 453)A07

EERC 76-21 "Capacity of Columns with Splice Imperfections," by E.P. Popov, R.M. Stephen and R. Philbrick - 1976 (PB 260 378)A04

EERC 76-22 "Response of the Olive View Hospital Main Building during the San Fernando Earthquake," by S. A. Mahin, V.V. Bertero, A.K. Chopra and R. Collins - 1976 (PB 271 425)A14

EERC 76-23 "A Study on the Major Factors Influencing the Strength of Masonry Prisms," by N.M. Mostaghel, R.L. Mayes, R. W. Clough and S.W. Chen - 1976 (Not published)

EERC 76-24 "GADFLEA - A Computer Program for the Analysis of Pore Pressure Generation and Dissipation during Cyclic or Earthquake Loading," by J.R. Booker, M.S. Rahman and H.B. Seed - 1976 (PB 263 947)A04

EERC 76-25 "Seismic Safety Evaluation of a R/C School Building," by B. Bresler and J. Axley - 1976

EERC 76-26 "Correlative Investigations on Theoretical and Experimental Dynamic Behavior of a Model Bridge Structure," by K. Kawashima and J. Penzien - 1976 (PB 263 388)A11

EERC 76-27 "Earthquake Response of Coupled Shear Wall Buildings," by T. Srichatrapimuk - 1976 (PB 265 157)A07

EERC 76-28 "Tensile Capacity of Partial Penetration Welds," by E.P. Popov and R.M. Stephen - 1976 (PB 262 899)A03

EERC 76-29 "Analysis and Design of Numerical Integration Methods in Structural Dynamics," by H.M. Hilber - 1976 (PB 264 410)A06

EERC 76-30 "Contribution of a Floor System to the Dynamic Characteristics of Reinforced Concrete Buildings," by L.E. Malik and V.V. Bertero - 1976 (PB 272 247)A13

EERC 76-31 "The Effects of Seismic Disturbances on the Golden Gate Bridge," by F. Baron, M. Arikan and R.E. Hamati - 1976 (PB 272 279)A09

EERC 76-32 "Infilled Frames in Earthquake Resistant Construction," by R.E. Klingner and V.V. Bertero - 1976 (PB 265 892)A13

UCB/EERC-77/01 "PLUSH - A Computer Program for Probabilistic Finite Element Analysis of Seismic Soil-Structure Interaction," by M.P. Romo Organista, J. Lysmer and H.B. Seed - 1977

UCB/EERC-77/02 "Soil-Structure Interaction Effects at the Humboldt Bay Power Plant in the Ferndale Earthquake of June 7, 1975," by J.E. Valera, H.B. Seed, C.F. Tsai and J. Lysmer - 1977 (PB 265 795)A04

UCB/EERC-77/03 "Influence of Sample Disturbance on Sand Response to Cyclic Loading," by K. Mori, H.B. Seed and C.K. Chan - 1977 (PB 267 352)A04

UCB/EERC-77/04 "Seismological Studies of Strong Motion Records," by J. Shoja-Taheri - 1977 (PB 269 655)A10

UCB/EERC-77/05 "Testing Facility for Coupled-Shear Walls," by L. Li-Hyung, V.V. Bertero and E.P. Popov - 1977

UCB/EERC-77/06 "Developing Methodologies for Evaluating the Earthquake Safety of Existing Buildings," by No. 1 - B. Bresler; No. 2 - B. Bresler, T. Okada and D. Zisling; No. 3 - T. Okada and B. Bresler; No. 4 - V.V. Bertero and B. Bresler - 1977 (PB 267 354)A08

UCB/EERC-77/07 "A Literature Survey - Transverse Strength of Masonry Walls," by Y. Omote, R.L. Mayes, S.W. Chen and R.W. Clough - 1977 (PB 277 933)A07

UCB/EERC-77/08 "DRAIN-TABS: A Computer Program for Inelastic Earthquake Response of Three Dimensional Buildings," by R. Guendelman-Israel and G.H. Powell - 1977 (PB 270 693)A07

UCB/EERC-77/09 "SUBWALL: A Special Purpose Finite Element Computer Program for Practical Elastic Analysis and Design of Structural Walls with Substructure Option," by D.Q. Le, H. Peterson and E.P. Popov - 1977 (PB 270 567)A05

UCB/EERC-77/10 "Experimental Evaluation of Seismic Design Methods for Broad Cylindrical Tanks," by D.P. Clough (PB 272 280)A13

UCB/EERC-77/11 "Earthquake Engineering Research at Berkeley - 1976," - 1977 (PB 273 507)A09

UCB/EERC-77/12 "Automated Design of Earthquake Resistant Multistory Steel Building Frames," by N.D. Walker, Jr. - 1977 (PB 276 526)A09

UCB/EERC-77/13 "Concrete Confined by Rectangular Hoops Subjected to Axial Loads," by J. Vallenas, V.V. Bertero and E.P. Popov - 1977 (PB 275 165)A06

UCB/EERC-77/14 "Seismic Strain Induced in the Ground During Earthquakes," by Y. Sugimura - 1977 (PB 284 201)A04

UCB/EERC-77/15 "Bond Deterioration under Generalized Loading," by V.V. Bertero, E.P. Popov and S. Viwathanatepa - 1977

UCB/EERC-77/16 "Computer Aided Optimum Design of Ductile Reinforced Concrete Moment Resisting Frames," by S.W. Zagajeski and V.V. Bertero - 1977 (PB 280 137)A07

UCB/EERC-77/17 "Earthquake Simulation Testing of a Stepping Frame with Energy-Absorbing Devices," by J.M. Kelly and D.F. Tsztoo - 1977 (PB 273 506)A04

UCB/EERC-77/18 "Inelastic Behavior of Eccentrically Braced Steel Frames under Cyclic Loadings," by C.W. Roeder and E.P. Popov - 1977 (PB 275 526)A15

UCB/EERC-77/19 "A Simplified Procedure for Estimating Earthquake-Induced Deformations in Dams and Embankments," by F.I. Makdisi and H.B. Seed - 1977 (PB 276 820)A04

UCB/EERC-77/20 "The Performance of Earth Dams during Earthquakes," by H.B. Seed, F.I. Makdisi and P. de Alba - 1977 (PB 276 821)A04

UCB/EERC-77/21 "Dynamic Plastic Analysis Using Stress Resultant Finite Element Formulation," by P. Lukkunapvasit and J.M. Kelly - 1977 (PB 275 453)A04

UCB/EERC-77/22 "Preliminary Experimental Study of Seismic Uplift of a Steel Frame," by R.W. Clough and A.A. Huckelbridge 1977 (PB 278 769)A08

UCB/EERC-77/23 "Earthquake Simulator Tests of a Nine-Story Steel Frame with Columns Allowed to Uplift," by A.A. Huckelbridge - 1977 (PB 277 944)A09

UCB/EERC-77/24 "Nonlinear Soil-Structure Interaction of Skew Highway Bridges," by M.-C. Chen and J. Penzien - 1977 (PB 276 176)A07

UCB/EERC-77/25 "Seismic Analysis of an Offshore Structure Supported on Pile Foundations," by D.D.-N. Liou and J. Penzien 1977 (PB 283 180)A06

UCB/EERC-77/26 "Dynamic Stiffness Matrices for Homogeneous Viscoelastic Half-Planes," by G. Dasgupta and A.K. Chopra - 1977 (PB 279 654)A06

UCB/EERC-77/27 "A Practical Soft Story Earthquake Isolation System," by J.M. Kelly, J.M. Eidinger and C.J. Derham - 1977 (PB 276 814)A07

UCB/EERC-77/28 "Seismic Safety of Existing Buildings and Incentives for Hazard Mitigation in San Francisco: An Exploratory Study," by A.J. Meltsner - 1977 (PB 281 970)A05

UCB/EERC-77/29 "Dynamic Analysis of Electrohydraulic Shaking Tables," by D. Rea, S. Abedi-Hayati and Y. Takahashi 1977 (PB 282 569)A04

UCB/EERC-77/30 "An Approach for Improving Seismic - Resistant Behavior of Reinforced Concrete Interior Joints," by B. Galunic, V.V. Bertero and E.P. Popov - 1977 (PB 290 870)A06

UCB/EERC-78/01 "The Development of Energy-Absorbing Devices for Aseismic Base Isolation Systems," by J.M. Kelly and D.F. Tsztoo - 1978 (PB 284 978)A04

UCB/EERC-78/02 "Effect of Tensile Prestrain on the Cyclic Response of Structural Steel Connections, by J.G. Bouwkamp and A. Mukhopadhyay - 1978

UCB/EERC-78/03 "Experimental Results of an Earthquake Isolation System using Natural Rubber Bearings," by J.M. Eidinger and J.M. Kelly - 1978 (PB 281 686)A04

UCB/EERC-78/04 "Seismic Behavior of Tall Liquid Storage Tanks," by A. Niwa - 1978 (PB 284 017)A14

UCB/EERC-78/05 "Hysteretic Behavior of Reinforced Concrete Columns Subjected to High Axial and Cyclic Shear Forces," by S.W. Zagajeski, V.V. Bertero and J.G. Bouwkamp - 1978 (PB 283 858)A13

UCB/EERC-78/06 "Inelastic Beam-Column Elements for the ANSR-I Program," by A. Riahi, D.G. Row and G.H. Powell - 1978

UCB/EERC-78/07 "Studies of Structural Response to Earthquake Ground Motion," by O.A. Lopez and A.K. Chopra - 1978 (PB 282 790)A05

UCB/EERC-78/08 "A Laboratory Study of the Fluid-Structure Interaction of Submerged Tanks and Caissons in Earthquakes," by R.C. Byrd - 1978 (PB 284 957)A08

UCB/EERC-78/09 "Model for Evaluating Damageability of Structures," by I. Sakamoto and B. Bresler - 1978

UCB/EERC-78/10 "Seismic Performance of Nonstructural and Secondary Structural Elements," by I. Sakamoto - 1978

UCB/EERC-78/11 "Mathematical Modelling of Hysteresis Loops for Reinforced Concrete Columns," by S. Nakata, T. Sproul and J. Penzien - 1978

UCB/EERC-78/12 "Damageability in Existing Buildings," by T. Blejwas and B. Bresler - 1978

UCB/EERC-78/13 "Dynamic Behavior of a Pedestal Base Multistory Building," by R.M. Stephen, E.L. Wilson, J.G. Bouwkamp and M. Button - 1978 (PB 286 650)A08

UCB/EERC-78/14 "Seismic Response of Bridges - Case Studies," by R.A. Imbsen, V. Nutt and J. Penzien - 1978 (PB 286 503)A10

UCB/EERC-78/15 "A Substructure Technique for Nonlinear Static and Dynamic Analysis," by D.G. Row and G.H. Powell - 1978 (PB 288 077)A10

UCB/EERC-78/16 "Seismic Risk Studies for San Francisco and for the Greater San Francisco Bay Area," by C.S. Oliveira - 1978

UCB/EERC-78/17 "Strength of Timber Roof Connections Subjected to Cyclic Loads," by P. Gülkan, R.L. Mayes and R.W. Clough - 1978

UCB/EERC-78/18 "Response of K-Braced Steel Frame Models to Lateral Loads," by J.G. Bouwkamp, R.M. Stephen and E.P. Popov - 1978

UCB/EERC-78/19 "Rational Design Methods for Light Equipment in Structures Subjected to Ground Motion," by J.L. Sackman and J.M. Kelly - 1978 (PB 292 357)A04

UCB/EERC-78/20 "Testing of a Wind Restraint for Aseismic Base Isolation," by J.M. Kelly and D.E. Chitty - 1978 (PB 292 833)A03

UCB/EERC-78/21 "APOLLO - A Computer Program for the Analysis of Pore Pressure Generation and Dissipation in Horizontal Sand Layers During Cyclic or Earthquake Loading," by P.P. Martin and H.B. Seed - 1978 (PB 292 835)A04

UCB/EERC-78/22 "Optimal Design of an Earthquake Isolation System," by M.A. Bhatti, K.S. Pister and E. Polak - 1978 (PB 294 735)A06

UCB/EERC-78/23 "MASH - A Computer Program for the Non-Linear Analysis of Vertically Propagating Shear Waves in Horizontally Layered Deposits," by P.P. Martin and H.B. Seed - 1978 (PB 293 101)A05

UCB/EERC-78/24 "Investigation of the Elastic Characteristics of a Three Story Steel Frame Using System Identification," by I. Kaya and H.D. McNiven - 1978

UCB/EERC-78/25 "Investigation of the Nonlinear Characteristics of a Three-Story Steel Frame Using System Identification," by I. Kaya and H.D. McNiven - 1978

UCB/EERC-78/26 "Studies of Strong Ground Motion in Taiwan," by Y.M. Hsiung, B.A. Bolt and J. Penzien - 1978

UCB/EERC-78/27 "Cyclic Loading Tests of Masonry Single Piers: Volume 1 - Height to Width Ratio of 2," by P.A. Hidalgo, R.L. Mayes, H.D. McNiven and R.W. Clough - 1978

UCB/EERC-78/28 "Cyclic Loading Tests of Masonry Single Piers: Volume 2 - Height to Width Ratio of 1," by S.-W.J. Chen, P.A. Hidalgo, R.L. Mayes, R.W. Clough and H.D. McNiven - 1978

UCB/EERC-78/29 "Analytical Procedures in Soil Dynamics," by J. Lysmer - 1978

UCB/EERC-79/01	"Hysteretic Behavior of Lightweight Reinforced Concrete Beam-Column Subassemblages," by B. Forzani, E.P. Popov and V.V. Bertero - April 1979(PB 298 267)A06
UCB/EERC-79/02	"The Development of a Mathematical Model to Predict the Flexural Response of Reinforced Concrete Beams to Cyclic Loads, Using System Identification," by J. Stanton & H. McNiven - Jan. 1979(PB 295 875)A10
UCB/EERC-79/03	"Linear and Nonlinear Earthquake Response of Simple Torsionally Coupled Systems," by C.L. Kan and A.K. Chopra - Feb. 1979(PB 298 262)A06
UCB/EERC-79/04	"A Mathematical Model of Masonry for Predicting its Linear Seismic Response Characteristics," by Y. Mengi and H.D. McNiven - Feb. 1979(PB 298 266)A06
UCB/EERC-79/05	"Mechanical Behavior of Lightweight Concrete Confined by Different Types of Lateral Reinforcement," by M.A. Manrique, V.V. Bertero and E.P. Popov - May 1979(PB 301 114)A06
UCB/EERC-79/06	"Static Tilt Tests of a Tall Cylindrical Liquid Storage Tank," by R.W. Clough and A. Niwa - Feb. 1979 (PB 301 167)A06
UCB/EERC-79/07	"The Design of Steel Energy Absorbing Restrainers and Their Incorporation into Nuclear Power Plants for Enhanced Safety: Volume 1 - Summary Report," by P.N. Spencer, V.F. Zackay, and E.R. Parker - Feb. 1979(UCB/EERC-79/07)A09
UCB/EERC-79/08	"The Design of Steel Energy Absorbing Restrainers and Their Incorporation into Nuclear Power Plants for Enhanced Safety: Volume 2 - The Development of Analyses for Reactor System Piping,""Simple Systems" by M.C. Lee, J. Penzien, A.K. Chopra and K, Suzuki "Complex Systems" by G.H. Powell, E.L. Wilson, R.W. Clough and D.G. Row - Feb. 1979(UCB/EERC-79/08)A10
UCB/EERC-79/09	"The Design of Steel Energy Absorbing Restrainers and Their Incorporation into Nuclear Power Plants for Enhanced Safety: Volume 3 - Evaluation of Commercial Steels," by W.S. Owen, R.M.N. Pelloux, R.O. Ritchie, M. Faral, T. Ohhashi, J. Toplosky, S.J. Hartman, V.F. Zackay and E.R. Parker - Feb. 1979(UCB/EERC-79/09)A04
UCB/EERC-79/10	"The Design of Steel Energy Absorbing Restrainers and Their Incorporation into Nuclear Power Plants for Enhanced Safety: Volume 4 - A Review of Energy-Absorbing Devices," by J.M. Kelly and M.S. Skinner - Feb. 1979(UCB/EERC-79/10)A04
UCB/EERC-79/11	"Conservatism In Summation Rules for Closely Spaced Modes," by J.M. Kelly and J.L. Sackman - May 1979(PB 301 328)A03
UCB/EERC-79/12	"Cyclic Loading Tests of Masonry Single Piers; Volume 3 - Height to Width Ratio of 0.5," by P.A. Hidalgo, R.L. Mayes, H.D. McNiven and R.W. Clough - May 1979(PB 301 321)A08
UCB/EERC-79/13	"Cyclic Behavior of Dense Course-Grained Materials in Relation to the Seismic Stability of Dams," by N.G. Banerjee, H.B. Seed and C.K. Chan - June 1979(PB 301 373)A13
UCB/EERC-79/14	"Seismic Behavior of Reinforced Concrete Interior Beam-Column Subassemblages," by S. Viwathanatepa, E.P. Popov and V.V. Bertero - June 1979(PB 301 326)A10
UCB/EERC-79/15	"Optimal Design of Localized Nonlinear Systems with Dual Performance Criteria Under Earthquake Excitations," by M.A. Bhatti - July 1979(PB 80 167 109)A06
UCB/EERC-79/16	"OPTDYN - A General Purpose Optimization Program for Problems with or without Dynamic Constraints," by M.A. Bhatti, E. Polak and K.S. Pister - July 1979(PB 80 167 091)A05
UCB/EERC-79/17	"ANSR-II, Analysis of Nonlinear Structural Response, Users Manual," by D.P. Mondkar and G.H. Powell - July 1979(PB 80 113 301)A05
UCB/EERC-79/18	"Soil Structure Interaction in Different Seismic Environments," A. Gomez-Masso, J. Lysmer, J.-C. Chen and H.B. Seed - August 1979(PB 80 101 520)A04
UCB/EERC-79/19	"ARMA Models for Earthquake Ground Motions," by M.K. Chang, J.W. Kwiatkowski, R.F. Nau, R.M. Oliver and K.S. Pister - July 1979(PB 301 166)A05
UCB/EERC-79/20	"Hysteretic Behavior of Reinforced Concrete Structural Walls," by J.M. Vallenas, V.V. Bertero and E.P. Popov - August 1979(PB 80 165 905)A12
UCB/EERC-79/21	"Studies on High-Frequency Vibrations of Buildings - 1: The Column Effect," by J. Lubliner - August 1979 (PB 80 158 553)A03
UCB/EERC-79/22	"Effects of Generalized Loadings on Bond Reinforcing Bars Embedded in Confined Concrete Blocks," by S. Viwathanatepa, E.P. Popov and V.V. Bertero - August 1979
UCB/EERC-79/23	"Shaking Table Study of Single-Story Masonry Houses, Volume 1: Test Structures 1 and 2," by P. Gülkan, R.L. Mayes and R.W. Clough - Sept. 1979
UCB/EERC-79/24	"Shaking Table Study of Single-Story Masonry Houses, Volume 2: Test Structures 3 and 4," by P. Gülkan, R.L. Mayes and R.W. Clough - Sept. 1979
UCB/EERC-79/25	"Shaking Table Study of Single-Story Masonry Houses, Volume 3: Summary, Conclusions and Recommendations," by R.W. Clough, R.L. Mayes and P. Gülkan - Sept. 1979
UCB/EERC-79/26	"Recommendations for a U.S.-Japan Cooperative Research Program Utilizing Large-Scale Testing Facilities," by U.S.-Japan Planning Group - Sept. 1979(PB 301 407)A06
UCB/EERC-79/27	"Earthquake-Induced Liquefaction Near Lake Amatitlan, Guatemala," by H.B. Seed, I. Arango, C.K. Chan, A. Gomez-Masso and R. Grant de Ascoli - Sept. 1979(NUREG-CR1341)A03
UCB/EERC-79/28	"Infill Panels: Their Influence on Seismic Response of Buildings," by J.W. Axley and V.V. Bertero - Sept. 1979(PB 80 163 371)A10
UCB/EERC-79/29	"3D Truss Bar Element (Type 1) for the ANSR-II Program," by D.P. Mondkar and G.H. Powell - Nov. 1979 (PB 80 169 709)A02
UCB/EERC-79/30	"2D Beam-Column Element (Type 5 - Parallel Element Theory) for the ANSR-II Program," by D.G. Row, G.H. Powell and D.P. Mondkar - Dec. 1979(PB 80 167 224)A03
UCB/EERC-79/31	"3D Beam-Column Element (Type 2 - Parallel Element Theory) for the ANSR-II Program," by A. Riahi, G.H. Powell and D.P. Mondkar - Dec. 1979(PB 80 167 216)A03
UCB/EERC-79/32	"On Response of Structures to Stationary Excitation," by A. Der Kiureghian - Dec. 1979(PB 80166 929)A03
UCB/EERC-79/33	"Undisturbed Sampling and Cyclic Load Testing of Sands," by S. Singh, H.B. Seed and C.K. Chan - Dec. 1979(
UCB/EERC-79/34	"Interaction Effects of Simultaneous Torsional and Compressional Cyclic Loading of Sand," by P.M. Griffin and W.N. Houston - Dec. 1979

UCB/EERC-80/01 "Earthquake Response of Concrete Gravity Dams Including Hydrodynamic and Foundation Interaction Effects," by A.K. Chopra, P. Chakrabarti and S. Gupta - Jan. 1980(AD-A087297)A10

UCB/EERC-80/02 "Rocking Response of Rigid Blocks to Earthquakes," by C.S. Yim, A.K. Chopra and J. Penzien - Jan. 1980 (PB80 166 002)A04

UCB/EERC-80/03 "Optimum Inelastic Design of Seismic-Resistant Reinforced Concrete Frame Structures," by S.W. Zagajeski and V.V. Bertero - Jan. 1980(PB80 164 635)A06

UCB/EERC-80/04 "Effects of Amount and Arrangement of Wall-Panel Reinforcement on Hysteretic Behavior of Reinforced Concrete Walls," by R. Iliya and V.V. Bertero - Feb. 1980(PB81 122 525)A09

UCB/EERC-80/05 "Shaking Table Research on Concrete Dam Models," by A. Niwa and R.W. Clough - Sept. 1980(PB81 122 368)A06

UCB/EERC-80/06 "The Design of Steel Energy-Absorbing Restrainers and their Incorporation into Nuclear Power Plants for Enhanced Safety (Vol 1A): Piping with Energy Absorbing Restrainers: Parameter Study on Small Systems," by G.H. Powell, C. Oughourlian and J. Simons - June 1980

UCB/EERC-80/07 "Inelastic Torsional Response of Structures Subjected to Earthquake Ground Motions," by Y. Yamazaki April 1980(PB81 122 327)A08

UCB/EERC-80/08 "Study of X-Braced Steel Frame Structures Under Earthquake Simulation," by Y. Ghanaat - April 1980 (PB81 122 335)A11

UCB/EERC-80/09 "Hybrid Modelling of Soil-Structure Interaction," by S. Gupta, T.W. Lin, J. Penzien and C.S. Yeh May 1980(PB81 122 319)A07

UCB/EERC-80/10 "General Applicability of a Nonlinear Model of a One Story Steel Frame," by B.I. Sveinsson and H.D. McNiven - May 1980(PB81 124 877)A06

UCB/EERC-80/11 "A Green-Function Method for Wave Interaction with a Submerged Body," by W. Kioka - April 1980 (PB81 122 269)A07

UCB/EERC-80/12 "Hydrodynamic Pressure and Added Mass for Axisymmetric Bodies," by F. Nilrat - May 1980(PB81 122 343)A08

UCB/EERC-80/13 "Treatment of Non-Linear Drag Forces Acting on Offshore Platforms," by B.V. Dao and J. Penzien May 1980(PB81 153 413)A07

UCB/EERC-80/14 "2D Plane/Axisymmetric Solid Element (Type 3 - Elastic or Elastic-Perfectly Plastic) for the ANSR-II Program," by D.P. Mondkar and G.H. Powell - July 1980(PB81 122 350)A03

UCB/EERC-80/15 "A Response Spectrum Method for Random Vibrations," by A. Der Kiureghian - June 1980(PB81 122 301)A03

UCB/EERC-80/16 "Cyclic Inelastic Buckling of Tubular Steel Braces," by V.A. Zayas, E.P. Popov and S.A. Mahin June 1980(PB81 124 885)A10

UCB/EERC-80/17 "Dynamic Response of Simple Arch Dams Including Hydrodynamic Interaction," by C.S. Porter and A.K. Chopra - July 1980(PB81 124 000)A13

UCB/EERC-80/18 "Experimental Testing of a Friction Damped Aseismic Base Isolation System with Fail-Safe Characteristics," by J.M. Kelly, K.E. Beucke and M.S. Skinner - July 1980(PB81 148 595)A04

UCB/EERC-80/19 "The Design of Steel Energy-Absorbing Restrainers and their Incorporation into Nuclear Power Plants for Enhanced Safety (Vol 1B): Stochastic Seismic Analyses of Nuclear Power Plant Structures and Piping Systems Subjected to Multiple Support Excitations," by M.C. Lee and J. Penzien - June 1980

UCB/EERC-80/20 "The Design of Steel Energy-Absorbing Restrainers and their Incorporation into Nuclear Power Plants for Enhanced Safety (Vol 1C): Numerical Method for Dynamic Substructure Analysis," by J.M. Dickens and E.L. Wilson - June 1980

UCB/EERC-80/21 "The Design of Steel Energy-Absorbing Restrainers and their Incorporation into Nuclear Power Plants for Enhanced Safety (Vol 2): Development and Testing of Restraints for Nuclear Piping Systems," by J.M. Kelly and M.S. Skinner - June 1980

UCB/EERC-80/22 "3D Solid Element (Type 4-Elastic or Elastic-Perfectly-Plastic) for the ANSR-II Program," by D.P. Mondkar and G.H. Powell - July 1980(PB81 123 242)A03

UCB/EERC-80/23 "Gap-Friction Element (Type 5) for the ANSR-II Program," by D.P. Mondkar and G.H. Powell - July 1980 (PB81 122 285)A03

UCB/EERC-80/24 "U-Bar Restraint Element (Type 11) for the ANSR-II Program," by C. Oughourlian and G.H. Powell July 1980(PB81 122 293)A03

UCB/EERC-80/25 "Testing of a Natural Rubber Base Isolation System by an Explosively Simulated Earthquake," by J.M. Kelly - August 1980

UCB/EERC-80/26 "Input Identification from Structural Vibrational Response," by Y. Hu - August 1980(PB81 152 308)A05

UCB/EERC-80/27 "Cyclic Inelastic Behavior of Steel Offshore Structures," by V.A. Zayas, S.A. Mahin and E.P. Popov August 1980

UCB/EERC-80/28 "Shaking Table Testing of a Reinforced Concrete Frame with Biaxial Response," by M.G. Oliva October 1980(PB81 154 304)A10

UCB/EERC-80/29 "Dynamic Properties of a Twelve-Story Prefabricated Panel Building," by J.G. Bouwkamp, J.P. Kollegger and R.M. Stephen - October 1980

UCB/EERC-80/30 "Dynamic Properties of an Eight-Story Prefabricated Panel Building," by J.G. Bouwkamp, J.P. Kollegger and R.M. Stephen - October 1980

UCB/EERC-80/31 "Predictive Dynamic Response of Panel Type Structures Under Earthquakes," by J.P. Kollegger and J.G. Bouwkamp - October 1980(PB81 152 316)A04

UCB/EERC-80/32 "The Design of Steel Energy-Absorbing Restrainers and their Incorporation into Nuclear Power Plants for Enhanced Safety (Vol 3): Testing of Commercial Steels in Low-Cycle Torsional Fatigue," by P. Spencer, E.R. Parker, E. Jongewaard and M. Drory

UCB/EERC-80/33 "The Design of Steel Energy-Absorbing Restrainers and their Incorporation into Nuclear Power Plants for Enhanced Safety (Vol 4): Shaking Table Tests of Piping Systems with Energy-Absorbing Restrainers," by S.F. Stiemer and W.G. Godden - Sept. 1980

UCB/EERC-80/34 "The Design of Steel Energy-Absorbing Restrainers and their Incorporation into Nuclear Power Plants for Enhanced Safety (Vol 5): Summary Report," by P. Spencer

UCB/EERC-80/35 "Experimental Testing of an Energy-Absorbing Base Isolation System," by J.M. Kelly, M.S. Skinner and K.E. Beucke - October 1980(PB81 154 072)A04

UCB/EERC-80/36 "Simulating and Analyzing Artificial Non-Stationary Earthquake Ground Motions," by R.F. Nau, R.M. Oliver and K.S. Pister - October 1980(PB81 153 397)A04

UCB/EERC-80/37 "Earthquake Engineering at Berkeley - 1980," - Sept. 1980

UCB/EERC-80/38 "Inelastic Seismic Analysis of Large Panel Buildings," by V. Schricker and G.H. Powell - Sept. 1980 (PB81 154 338)A13

UCB/EERC-80/39 "Dynamic Response of Embankment, Concrete-Gravity and Arch Dams Including Hydrodynamic Interaction," by J.F. Hall and A.K. Chopra - October 1980(PB81 152 324)A11

UCB/EERC-80/40 "Inelastic Buckling of Steel Struts Under Cyclic Load Reversal," by R.G. Black, W.A. Wenger and E.P. Popov - October 1980(PB81 154 312)A08

UCB/EERC-80/41 "Influence of Site Characteristics on Building Damage During the October 3, 1974 Lima Earthquake," by P. Repetto, I. Arango and H.B. Seed - Sept. 1980(PB81 161 739)A05

UCB/EERC-80/42 "Evaluation of a Shaking Table Test Program on Response Behavior of a Two Story Reinforced Concrete Frame," by J.M. Blondet, R.W. Clough and S.A. Mahin

UCB/EERC-80/43 "Modelling of Soil-Structure Interaction by Finite and Infinite Elements," by F. Medina

UCB/EERC-81/01 "Control of Seismic Response of Piping Systems and Other Structures by Base Isolation," edited by J.M. Kelly - January 1981 (PB81 200 735)A05

UCB/EERC-81/02 "OPTNSR - An Interactive Software System for Optimal Design of Statically and Dynamically Loaded Structures with Nonlinear Response," by M.A. Bhatti, V. Ciampi and K.S. Pister - January 1981 (PB81 218 851)A09

UCB/EERC-81/03 "Analysis of Local Variations in Free Field Seismic Ground Motion," by J.-C. Chen, J. Lysmer and H.B. Seed - January 1981 (AD-A099508)A13

UCB/EERC-81/04 "Inelastic Structural Modeling of Braced Offshore Platforms for Seismic Loading," by V.A. Zayas, P.-S. B. Shing, S.A. Mahin and E.P. Popov - January 1981 (PB

UCB/EERC-81/05 "Dynamic Response of Light Equipment in Structures," by A. Der Kiureghian, J.L. Sackman and B. Nour-Omid - April 1981 (PB81 218 497)A04

UCB/EERC-81/06 "Preliminary Experimental Investigation of a Broad Base Liquid Storage Tank," by J.G. Bouwkamp, J.P. Kollegger and R.M. Stephen - May 1981

UCB/EERC-81/07 "The Seismic Resistant Design of Reinforced Concrete Coupled Structural Walls," by A.E. Aktan and V.V. Bertero - June 1981 (PB82 113 358)A11

UCB/EERC-81/08 "The Undrained Shearing Resistance of Cohesive Soils at Large Deformation," by M.R. Pyles and H.B. Seed - August 1981

UCB/EERC-81/09	"Experimental Behavior of a Spatial Piping System with Steel Energy Absorbers Subjected to a Simulated Differential Seismic Input," by S.F. Stiemer, W.G. Godden and J.M. Kelly - July 1981
UCB/EERC-81/10	"Evaluation of Seismic Design Provisions for Masonry in the United States," by B.I. Sveinsson, R.L. Mayes and H.D. McNiven - August 1981
UCB/EERC-81/11	"Two-Dimensional Hybrid Modelling of Soil-Structure Interaction," by T.-J Tzong, Sunil Gupta and J. Penzien - August 1981
UCB/EERC-81/12	"Studies on Effects of Infills in Seismic Resistant R/C Construction," by S. Brokken and V.V. Bertero - September 1981
UCB/EERC-81/13	"Linear Models to Predict the Nonlinear Seismic Behavior of a One-Story Steel Frame," by H. Valdimarsson, A.H. Shah and H.D. McNiven - September 1981
UCB/EERC-81/14	"TLUSH: A Computer Program for the Three-Dimensional Dynamic Analysis of Earth Dams," by T. Kagawa, L.H. Mejia, H.B. Seed and J. Lysmer - September 1981
UCB/EERC-81/15	"Three Dimensional Dynamic Response Analysis of Earth Dams," by L.H. Mejia and H.B. Seed - September 1981
UCB/EERC-81/16	"Experimental Study of Lead and Elastomeric Dampers for Base Isolation Systems," by J.M. Kelly and S.B. Hodder - October 1981
UCB/EERC-81/17	"The Influence of Base Isolation on the Seismic Response of Light Secondary Equipment," by J.M. Kelly - April 1981
UCB/EERC-81/18	"Studies on Evaluation of Shaking Table Response Analysis Procedures," by J. Marcial Blondet - November 1981
UCB/EERC-81/19	"DELIGHT.STRUCT: A Computer-Aided Design Environment for Structural Engineering," by R.J. Balling, K.S. Pister and E. Polak - December 1981
UCB/EERC-81/20	"Optimal Design of Seismic-Resistant Planar Steel Frames," by R.J. Balling, V. Ciampi, K.S. Pister and E. Polak - December 1981